Descending Control
in a Locomotor System

Inaugural-Dissertation

zur

Erlangung des Doktorgrades

der Mathematisch-Naturwissenschaftlichen Fakultät

der Universität zu Köln

vorgelegt von

Felix Clotten

aus Troisdorf

Köln

2020

Berichterstatter/in: PD Dr. Carmen Wellmann

Prof. Dr. Ansgar Büschges

Tag der mündlichen Prüfung: 25. September 2019

... Du wirst immer da sein ...

Contents

Zusammenfassung

Lokomotion ist sehr variabel, da sie sich an eine Vielzahl von Verhaltenskontexten anpassen muss. Daher müssen die Motorleistung und die zugrunde liegenden neuronalen Netzwerke an die Umgebungsbedingungen angepasst werden, in dem sie z.B. in Bezug auf Geschwindigkeit, Stärke oder Richtung moduliert werden. Vor allem muss Lokomotion initiiert werden, um eine zielgerichtete Bewegungen zu erzeugen, und zu einem anderen Zeitpunkt muss sie beendet werden. Bei einer Vielzahl von Tieren, sowohl Vertebraten als auch Invertebraten, wurde gezeigt, dass Lokomotion durch absteigende Informationen gesteuert wird, welche außerhalb des Bewegungsapparates entstehen. Im zentralen Nervensystem (ZNS) von Wirbeltieren werden diese Informationen von neuronalen Gruppen bereitgestellt, die eine große Anzahl von Neuronen umfassen. Bei wirbellosen ZNSs führte die geringere Anzahl von Neuronen jedoch zur Entdeckung einzelner Neurone, die die Fähigkeit besitzen, komplexe Verhaltensweisen zu initiieren oder zu beenden.

Das Netzwerk zur Bewegungskontrolle der Schwimmbeine von Flusskrebsen ist ein ausführlich beschriebenes System zur Untersuchung neuronaler Mechanismen, die der Motorleistung und Koordination mehrerer Gliedmaßen zugrunde liegen. Die Schwimmbeine sind vier gepaarte Pleopoden am Abdomen des Tieres. Beim Schwimmen des Flusskrebses bewegen sich die Schwimmbeine in alternierender Protraktion und Retraktion. Das neuronale Netzwerk, das diese Bewegungen erzeugt, wurde detailliert untersucht und es konnte gezeigt werden, dass zwei Klassen von Interneuronen den zentralen Mustergenerator (*central pattern generator*, CPG) bilden. Die Aktivität jedes Schwimmbeines wird von einem eigenen CPG gesteuert. Zusätzlich wurden absteigende Kommandoneurone beschrieben, die eine fiktive Lokomotion in isolierten Präparationen des Nervensystems initiieren oder beenden. Die Frage, wie diese Neurone die CPGs ansprechen, blieb jedoch bisher unbeantwortet.

Um diese Frage zu beantworten, habe ich einzelne Axonbündel innerhalb des Nervensystems stimuliert und extrazelluläre und intrazelluläre Aufnahmen der fiktiven Aktivität der Schwimmbeine gemacht. Ich konnte erfolgreich zeigen, dass meine Stimulationen einzelne Kommandoneurone rekrutierten, die fiktive Lokomotion initiierten und beendeten. Interessanterweise

konnte ich weiter zeigen, dass erregende Kommandoneurone die fiktive Lokomotion auch beschleunigen und verstärken können. Während die Beschleunigung bilateral identisch ist, ist die Verstärkung der Bewegung auf beiden Seiten unterschiedlich. Ich habe weiter gezeigt, dass hierbei nur eine Klasse von CPG-Neuronen direkten exzitatorischen Eingang bekommt. Darüber hinaus werden die CPGs einseitig angesteuert, was einen Mechanismus zur Initiierung eines bestimmten Verhaltens, z.B. Kurvenschwimmen, widerspiegeln könnte. Dies ist der erste Beweis dafür, wie absteigende Kontrolle die Bewegung der Schwimmbeine moduliert und liefert neue Einblicke in die allgemeine Kontrolle von Lokomotion.

Abstract

Locomotion is highly variable because it needs to adapt to a wide range of behavioral contexts. Consequently, the motor output and the underlying neuronal circuits need to be adapted in order to fit into the environmental circumstances, e.g. modulated in terms of speed, strength, or direction. Most importantly, locomotion needs to be initiated to generate necessary movements and under different circumstances it needs to be terminated. It was shown in a broad range of animals, both vertebrates and invertebrates, that motor output is controlled by descending information that arise outside of the locomotor systems. In the central nervous systems (CNS) of vertebrates these information are provided by distinct neuronal groups that comprise large numbers of neurons. In invertebrate CNSs, however, the smaller number of neurons had led to the discovery of individual neurons that possess the ability to initiated or terminate complex behaviors.

The swimmeret system of crayfish is a well characterized system to investigate the neuronal mechanisms underlying locomotion and coordination of multiple pairs of limbs. It consists of four paired limbs on the animal's abdomen that perform cycles of alternating power and return stroke movements when the crayfish swims. On the one hand, the neuronal network that generates these movements was investigated in great detail. The activity of each limb is driven by two classes of interneurons which form the central pattern generator (CPG). On the other hand, descending command neurons were found that initiate or terminate fictive locomotion in the isolated swimmeret system. However, the question of how these neurons affect the CPGs of the swimmeret system remained unanswered.

In order to address this question, I stimulated separated axon bundles within the abdominal nerve cord and performed extracellular and intracellular recordings of the swimmeret system's activity. I successfully showed that my stimulations recruited individual command neurons that affected fictive locomotion in terms of initiation and termination. Interestingly, I was able to show that excitatory command neurons can accelerate and strengthen fictive locomotion. While acceleration is implemented bilaterally, strengthening of the motor output contains a side-specific component. I further demonstrated that only one class of CPG neurons is directly targeted by

descending excitatory input. Furthermore, the CPGs are unilaterally targeted which may reflect a mechanism to initiate a specific behavior, e.g. turning. This is the first evidence of how descending input modulates the swimmeret system's motor output and gives new insights into the general control of locomotion.

1 Introduction

1.1 Descending control of rhythmic behavior

Perhaps the most striking characteristic that all species within the animal kingdom have in common is the ability to perform movements. Movements form the basis for any form of behavior and therefore, addressing the inherent mechanisms of the motor activity underlying it had always been a great incentive in the field of neuroscience. Within the wide range of behaviors that animals perform, periodic movements fascinated early researchers the most and never lost attraction since. The biological relevance of rhythmic movements is strongly emphasized by the fact that the rhythmicity of the heartbeat represents the very first movement performed during the embryonic development of vertebrates [Wernicke, 1876; Sylva et al., 2013]. The sinus node of the vertebrate heart consists of specialized muscle cells that are spontaneously active and act as pacemaker cells. No additional neuronal innervation is necessary to maintain the cardial rhythm. In comparison, early research on insects [Alexandrowicz, 1926] or crustaceans [Carlson, 1904] had shown that the neurogenic hearts of invertebrates are innervated by a specialized neuronal cluster, the cardiac ganglion (see Cooke [2002] for a review). Moreover, Carlson [1904] already demonstrated that within the cardiac ganglion, certain neurons drive the rhythmic activity of the decapod heart and this neuronal subset can be referred to as a central pattern generator (CPG). CPGs either can consist of single neurons that show specific activity oscillations due to their intrinsic properties (Alving [1968], to some extent Bal et al. [1988]), or are formed by multiple neurons and rely on the neuron's interconnections [Smarandache-Wellmann et al., 2013; Friesen et al., 1976]. All CPGs share the common feature that they generate rhythmic activity without any timed sensory or descending input being necessary [Marder and Bucher, 2001]. Besides regulation of the invertebrate heart beat, such CPGs were found in a wide range of investigated animals and performed behaviors like breathing (see Negro et al. [2018] for a review), chewing (see Westberg and Kolta [2011] for a review), or locomotion. In fact, CPGs underlying motor activity during locomotion are investigated perhaps on the most detailed level. In invertebrates, they had been extensively shown to control different

forms of locomotion like flying in locust [Wilson, 1961], walking in cockroaches [Pearson and Iles, 1970], or swimming in leeches [Kristan and Calabrese, 1976]. On the one hand, locomotion is reflected by alternating activity of two antagonistic muscle groups. On the other hand, separated body segments or limbs can be active during locomotion and it could be shown that individual CPGs control for the respective motor output of these segments [Murchison et al., 1993; Brodfuehrer et al., 1995]. In order to combine their separated activities, intersegmental coordination is essential to form a goal-directed motor output on a system's level. In different systems, this coordination could be shown to depend on sensory feedback [Cang and Friesen, 2000; Borgmann et al., 2009] or to be maintained by a specialized neuronal network, which had been successfully demonstrated in the crustacean swimmeret system [Namba and Mulloney, 1999; Mulloney and Hall, 2003; Smarandache-Wellmann and Grätsch, 2014; Smarandache-Wellmann et al., 2014].

The picture of locomotion is not complete by only describing the neuronal mechanisms that generate and maintain a specific locomotor behavior. On the output level, the most crucial aspect of locomotion is the ability to modulate the motor activity. Since locomotion is necessary for food acquisition, predator avoidance, or sexual reproduction, modulation is the prerequisite to ensure adaptation and survival in different environmental contexts. In general, modulation can be achieved in two different ways. On the one hand, local proprioceptive feedback can directly act on the neuronal microcircuits that generate or coordinate locomotion [Büschges, 2005; Borgmann et al., 2009; Zill et al., 2004]. On the other hand, modulatory information arising upstream of a locomotor system has been shown to be transmitted by descending pathways. Modulation by such pathways is predominantly reflected by termination and initiation of locomotion but also occurs in terms of acceleration or strengthening. In addition, turning behavior or postural stabilization can be achieved by modulating the activity of two body sides differently. Ullén et al. [1995] showed that bilateral descending input from the vestibular system controls for the rightening response in lampreys and Zelenin et al. [2000] further investigated these findings on a neuronal level. In addition, Karayannidou et al. [2007] could demonstrate that the same bilateral pathways account for the control of horizontal orientation. In parallel to these modulations, ensuring the maintenance of proper locomotion, sensory information can also initiate locomotion. Lampreys for example completely depend on olfactory sensation to find a food source. In preparations of the isolated nervous system of the lamprey, olfactory input activates a poly-synaptic pathway that produces fictive locomotion [Derjean et al., 2010; Daghfous et al., 2018]. Within this neuronal pathway, reticulospinal neurons activate the locomotor networks in the spinal cord [Di Prisco et al., 1997; Dubuc et al., 2008]. However, Grätsch et al. [2018]

could recently show that a subpopulations of reticulospinal neurons are additionally involved in a parallel descending pathway that terminates locomotion. Analogous descending pathways initiating locomotor responses were also described in other vertebrates. To name only a few, Mauthner cells trigger escape response in fish [Eaton et al., 2001], electrical stimulation of the mesencephalic locomotor region (MLR) initiates locomotion in salamanders [Cabelguen et al., 2003] and cats (see [Whelan, 1996] for a review), and optogenetic activation even of distinct neuron populations within the MLR can initiate and modulate motor output in mice [Josset et al., 2018]. In addition, descending pathways that terminate locomotion were also described in frog tadpoles [Perrins et al., 2002], cats [Takakusaki et al., 2003], and mice [Bouvier et al., 2015].

Despite immense methodical advances in recent times, descending pathways in vertebrates were so far mostly described on a level of distinct populations of neurons. Due to smaller numbers of neurons and considerably lower complexity, invertebrate systems offer the great advantage to investigate the function of individual neurons within these pathways. For example, Zorović and Hedwig [2012] intracellularly recorded from descending interneurons in the cricket and demonstrated their role in activation and modulation of walking. In fruit flies, Bidaye et al. [2014] identified a bilateral pair of descending interneurons that trigger backward walking and Sen et al. [2017] could show, that asymmetric activation of these neurons induces backward turning. In terms of swimming, individual neurons for both initiation [Brodfuehrer and Friesen, 1986] and termination [O'Gara and Friesen, 1995] were discovered in leech. Interestingly, the very first description of descending neurons commanding locomotor movements was also related to a swimming movement, the escape response of crayfish, when Wiersma [1947] described, that electrical stimulation of the giant fibers within the connectives evoked contraction of flexor muscles of the animals abdomen (see [Edwards et al., 1999] for a review). Several years later, Wiersma and Ikeda [1964] also demonstrated individual neurons that initiate and terminate swimming behavior in isolated preparations of the abdominal nervous system of the crayfish and referred to them as *command neurons* of the swimmeret system.

1.2 The swimmeret system

The swimmeret system of crustaceans provides a well established system to reveal fundamental mechanisms that underlie locomotor movements. Like all arthropods, crustaceans have a segmented body with paired limbs on each segment. Different segments contain limbs specialized for a specific function. The swimmerets are the limbs located on the animal's abdomen and besides their function in turning behavior [Copp and Hodes, 2001] and righting response [Davis, 1968a], they perform the locomotor movements used during swimming. For researchers, the swimmeret system combines several aspects that emphasize its important role in studying locomotion. First of all, preparations of the isolated abdominal nerve cord of crayfish, i. e. preparations lacking any sensory or proprioceptive feedback, express the same motor pattern as it is observed *in vivo* [Wiersma and Hughes, 1961]. This so called fictive locomotion is expressed without experimental application of neuromodulatory substances and enables detailed investigations under this reduced conditions [Wiersma and Ikeda, 1964]. In addition, the isolated preparation provides great accessibility regarding intracellular recordings or drug application, even to distinct parts of the nervous system. Finally, the neuronal circuits underlying the swimmeret system's motor output, i.e. alternating motor neuron activities and intersegmental coordination, were characterized in great detail. Hence, the swimmeret system offers the possibility to address specific questions regarding neuronal control of locomotion (see Mulloney and Smarandache-Wellmann [2012] for a review).

1.2.1 Neuronal circuitry

The swimmeret system of the signal crayfish, *Pacifastacus leniusculus* (DANA, 1842)*, consists of four pairs of swimmerets on abdominal segments two to five (Figure 1.1 A). The pair of limbs on the first abdominal segment is only developed in male crayfish and is modified for sexual reproduction. Propulsion during swimming is achieved by rhythmical movements of the four pairs of swimmerets by performing cycles of alternating power-stroke (PS, retraction) and return-stroke (RS, protraction) movements. During straight forward swimming, the two swimmerets of one abdominal segment are active synchronously [Davis, 1968a]. However, the mechanism of this bilateral coupling remains unknown and I will further only address the unilateral activity pattern of the swimmeret system. The PS generates the actual driving force and the RS returns the swimmeret to the initial position, required for performing a subsequent power-stroke (Figure 1.1 B). The muscles underlying these movements are controlled by PS and RS motor neurons, located in the ipsilateral hemiganglion of the corresponding abdominal

ganglia A2 to A5 (Figure 1.1 C). They project their axons through the first nerve (N1) and can be pooled in four functional groups: PS Exciters (PSE), PS Inhibitors (PSI), RS Exciters (RSE) and RS Inhibitors (RSI). The axons of PSE and PSI project through the posterior and the axons of RSE and RSI through the anterior branch of N1, respectively [Mulloney and Hall, 2000]. Extracellular recordings from these branches reveal alternating discharge patterns of PSE and RSI motor neurons on the one hand, and RSE and PSI motor neurons on the other hand. PS muscles are inhibited when RS muscles are excited, and vice versa. Although direct synaptic connections between small subsets of motor neurons were shown to exist [Sherff and Mulloney, 1996], it was hypothesized that these monosynaptic connections do not play a crucial role in maintaining their alternating activity. Instead, it was shown that the alternating activity of different motor neuron pools is driven by a local CPG, located in each hemiganglion [Heitler and Pearson, 1980; Murchison et al., 1993].

The local CPGs consist of two populations of non-spiking interneurons that drive motor neuron activity by graded, inhibitory transmitter release [Paul and Mulloney, 1985b,a; Mulloney, 2003]. Smarandache-Wellmann et al. [2013] described three types of interneurons inhibiting PSEs and RSIs and two types of interneurons inhibiting RSEs and PSIs. They assigned these neurons to previous descriptions of CPG neurons and renamed them as Inhibitors of PS (IPS) and Inhibitors of RS (IRS). Each IPS type was found as single copies in each hemiganglion and, although the three types are distinguishable by their specific morphology, they were not found to have different effects on the fictive motor pattern. Depolarizing current injection in IPS, inhibits PS activity and excites RS activity of the respective hemiganglion. Vice versa, hyperpolarization of IPS excites PS and inhibits RS activity. In contrast to IPSs, Smarandache-Wellmann et al. [2013] only characterized two different types of IRS with absolute certainty. IRS *hook* (IRSh) and IRS *no hook* (IRSnh) can be distinguished by their morphology and were also described to be present as single copies within each hemiganglion. Depolarization of either IRSs excites PS and inhibits RS activity, whereas hyperpolarization inhibits PS and excites RS activity. However, occasional dye-coupling of two similar neurons gave evidence for the existence of an additional IRSnh, electrically coupled to the already described IRSnh. Whether this finding reflects a distinct, third type of IRS had not been demonstrated so far. Interestingly, IRSh, but not IRSnh, is electrically coupled to Commissural Interneuron 1 (CI1), which takes a crucial role in intersegmental coordination [Smarandache-Wellmann et al., 2014]. In the active swimmeret system, the membrane potentials (V_m) of IPSs and IRSs oscillate in antiphase to each other due to reciprocal inhibition [Murchison et al., 1993; Skinner and Mulloney, 1998]. The alternating motor activity of PS and RS is shaped by this opposing oscillations and consequently fully

relies on the interplay of IPS and IRS.

During forward swimming in intact animals, as well as during fictive locomotion in isolated preparations, swimmeret activity reveals a stable posterior-to-anterior progression from A5 to A2 [Ikeda and Wiersma, 1964; Davis, 1968b]. The movements of different pairs of swimmerets are temporally shifted among each other, i.e. the cycle of movement starts with the most posterior pair and the anterior ones follow with a phase lag of approximately 25 % between segments, independent of the swimming speed [Davis, 1968b; Mulloney and Smarandache-Wellmann, 2012, (Blumenthal and Smarandache-Wellmann, unpublished)]. This metachronous wave from posterior to anterior is maintained by an ipsilateral coordinating network that consists of three neurons, located as single copies in each hemiganglion. Two different types of coordinating neurons encode information about the motor activity of their own hemiganglion and send it in ascending (Ascending Coordinating Neuron, ASC_E) and descending (Descending Coordinating Neuron, DSC) direction to neighboring hemiganglia [Namba and Mulloney, 1999; Smarandache-Wellmann and Grätsch, 2014]. The third neuron, CI1, decodes the coordinating information from all neighboring ganglia and feeds it back to the CPG of its own hemiganglion [Mulloney and Hall, 2003; Smarandache-Wellmann et al., 2014].

1.2.2 Microcircuits at a silent state

Since research on the swimmeret system mostly aimed to investigate the neuronal basis of oscillatory activity, i.e. alternating PS and RS activity, information about the microcircuits in an inactive state is sparse. On a behavioral level, Davis [1968a] showed that during righting responses in intact lobster, one side of the paired swimmerets is inactive. In this case, the swimmerets are protracted in the RS position. This can also be observed in intact crayfish not performing any swimmeret movements (personal observations). These animals keep all swimmerets in a horizontal position directed anteriorly. This position could either be determined by the morphological or anatomical structure of the swimmerets, or indicates a tonic activity of the RS muscles while the PS muscles are inactive. In lobster, Davis [1969] performed recordings from swimmeret muscles and distinguished the activity of individual motor neurons. He described tonic activity of motor neurons when no swimmeret movements were observed and stated that this might be associated with holding the swimmeret at a specific position. Unfortunately, it is not possible to assign this tonic activity to one functional group of motor neurons, i.e. PSE or PSI, or RSE or RSI, respectively. Generally, an inactive state of the isolated preparation of the swimmeret system is defined as the absence of PS activity. Intracellular recordings performed in crayfish further revealed that the membrane potential (V_m) of motor neurons does
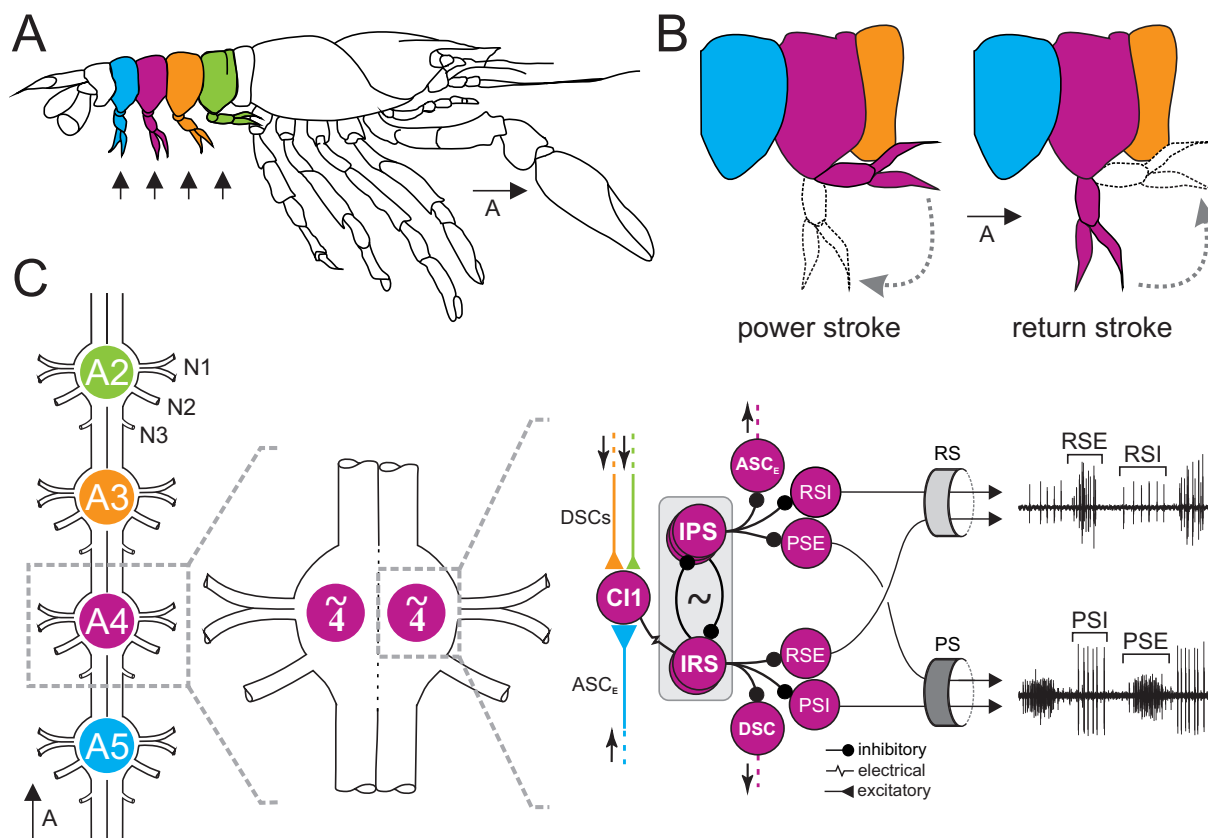
Figure 1.1: The swimmeret system of the crayfish, *Pacifastacus leniusculu*s. **A:** Schematic drawing of a crayfish. The swimmerets (arrows) are paired limbs on the animal's abdomen. **B:** During forward swimming, swimmerets perform alternating power (PS) and return (RS) strokes. **C:** *From left to right*: Schematic drawing of the four abdominal ganglia that innervate the swimmerets. The activity of a single swimmeret is controlled by a neuronal micro circuit located in the corresponding hemiganglion. Two groups of neurons (IPS, IRS) form the CPG that the alternating discharge of RS and PS motor neurons (RSE / PSI, and PSE / RSI). Three neurons (CI1, DSC, ASC_E) form a coordinating network that coordinates the activities of ipsilateral hemiganglia. A detailed description is given in the text. Abdominal body segments and corresponding ganglia are colored (2nd: *green*, 3th: *orange*, 4th: *purple*, 5th: *blue*). **RS** *return stroke*, **PS** *power stroke*, **N1** *first nerve root*, **N2** *second nerve root*, **N3** *third nerve root*, **A2-A5** *abdominal ganglia*, **CI1** *Commissural Interneuron 1*, **DSC** *Descending Coordinating Neuron*, **ASC_E** *Ascending Coordinating Neuron*, **IPS** *Inhibitor of Power Stroke*, **IRS** *Inhibitor of Return Stroke*, **RSI** *Return Stroke Inhibitor*, **RSE** *Return Stroke Exciter*, **PSI** *Power Stroke Inhibitor*, **PSE** *Power Stroke Exciter*.

not oscillate in this silent state [Heitler, 1978; Sherff and Mulloney, 1997; Mulloney, 2003]. At this *non-oscillating potential* (NOP), Sherff and Mulloney [1997] described that "a few motor neurons fired action potentials tonically, but most were quiet" but did not further distinguish between different functional groups. However, Mulloney [2003] assigned his observations in a silent state to specific groups of motor neurons. In his experiments, the axons of PSE did not show any neuronal discharge "while a few RSE and RSI axons fired steadily". If a preparation became active, PSEs fired bursts of action potentials and RSEs and RSIs "changed from steady firing to periodic bursting". Mulloney [2003] additionally described these changes at the intracellular level and specifically reported that the V_m of one RSE started to oscillate "around it's resting potential [in this thesis: NOP]".

Absent PS and tonic RS activity during a silent state of the swimmeret system, indicates that PSEs and RSEs are locked at a comparatively hyper- or depolarized V_m , respectively. Since phasic inhibition from the CPG neurons gradually modulates the V_m of motor neurons when the system is active, this constant, stable synaptic inputs represent a potential source for the lack of oscillations in different motor neuron groups. Heitler and Pearson [1980] performed simultaneous intracellular recordings from one PSE and one presynaptic, non-spiking interneuron, presumably IRS. Depolarization of the interneuron decreased the amplitude of V_m oscillations in the PSE "with the membrane potential remaining in the depolarized phase", indicating reduced inhibition. In addition, they observed a strong excitation of other PS motor neurons and inhibition of RS motor neurons that were recorded extracellularly. In contrast, hyperpolarization of the interneuron silenced the system, i.e. PS activity was absent and RS became tonically active. The V_m oscillations of PSE were again "much reduced with the membrane remaining hyperpolarized". Smarandache-Wellmann et al. [2013] could reproduce these effects by current injections into identified IRSs and observed the opposite effects on motor neurons regarding IPS. Depolarization of IPS silenced PS activity and evoked tonic RS activity. In addition, their intracellular recordings indicate that the amplitudes of V_m oscillations of IRS and IPS decreased when the neurons were hyperpolarized or depolarized, respectively. This could indicate, that the NOP in a silent state is respectively hyper- or depolarized, compared to V_m oscillations in an active state.

The observations made by Heitler and Pearson [1980] and Smarandache-Wellmann et al. [2013] are due to artificial interfering with the rhythmicity of the swimmeret system, i.e. altering the activity of a single neuron with current injections. However, spontaneous transition from one state into the other might be underlined by different shifts in the V_m. Only little information is available about spontaneous activity transition at the level of interneurons of the swimmeret

system. Paul and Mulloney [1985b] showed one recording of IPS (previously *Interneuron 1*, Figure 2 A in Paul and Mulloney [1985b]), whose V_m started to oscillate spontaneously. In this case, the peak potential (PP) during oscillations was at the V_m of the NOP. Analog to motor neurons, the coordinating neurons DSC and ASC_E also receive synaptic inhibition from the CPG interneurons and Schneider [2017] showed two examples of spontaneous activity transition of these neurons. She demonstrated that the NOP of DSC is at the V_m of the PP, whereas the NOP of ASC_E is at the V_m of the trough potential (TP) during oscillation. Finally, Blumenthal [2018] presented one example of spontaneous transition, revealing that the NOP of CI1 equals it's TP.

1.2.3 Descending control

As extensively described in chapter 1.1, locomotion can be modulated by descending input from higher centers of the CNS, i.e. neuronal populations upstream of locomotor systems. Here, sensory information plays a crucial role and was shown to affect the activity of the swimmeret system. The righting response of crustaceans, as described by Davis [1968a], relies on information provided by the statocysts system. In the crayfish species *Procambarus clarkii*, statocyst-driven descending interneurons (SDI) were described both at the level of the brain [Nakagawa and Hisada, 1989] and within the abdominal connectives [Takahata and Hisada, 1982]. Takahata and Hisada [1982] described four pairs of SDIs projecting throughout the entire nervous system to the most posterior ganglion A6. Two of them receive input from the contralateral, one from the ipsilateral side, and one pair receives bilateral input. Even if it is not demonstrated so far, the projection pattern of SDIs and the contribution of swimmerets in righting responses indicate that SDIs can potentially affect the swimmeret system. Subsequent research has shown that the activity of SDIs is affected by proprioception of the walking legs [Hama and Takahata, 2003], the behavioral context, i.e. the direction of walking [Takahata et al., 1984], and to some extent by the visual system [Takahata and Hisada, 1982]. At the level of the brain, statocyst-driven local interneurons that are most likely presynaptic to SDIs [Nakagawa and Hisada, 1989], were shown to be modulated by sensory information from the walking legs [Hama and Takahata, 2005]. Furthermore, the dendritic projections of SDIs and their presynaptic partners within the brain suggest interaction with other sensory neurons [Nakagawa and Hisada, 1989]. Therefore, SDIs can be assumed to be multimodal interneurons and Takahata and Hisada [1982] discussed a potential role as command neurons of the righting response. In fact, this idea is strongly emphasized since Fraser [1975] was able to evoke a righting response in the crab, *Scylla serrata*, by electrical stimulation of a single SDI.

Command neurons were also described in the swimmeret system. Descending axons within the abdominal connectives that modulate fictive locomotion were first extensively investigated in *P. clarkii* by Wiersma and Ikeda [1964]. They described five pairs of excitatory command neurons that, when electrically stimulated, initiated fictive locomotion in isolated preparations of the abdominal nervous system. The period of the evoked activity depends on the stimulation frequency [Stein, 1971; Atwood and Wiersma, 1967] and early studies stated that stimulation of different command neurons evoked slightly different effects within the swimmeret system [Atwood and Wiersma, 1967]. Acevedo et al. [1994] demonstrated the existence of the same neurons in *P. leniusculus* and named then E_A to E_E according to the locations described by Wiersma and Ikeda [1964] and their *excitatory* effect (Figure 1.2 A, B). In contrast to Atwood and Wiersma [1967], she described similar motor activities evoked by stimulation of individual excitatory command neurons. Furthermore, she compared the resulting fictive locomotion to spontaneous and proctolin-induced (PR) locomotion, and did not find any differences. A remarkable bioassay and antibody labeling against PR, gave evidence that at least a portion of the excitatory command neurons contain PR that is released within the abdominal ganglia during stimulation of these neurons [Acevedo, 1990; Acevedo et al., 1994] (Figure 1.2 C).

Analog to excitatory command neurons, Wiersma and Ikeda [1964] and Acevedo et al. [1994] also described inhibitory command neurons of the swimmeret system. Electrical stimulation of the axons of these neurons completely terminated PS activity, applicable for both spontaneous locomotion or locomotion evoked by stimulation of an excitatory command neuron. The locations of the axons within the abdominal connectives are close to some of the excitatory command neurons, and Acevedo et al. [1994] named then I_A, I_C and I_E due to their *inhibitory* effect (Figure 1.2 B). It was shown that octopamine (OA) terminates fictive locomotion, making OA a potential neurotransmitter to be released by inhibitory command neurons [Mulloney et al., 1987]. Mulloney et al. [1987] further demonstrated that bath application of phentolamine, an OA antagonist, partially blocked the termination caused by the stimulation of inhibitory command neurons.

Although descending input that affects the swimmeret system was described in detail, we are still lacking knowledge about the neuronal targets of inhibitory and excitatory command neurons within the microcircuits. Frequency-dependent effects on the period and on the excitement of PS motor neurons [Davis and Kennedy, 1972a], suggest that both the CPG neurons and the motor neurons are targeted. However, if they are affected within the same magnitude or with bilateral differences was not investigated on a cellular level. In addition, it is unknown which input command neurons receive and how they interact with other descending input, e.g. SDIs.
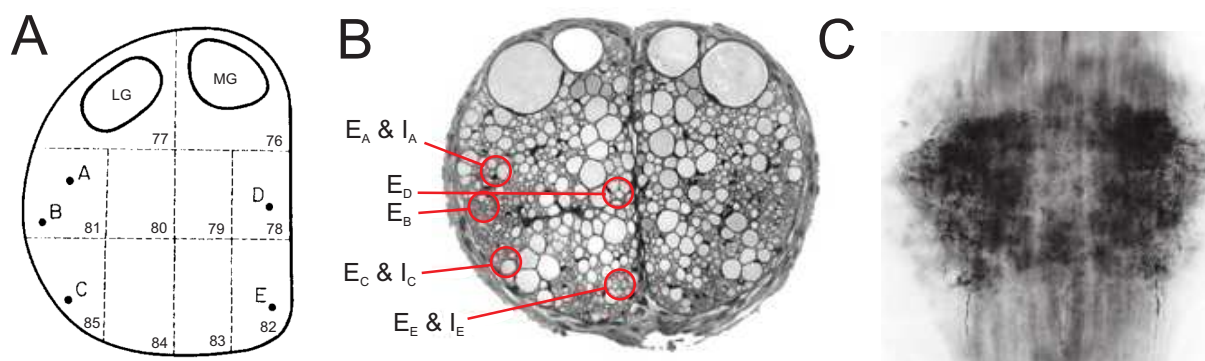
Figure 1.2: Command neurons of the swimmeret system. **A:** Schematic drawing of an abdominal hemiconnective. Numbers refer to areas described by Wiersma and Hughes [1961]. Letters A to E indicate the locations of excitatory command neurons E_{A-E}. Modified from Wiersma and Ikeda [1964]. **B:** Cross section of one abdominal connectives in *Pacifastacus leniusculus*. Letters E_{A-E} and $I_{A,C,E}$ indicate the locations of excitatory and inhibitory command neurons, respectively. Adopted from Mulloney and Smarandache-Wellmann [2012]. **C:** Anti-proctolin antibody labeling in the abdominal ganglion A2 (dorsal view, anterior at the top). Dense labeling is present in ganglion, predominantly in the lateral neuropil. Adopted from Acevedo et al. [1994]. **LG** *lateral giant fiber*, **MG** *medial lateral giant fiber*, **E_X** *excitatory command neuron*, **I_X** *inhibitory command neuron*.

1.3 Aim of study

The first aim of my thesis was to revise previous studies of command neurons of the swimmeret system that were shown to provide descending control of locomotion. In addition to already described termination and initiation of fictive locomotion, I wanted to address further modulatory effects on the motor output, e.g. a potential enhancement of fictive locomotion. Therefore, I performed electrical stimulations in areas that presumably contain the axons of inhibitory and excitatory command neurons and extracellularly recorded the motor output of the swimmeret system. Since the locations of the command neurons' axons were so far described only by visual estimation, I aimed to provide a histological proof of the stimulated axons and investigate their physiological properties, i.e. the extent of their axonal projection and the propagation of descending information. In future, these anatomical and physiological approach will ensure proper comparison between different experiments and studies. They are further necessary to relate the evoked modulations of fictive locomotion to different descending inputs (e.g. statocyst input, Yoshino et al. [1980]; Takahata and Hisada [1982]) and to other behaviors observed in intact animals (e.g. turning, Bowerman and Larimer [1974]).

The second aim of my thesis was to study transitions between different states of activity at the level of the neuronal microcircuits. Therefore, I investigated activity changes in individual neurons by performing intracellular recordings. The membrane potentials (V_m) of these neurons

oscillate between phases of depolarization (peak potential, PP) and hyperpolarization (trough potential, TP) when the swimmeret system expresses fictive locomotion but are stable at a silent state (non-oscillating potential, NOP). As suggested by behavioral observations and physiological descriptions, different neuronal groups are locked at specific phases of V_m oscillations, i.e. they are either continuously depolarized or hyperpolarized (Chapter 1.2.2). Based on these finding, I hypothesized a silent state of the microcircuits in which the NOP of each neuron is assigned to be either at the PP or the TP (Figure 1.3). The absence of rhythmic power stroke (PS) motor activity indicates tonic hyperpolarization of PS excitatory motor neurons (PSE) at the TP and continuous depolarization of PS inhibitory motor neurons (PSI) at the PP. Vice versa, continuous return stroke (RS) activity indicates continuous depolarization of RS excitatory motor neurons (RSE) at the PP and continuous hyperpolarization of RS inhibitory motor neurons (RSI) at the TP. Due to the known neuronal circuitry, I assume that the specific NOP of a motor neuron is determined by either tonic or absent inhibition by the respective interneurons of the central pattern generator (CPG). The NOPs of these CPG neurons consequently determine the NOPs of the neurons forming the coordinating network (Figure 1.3 B).

My final aim was to identify the local targets of command neurons. Termination and initiation of fictive locomotion is achieved by unilateral stimulations of command neurons that bilaterally affect PS motor activity [Wiersma and Ikeda, 1964; Mulloney et al., 1987; Acevedo et al., 1994]. Consequently, I assumed that both hemiganglia of one segment are equally targeted by unilateral command neurons. In addition, initiated fictive locomotion is reflected by constant coordination that is independent of the evoked period of the motor output. This suggests that the neurons of the coordinating networks are not affected by command neurons. Instead, there is evidence that the period and the strength of fictive locomotion depend on varying input from excitatory command neurons, indicating that CPG neurons and motor neurons are direct targets of these neurons.
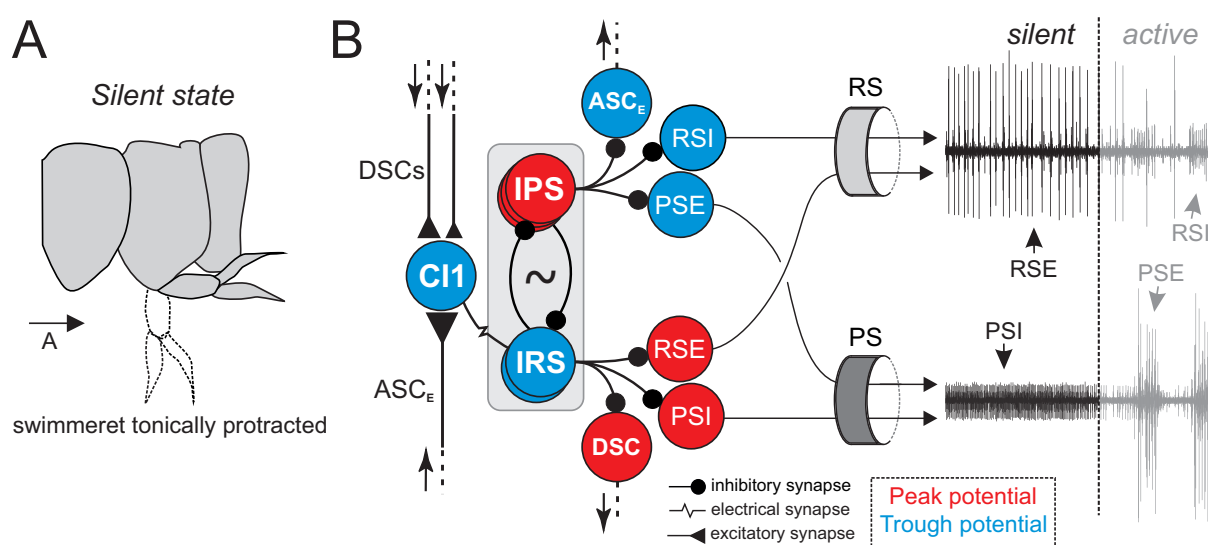
Figure 1.3: Illustration of a hypothetical silent state of the microcircuit. **A:** In freely behaving crayfishes, swimmerets are tonically protracted in the return stroke (RS) position, indicating tonic excitation of RS muscles and tonic inhibition of PS muscles. **B:** During swimming, the membrane potentials of neurons within the micro circuits oscillate between the peak (PP, depolarized phase) and the trough (TP, hyperpolarized phase) potential to generate alternating activity (not shown). In a silent state, different neuronal groups are locked at one of these phases to generate tonic discharge of RS exciters (RSE) and PS inhibitors (PSI), and suppress discharge of PS exciters (PSE) and RS inhibitors (RSI). The corresponding activities of motor neurons at a silent and an active state are illustrated by extracellular recordings of the posterior (PS) and anterior (RS) branch of the first nerve root. A detailed description is given in the text. **RS** *return stroke*, **PS** *power stroke*, **CI1** *Commissural Interneuron 1*, **DSC** *Descending Coordinating Neuron*, **ASC$_E$** *Ascending Coordinating Neuron*, **IPS** *Inhibitor of Power Stroke*, **IRS** *Inhibitor of Return Stroke*, **RSI** *Return Stroke Inhibitor*, **RSE** *Return Stroke Exciter*, **PSI** *Power Stroke Inhibitor*, **PSE** *Power Stroke Exciter*.

2 Materials and Methods

All surgical and experimental procedures were performed observing the guidelines of the animal protection act of the Federal Republic of Germany. Signal crayfish, *Pacifastacus leniusculus*, were caught in different waters of North Rhine-Westphalia by local fishermen or members of our research group. Animals were kept in aerated fresh water maintained at 14° C and fed once a week with organic carrots and shrimp pallets (The Hartz Mountain Corporation, New Jersey, USA). For this study, I performed experiments on 107 adult animals of both sexes.

2.1 Animal preparation

Directly prior to an experiment, I took a single crayfish from the animal holding tanks and anesthetized it on ice for 30 minutes. Both claws were cut at their bases, the left and right uropod were removed and the crayfish exsanguinated through the claw openings with 50 ml cold normal crayfish saline (CS) (5.4 mM KCl, 2.6 mM $MgCl^2$, 13.5 mM $CaCl^2$ and 195 mM NaCl, buffered with 10 mM Tris base and 4.7 mM maleic acid at pH 7.4 - 7.6 and oxygenated for 2 hours). The crayfish was decapitated and the abdominal nerve cord together with the forth and fifth thoracic ganglia was isolated and pinned out straight with the dorsal side up in a Petri dish lined with transparent Sylgard (Sigma-Aldrich, St. Louis, MO, USA). For a detailed description of the preparation steps see Seichter et al. [2014]. In the experiments presented in chapter 3.2.5, I isolated additional portions of the nervous system. In addition to the abdominal chain of ganglia, these preparations either included only the thoracic ganglia T1 to T5, the subesophageal ganglion, or the entire nervous system as far as to the level of the brain. All ganglia were desheathed on the dorsal side using fine forceps and scissors to ensure proper oxygen supply of the nervous tissue. If necessary for the experiment, I isolated the nerves innervating the walking leg muscles in T4.

For electrical stimulations the connectives between the first (A1) and second (A2) abdominal ganglia (cA1/A2) were completely desheathed. The dorsal portion of one hemiconnective, i.e. divisions 76 and 77 [Wiersma and Hughes, 1961], were removed to preclude stimulation of the

medial (MG, 76) and lateral (LG, 77) giant fibers. The remaining portion of the hemiconnective was split into separated axon bundles using a sharpened insect pin while care was taken to prevent axon damages. In some experiments I performed stimulations at different levels of the nervous system. The respective portion of the connectives was prepared according to the description for cA1/A2. In addition, the connective between A5 and A6 (cA5/A6) was also desheathed to facilitate extracellular recordings using a hook electrode. To improve the recording quality, the hemiconnective of cA5/A6 ipsilateral to the stimulation was subdivided into two dorsal and two ventral sections.

2.2 Experimental procedure

2.2.1 Electrical stimulation

I electrically stimulated separated axon bundles at the level of cA1/A2 using a suction electrode (Figure 2.1 A). Suction electrodes were pulled on a micropipette horizontal puller (P-87, Sutter Instruments) with filament (Sutter Instruments) from fire polished borosilicate glass capillaries (outer/inner diameter: 1.5 mm/0.86 mm). I manually broke the tips under visual control using a dissection microscope to generate tip openings suitable for axon bundle diameters used in this study. A single axon bundle was cut posterior to A2 and carefully sucked into the suction electrode (Figure 2.1 B). The reference electrode was placed in the bath solution. Stimuli were generated with a Universal Digital Stimulator (MS 501, Electronic Lab), further processed by an Universal Stimulus Isolater (Model 401, Electronic Lab, University of Cologne, Germany) and send to a preamplifier (MA 103, Electronic Lab) connected to the electrode. The stimulus signal was digitized by an A / D converter (Digidata 1440A, Molecular Devices, Sunnyvale, CA, USA or Micro1401 mkII, Cambridge Electronic Design, Cambridge, England) and recorded on a computer with Spike2 (v7.09, Cambridge Electronic Design) or pClamp software (v10.2.0.18, Molecular Devices).

Within an experiment, I stimulated different axon bundles until a reproducible stimulation effect was evoked by the stimulation of the same bundle. Please note that I stimulated several axon bundles in each preparation but not all of them had an effect on the swimmeret system. In this study I present only the data from successful stimulations, i.e. stimulations that initiated, terminated or enhanced fictive locomotion of the swimmeret system. I used silent preparations, i.e. preparations not being spontaneously active in normal crayfish saline, to initially investigate the initiation of fictive locomotion. Afterwards, a stable expression of fictive locomotion

was elicited by using crayfish saline containing carbolic (CCh, Sigma-Aldrich, St. Louis, MO, USA). Analogously, I used active preparations (spontaneously or CCh-induced) to investigate the termination of fictive locomotion by electrical stimulations.

The stimuli I used in this study, were trains of rectangular pulses with a duration of 1 ms and a frequency of 30 Hz delivered in bouts lasting from one second up to one minute. For every single stimulation configuration, the stimulus amplitude was individually set depending on stimulated axons and the seal between the axon bundle and the suction electrode. Therefore, the amplitude was gradually increased until a stimulation effect was reproducible observed, eventually ranging from 0.01 to 0.1 mA for individual stimulations. In some experiments, in order to investigate the effect of changes in stimulation frequency and amplitude, I tested different stimulation frequencies (10 to 50 Hz). Occasionally, I tested additional stimulation amplitudes above or below the initial value.
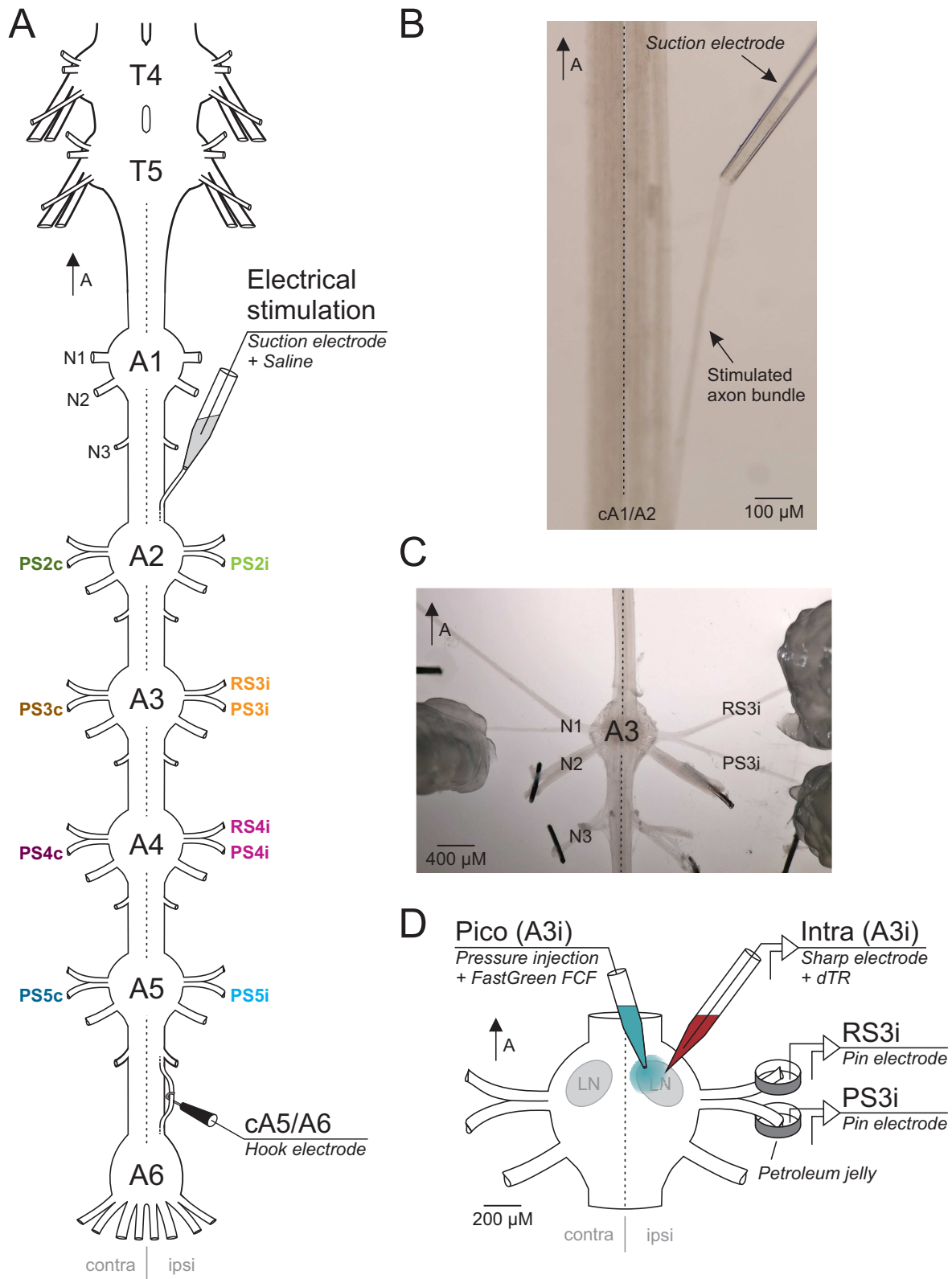
Figure 2.1: Experimental setup. Dorsal views. Dashed lines indicate midline. **A:** Schematic drawing of the preparation consisting of ganglia T4 to A6. The extracellular recordings of the motor output of abdominal ganglia A2 to A5 are listed using the corresponding color code. Electrical stimulations using a suction electrode were performed anterior to the swimmeret system, i.e. cA1/A2, and recordings of stimulus-correlated activity at the level of cA5/A6 using a hook electrode. **B:** Picture of an electrical stimulation of a separated axon bundle at the level of cA1/A2. **C:** Picture of a representative ganglion, i.e. A3. The anterior and posterior branches of N1 contain the axons of RS and PS motor neurons, respectively. **D:** Schematic drawing of an individual ganglion. Extracellular recordings of RS and PS activity were performed using pin electrodes. Intracellular recordings of individual neurons using sharp microelectrodes and focal drug application using a suction electrode were performed within the lateral neuropil. For clarity reasons, only recordings ipsilateral to the electrical stimulation are depicted here. **RSi** *ipsilateral return stroke*, **PSi** *ipsilateral power stroke*, **PSc** *contralateral power stroke*, **N1** *first nerve*, **N2** *second nerve*, **N3** *third nerve*, **T4-T5** *thoracic ganglia*, **A1-A6** *abdominal ganglia*, **cA1/A2** *connective between A1 and A2*, **LN** *lateral neuropil*.

2.2.2 Electrophysiology

I extracellularly recorded the activity of motor neurons using stainless steel pin electrodes [Seichter et al., 2014] (Figure 2.1 A). I recorded power stroke (PS) motor neurons bilaterally from ganglia A2 to A5 and return stroke (RS) motor neurons from ganglia A3 and A4 ipsilateral to the electrical stimulation. Electrodes were inserted into the Sylgard close to the posterior or anterior branch of N1 for recording of the PS or RS, respectively. The respective nerve branch was wrapped around the electrode and insulated from the bath solution using petroleum jelly (Figure 2.1 C and D). The reference electrodes were inserted into the Sylgard close to the corresponding recording electrode .

To investigate the propagation of neuronal signals that were potentially evoked by the electrical stimulation, I aimed for picking up stimulus-correlated activity at the most posterior level of the abdominal nervous system, i. e. cA5/A6. Therefore, I used a hook electrode (Electronic Lab) connected to a preamplifier (MA 101, Electronic Lab) to extracellularly record from a separated portion of the hemiconnective ipsilateral to the stimulation (Figure 2.1 A). I insulated the hook electrode together with the respective axon bundle from the bath solution using petroleum jelly and placed the reference electrode nearby into the bath.

I performed intracellular recordings in the dendritic processes within the lateral neuropil (LN) using sharp microelectrodes to investigate the stimulation effect on individual neurons (Figure 2.1 D). Characterization of neurons was based on their physiological properties, i. e. spiking activity, phase of membrane potential oscillations, and the effect on the motor output of the corresponding hemiganglion (see chapter 1.2.1). Motor neurons were finally characterized by identifying intracellularly recorded action potentials on corresponding extracellular PS or RS recordings. In contrast to that, the non-spiking interneurons of the CPGs were only considered in this study if they matched the neurons' morphology and physiology [Smarandache-Wellmann et al., 2013]. Microelectrodes were pulled on a micropipette horizontal puller (P-1000, Sutter Instruments, Novato, CA, USA) from fire polished borosilicate glass capillaries (outer / inner diameter: 1 mm / 0.5 mm) and filled with 1 % dextran Texas Red (dTR; Invitrogen, Carlsbad, CA, USA) or 1 % dextran Fluorescein (FITC, Life Technologies, CA, USA) in 1 M KAc + 0.1 M KCl, resulting in tip resistances of 30 - 60 MΩ. To identify intracellular recorded neurons by their morphology, I iontophoretically stained the neurons with dTR or FITC by applying trains of rectangular pulses (1 nA, 500 ms, 1 Hz) for at least 15 minutes and kept the preparations overnight at 7° C to allow dye diffusion.

The extracellularly recordings were amplified (1000 x) and filtered (300 - 2000 Hz) using an

extracellular amplifier (Model 102, Electronic Lab). Intracellular signals were amplified (10 x) using a SEC 05X amplifier (npi Electronics Instruments, Tamm, Germany). All recordings were digitized by an A / D converter (Digidata 1440A, Molecular Devices or Micro1401 mkII, Cambridge Electronic Design) with a sampling frequency of 10 kHz, recorded on a computer (Dell, Round Rock, TX, USA) with Spike2 or pClamp software and saved for later analysis.

2.2.3 Drug application

If a stable expression of rhythmic motor output was required within an experiment, I used the cholinergic agonist carbachol (CCh, 1 - 5 µM) to activate an initially inactive preparation. CCh acts on both muscarinic and nicotinic acetylcholine receptors and elicits fictive locomotion of the swimmeret system [Braun and Mulloney, 1993]. For each preparation I gradually increased the CCh concentration until stable fictive locomotion was elicited, predominantly at 1 - 2 µM CCh. However, if the preparation was spontaneously active the experiment was performed in CS. In some experiments, I applied octopamine (OA, 1 - 100 µM, Alfa Aesar, Ward Hill, MA, USA), proctolin (PR, 1 µM, Alfa Aesar) and epinastine (10 µM, Sigma-Aldrich) to either test their effect on the spontaneous or CCh-induced rhythmic motor output directly, or to test if these substances are affecting the observed stimulation effects.

Drug solutions with the desired concentration were always prepared just prior to the experimental usage by diluting the stock solution in CS. Stock solutions of CCh (6 mM in CS) were stored in a freezer at - 20° C. Stock solutions of PR (147 µM) and Epinastine (10 mM) were prepared in aqua destillata (aq. dest) and stored in a fridge at 7° C. Due to the photoinstability of dissolved OA, it was kept as a solid at room temperature. Stock solutions of OA (20 mM in purified water) were stored in a fridge at 7° C and used not longer than five days.

In order to apply drugs to the entire abdominal nervous system, I used a custom-built, gravitational perfusion system and replaced the bathing solution with the drug solution. At least 50 mL were washed in to ensure that the desired drug concentration was reached. In addition, I used a pressure ejection system (PDES-2DX, npi Electronics Instruments) to focally apply drugs to the lateral neuropil of individual hemiganglia. Focal application was achieved using suction electrodes (see chapter 2.2.1) with fine tip diameters as an application electrode. I filled the application electrode with the drug solution by applying negative pressure, carefully inserted the tip of the electrode into the neuronal tissue, and applied the drug solution by giving single pulses of positive pressure (1 ms, 0.7 psi). For focal application experiments, Fast Green FCF (Sigma-Aldrich) was added to visualize the extent of application (Figure 2.1 D).

2.3 Histological methods

2.3.1 Backfills of axon bundles

To identify the location of axons that were successfully stimulated or recorded, I performed backfills of the respective axon bundles. Therefore, I cut the nerve bundles at a maximal distal level, isolated the cut ends using petroleum jelly and briefly pre-incubated them in distilled water. Afterwards, I incubated the cut ends in dextran tetramethylrhodamine (TRDA, 1 % in aq. dest., Life Technologies, CA, USA) or FITC (1 % in aq. dest.) for 48 - 96 h at 8°C. After fixation (see chapter 2.3.2), I removed the desired portions of the connectives, e.g. cA2/A3 or cA4/A5, and embedded tissue samples in agar-agar (4 % in 1 M PBS, Merck, Darmstadt, Germany). I prepared transversal cross sections (50 - 100 μM) using a vibratome (Leica VT1200 S, Leica Biosystems, Wetzlar, Germany) and transferred the sections to microscope slides for picture acquisition.

2.3.2 Histological development

In the following I describe the standardized histological development of abdominal ganglia with intracellular stained neurons (Chapter 2.2.2) or backfilled axon bundles (Chapter 2.3.1). If not mentioned differently, all steps were performed at room temperature (22 °C). The protocol for antibody staining is separately described (Chapter 2.3.3). Due to the usage of photosensitive fluorescent dyes in this study, I performed all steps with a maximum protection from light.

After removal of the dyes, I washed the preparations three times with cold CS and fixed them in paraformaldehyde (PFA, 4 % in PBS, Serva, Heidelberg, Germany) at 4°C overnight or at room temperature for 2 hours on a shaker. Preparations were then washed in PBS (1 M), dehydrated in an ascending ethanol series (50 %, 70 %, 90 %, 100 %, 10 minutes each), transferred to a Permanox® Petri dish and cleared in methyl salicylate (Carl Roth, Karlsruhe, Germany) for picture acquisition.

2.3.3 Antibody staining

In order to investigate the distribution of proctolin (PR) within the abdominal nervous system, I performed immunohistochemical stainings using primary antibodies against PR (anti-Proctolin, raised in rabbit, Jena Bioscience, Jena, Germany). After fixation (see chapter 2.3.2), I preincubated selected preparations in PBST-NGS (1 M PBS; + 1 % Triton-X-100, Fluka Chemie AG,

Buchs, Switzerland; + 5 % normal goat serum, Vector Laboratories, Burlingame, CA, USA; + 0.1 % sodium azide, Sigma-Aldrich) for 2 h. Afterwards, I applied the primary antibody (1 : 1000) and incubated at 4 °C (2 x, 24 h each). After the preparations were washed in PBST-NGS (6 x, 1 h each), I applied the secondary antibody (1 : 200, donkey anti-rabbit conjugated to Alexa Fluor 488, Abcam plc, Cambridge, UK) and incubated again at 4 °C (2 x, 24 h each). Before picture acquisition, preparations were washed in PBS (3 x, 1 h each), dehydrated in an ascending ethanol series (50 %, 70 %, 90 %, 100 %, 10 minutes each) and cleared in methyl salicylate. In addition to taking pictures as whole mounts of abdominal ganglia, I also prepared transversal cross sections of the connectives (see chapter 2.3.1).

2.3.4 Picture acquisition

Pictures were acquired using a fluorescence microscope (BX61, Olympus, Hamburg, Germany) or stereomicroscope (MVX10, Olympus). I took pictures of transversal cross sections of the connectives within one plane. Whole mounts of abdominal ganglia were either pictured in one plane or scanned as z-stacks (5 - 20 µm). Further processing was performed using ImageJ (National Institutes of Health, USA), Adobe Photoshop (CS5, Adobe, San José, CA) and CorelDRAW (X6, Corel, Ottawa, ON, Canada). Afterwards ganglia were rehydrated to 70 % Ethanol and stored in a freezer at - 20 °C.

2.4 Analysis

I removed stimulus artifacts caused by electrical stimulation using the "ArtRem6" script for Spike2 (by Cambridge Electronic Design, www.ced.co.uk). If the stimulus signal was not recorded, I manually defined the stimulus artifacts within the extracellular recordings. If the stimulus signal was available for a given experiment, stimuli were defined by this. In both cases, an appropriate time range for each stimulus was cut out of the data [3 to 5 ms]. The gaps were filled with a straight line to ensure further data analysis. Afterwards, I analyzed the rhythm using the "Crab-Analyzer" script (by Mark Beenhakker and Wolfgang Stein, www.neurobiologie.de) to calculate the burst on- and off-sets, period, burst durations, phases and duty cycles of the rhythm for each PS recording.
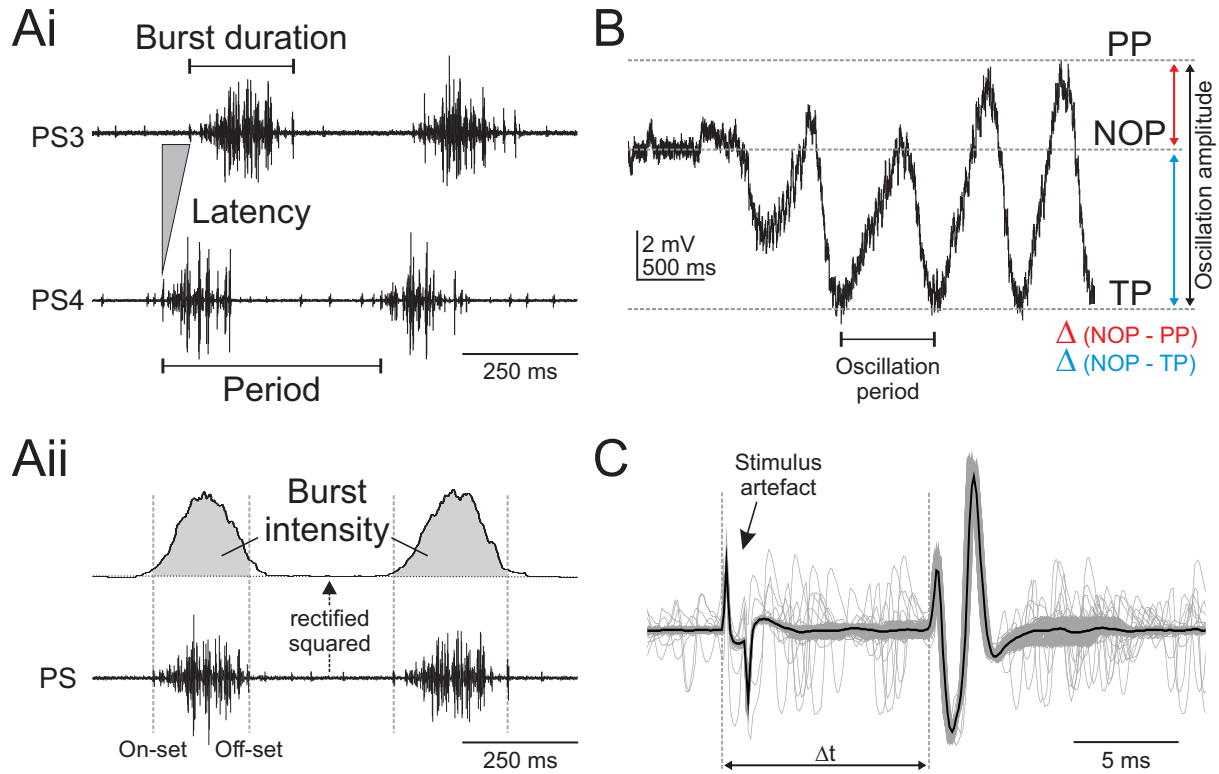
2.4.1 Parameters of the swimmeret rhythm

If fictive locomotion occurs spontaneously or is evoked by bath application of CCh [Braun and Mulloney, 1993] or PR [Mulloney et al., 1987; Acevedo et al., 1994], the two hemiganglia in each abdominal segment are simultaneously active (see chapter 1.2). Therefore, analyzing the parameters of the rhythm is sufficient for one side of the swimmeret system. However, for fictive locomotion evoked by unilateral stimulation of descending input, the parameters refer to PS activity recorded ipsilateral to the stimulation if not mentioned differently.

An overview about the analyzed parameter is shown in figure 2.2 Ai. On- and off-set are the beginning and the end of a single burst, respectively. The period, meaning the time span of one complete cycle, is defined by the time interval between the on-set of a PS burst and the on-set of a consecutive PS burst. The period was calculated using the most posterior recorded PS. The burst duration is the time from the on-set to the off-set of each burst. The phase of one PS burst describes the percentage time points within the cycle at which the corresponding burst begins. The on-set of the PS burst in A5 is the reference for calculating the phases of the more anterior PS bursts. Phases are calculated by dividing the latency of a PS burst on-set by the period. As the phase reflects the percentage of the period at which a particular PS burst occurs within the whole cycle, the duty cycle shows how much percent of a period is captured by the activity of a PS burst. It is calculated by dividing the burst duration by the period.

The strengths of individual PS bursts were analyzed by calculating the integral under a digital filtered PS recording as described by Mulloney [2005]. Baseline drifts were removed (DC removal) and the voltages were squared (rectification). Afterwards the recordings were smoothed

to ensure proper measurement of the underlying integral (Figure 2.2 Aii). The calculated integrals were divided by the respective burst duration and normalized to the mean within one experiment.

Figure 2.2: Analysis of physiological properties. **Ai:** Power stroke (PS) activity in ganglia A3 and A4 illustrating the parameters of the swimmeret rhythm. The phase of a PS burst is calculated by dividing the respective latency by the period. **Aii:** Calculation of burst intensity. Upper trace shows the rectified and smoothed voltages of the PS recording in the lower trace. **B:** Analyzed parameters of intracellular recordings. Peak and trough potential are defined during V_m oscillations and non-oscillating potential at a stable V_m. **C:** Example of an hook recording at the level of cA5/A6, illustrating a stimulus-correlated activity with the latency Δt. **PS3-4** *power stroke in abdominal ganglia A3 and A4*, **PP** *peak potential*, **TP** *trough potential*, **NOP** *non-oscillating potential*.

2.4.2 Intracellular recordings

I analyzed the activity of individual neurons by calculating the peak potential (PP), the trough potential (TP), the amplitude, and the period of membrane potential (V_m) oscillations. The PP and TP are the most depolarized and hyperpolarized states during V_m oscillations, respectively. However, please note that for spiking neurons I did not consider the deflections of action potentials for calculation of the PP. The amplitude of V_m oscillations is the difference between the PP and the TP, and the period of V_m oscillations is the time between two consecutive TPs. If the recorded neuron did not show any oscillations of V_m at specific times of the experimental procedure, e.g. during termination of the swimmeret rhythm by electrical stimulation, I defined

the stable V_m as the non-oscillating potential (NOP). I further used the NOP to analyze the shifts in V_m during activity transition of the swimmeret system, by calculating the differences between the NOP and the PP (Δ PP - NOP) and TP (Δ TP - NOP), respectively (Figure 2.2 B).

2.4.3 Hook electrode recordings

I performed multisweeps of extracellular hook electrode recordings triggered to individual stimulation pulses and calculated the latencies of stimulus-correlated activities (Figure 2.2 C). The time points of the stimulation pulses were either given by the recorded stimulus signal or defined manually. I defined distinct triphasic activity as the activity of a single unit. Activity with four or more phases indicated the overlap of the activity of more than one unit. To compare units across different experiments, I calculated the conduction velocity by dividing the distance between the stimulation and hook electrodes by the latency. The distance between both electrodes was either measured or calculated using the animal's body length (see appendix, Figure 5.1).

2.4.4 Statistics and data presentation

I calculated the parameters of fictive locomotion by analyzing eleven consecutive cycles of PS activity for each condition within a single experiment (n = 11). For individual neurons, I analyzed ten consecutive V_m oscillations (n = 10). For all datasets, the median (mdn) and the interquartile range (iqr, Q1 - Q3) are presented if not mentioned differently. *N* gives the number of experiments. I used nonparametric statistical tests for both unpaired (Wilcoxon rank-sum test) and paired data sets (Wilcoxon signed rank test, N $\geq$ 5) with a significance level of P $\leq$ 0.05. For datasets including more than two conditions I corrected the significance level by Bonferroni (P = 0.05 divided by the number of paired conditions). Datasets were obtained in Spike2 and further processed in Microsoft Office Excel 2007 (Microsoft, Redmond, WA, USA). Statistical testing and preparation of diagrams was performed in OriginPro (v8, OriginLab Corporation, Northampton, MA, USA). Figures were finally prepared in CorelDRAW.

3 Results

3.1 Stimulation of descending command neurons

The general aim of this thesis was to investigate the effect of descending command neurons on the swimmeret system (see chapter 1.3). On the one hand, my experimental approach, as well as the limited knowledge regarding the exact locations of the axons of these neurons, did not allow to precisely and exclusively stimulate individual command neurons. On the other hand, the approximate axon locations within the abdominal connectives (described by Wiersma and Ikeda [1964] and Acevedo et al. [1994]) offered the possibility to stimulate separated axon bundles, potentially containing the axons of individual command neurons. In order to verify the stimulation of command neurons in my experiments, I histologically examined the stimulation sites and compared them to previously described locations (Chapter 3.1.1). In addition, I controlled for the propagation of stimulus-evoked activity within the entire swimmeret system by performing extracellular recordings at the most posterior level, i.e. between abdominal ganglia A5 and A6. Afterwards, I used histological methods to identify the axon locations of specifically activated neurons and revealed similar locations as described for command neurons (Chapter 3.1.2).

3.1.1 Histological identification of stimulated axons

To histological identify the location of stimulated axons, I made backfills of the stimulated axon bundles and prepared cross sections of the abdominal connectives between the second and third abdominal ganglia (cA2/A3, Figure 3.1). For this thesis, I only stimulated axon bundles in the lateral part of one hemiconnective, including areas 81 and 85. Within each experiment all labeled axons, i.e. the stimulation sites, were restricted to these areas (Figure 3.1 Ai). Due to the fact that I stimulated anterior to A1 and prepared the cross sections anterior to A2, this indicates that the locations of the stimulated axons remain constant in between different ganglia. In order to further compare the stimulation sites across experiments they were transferred to a

standardized map derived from Wiersma and Hughes [1961], using the medial and lateral giant fibers as well as the midline as landmarks. The overall location of stimulation sites referring to either termination (Figure 3.1 Aii), initiation (Figure 3.1 B), or enhancement (Figure 3.1 C) of fictive locomotion were overlapping. Please note, that some stimulations resulted in both initiation and enhancement and are presented for both conditions (see chapter 3.2). Generally, the stimulation sites indicate that I stimulated previously described command neurons of the swimmeret system. On the one hand, stimulation of two excitatory (E_D, E_E) and one inhibitory (I_E) command neuron can be excluded since their axons are located in the medial portion of the hemiconnectives. On the other hand, I potentially stimulated three excitatory (E_A, E_B, E_C) and two inhibitory (I_A, I_C) command neurons. Due to the size of the stimulation sites, simultaneous activation of two command neurons can not be ruled out. In addition, even within single experiments differentiation between the lateral command neurons was limited and I observed similar stimulation effects independent of slightly varying stimulation sites. Therefore, I do not further distinguish between stimulation of E_A, E_B and E_C, or I_A and I_C, respectively.

In addition to cross sections of the connectives, I prepared whole mounts of the abdominal chain of ganglia. Due to passive diffusion of the dye and the length of the abdominal nervous system (approx. 30 mm), labeled axons were mostly restricted to ganglia A2 and A3. I did not observe any differences in the projection patterns regarding either termination, initiation, or enhancement of fictive locomotion (data not shown). In two individual preparations axons were labeled until the most posterior ganglion A6 (Figure 3.2). In both preparations, axonal projections were restricted to the lateral side and intense ramification was present in all ganglia. Whereas in figure 3.2 A ramification is mostly restricted to the hemiganglia ipsilateral to the stimulation site, the projection pattern in figure 3.2 B reveals additional ramification in the contralateral hemiganglia of A2 and A3. Somata were labeled in A2 and A3 (Figure 3.2 A), and A2 to A4 (Figure 3.2 B). Occasionally, a group of neurons in A2 or A3 showed intense labeling. Their somata were located ventrally at the midline and they showed similar projection patterns within both hemiganglia (Figure 3.2 B, ganglion A2). Interestingly, these neurons showed additional anterior directed projections in the lateral portion of the contralateral hemiconnective and intense ramification in A1 (Figure 3.2 B, ganglion A1). Projections continued in anterior direction and surpassed A1. Please note, that the stimulated axon bundles were always labeled in posterior direction only. Consequently, ipsilateral labeling within ganglion A1 and the connectives anterior to A2 may derived from non-axonal dye diffusion within the connective tissue or from axons that were not comprised in the stimulated bundle.
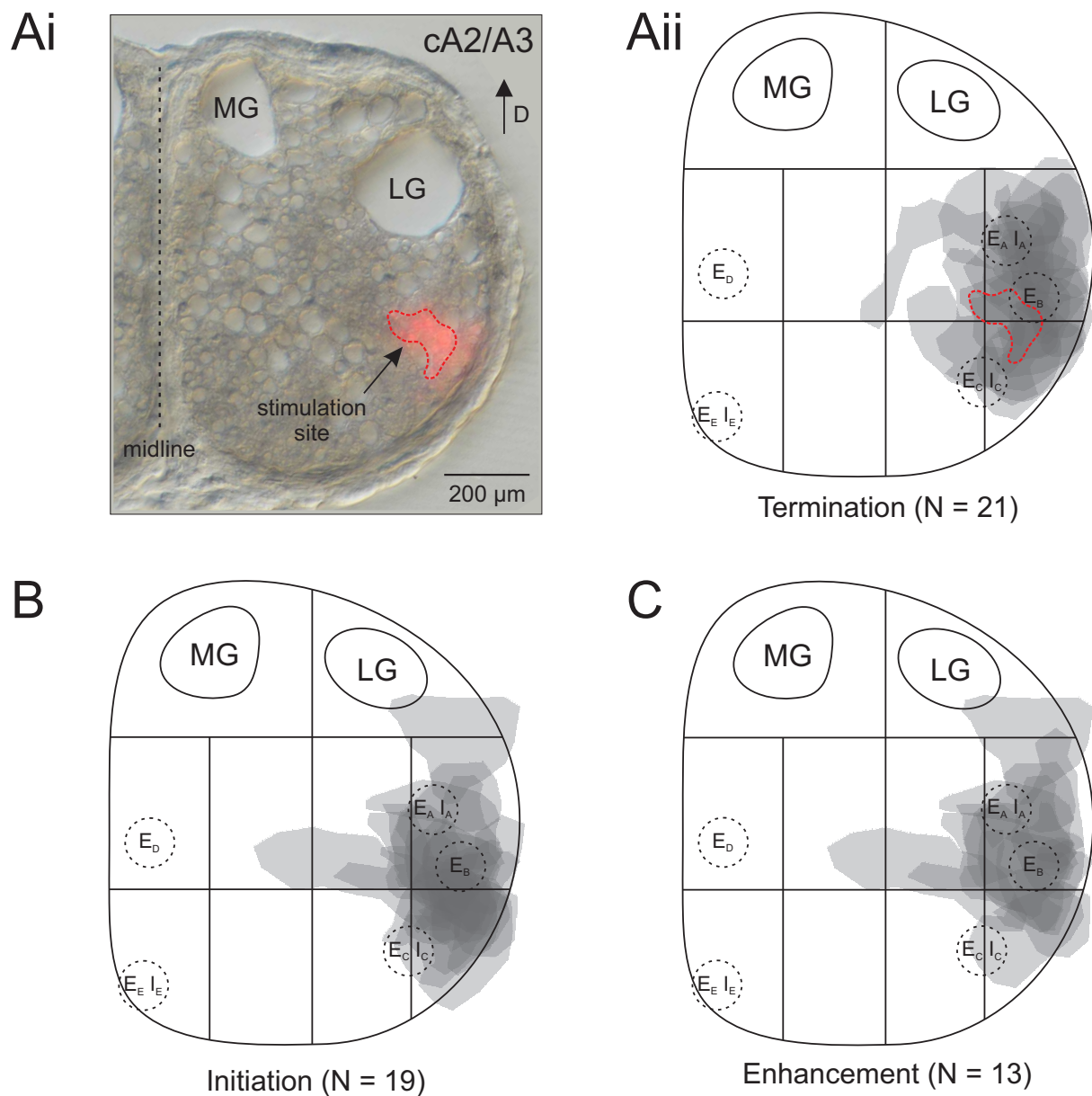
Figure 3.1: Histological identification of stimulation sites. **A:** Individual stimulation sites were identified and compared with previously described axon locations of command neurons introduced by Wiersma and Ikeda [1964] and Acevedo et al. [1994] (dashed circles). **Ai:** Cross section of a connective between ganglia A2 and A3. The stimulated axon bundle was stained to identify the axon locations (stimulation site) within its hemiconnective. **Aii:** Stimulation sites of stimulations terminating fictive locomotion of the swimmeret system. The stimulation site from (**Ai**) is indicated by the red, dashed line. Individual stimulation sites were pooled using a standardized map [Wiersma and Hughes, 1961]. **B:** Stimulation sites of stimulations initiating fictive locomotion. **C:** Stimulation sites of stimulations enhancing fictive locomotion. **cA2/A3** *connective between ganglia A2 and A3*, **MG** *medial giant fiber*, **LG** *lateral giant fiber*, **E$_X$** *excitatory command neuron*, **I$_X$** *inhibitory command neuron*.
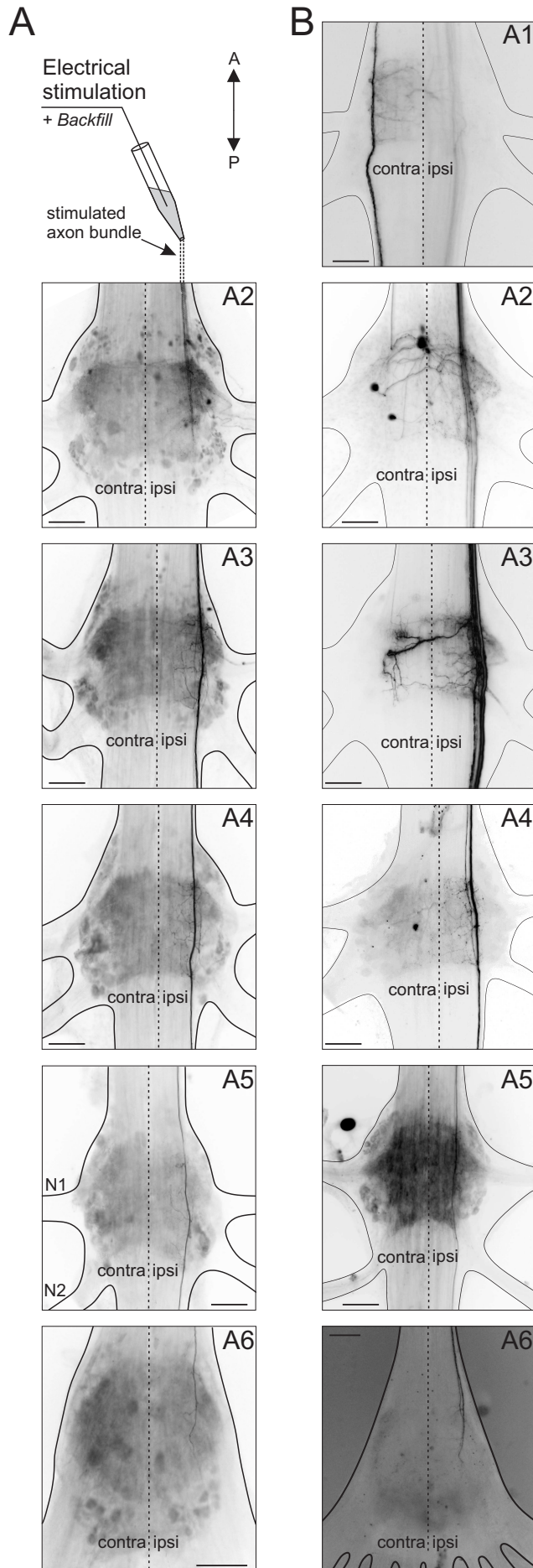
Figure 3.2: Stimulated axons project throughout the entire abdominal nervous system. Whole mounts of abdominal ganglia A1 to A6. Dorsal view. **A:** Backfill of a stimulated axon bundle anterior to A1, revealing the projection pattern within the abdominal ganglia. Projection was mostly restricted to hemiganglia ipsilateral to the stimulation site and one axon showed projection throughout the entire chain of ganglia. Somata and weak contralateral projections are visible in A2 and A3. **B:** The projection pattern of another backfill anterior to A1, indicating additional intense axon ramification in hemiganglia A2 and A3 contralateral to the stimulation site. Furthermore, labeled axons show contralateral projections in anterior direction in ganglia A2 and A3. Please note, that the stimulated axon bundle was labeled in posterior direction between A1 and A2 which is depicted in (**A**). A1 shows intense axon projections and ramifications contralateral to the stimulation site. Somata were labeled in A2 to A4. **A1-A6** *abdominal ganglia*, **N1** *first nerve*, **N2** *second nerve*.

3.1.2 Stimulations recruited distinct units

The stimulation method I used in this thesis comes along with the drawback of an unspecific stimulation of axons that might not project throughout the entire swimmeret system while still affecting its activity. To avoid this, I also recorded extracellularly from separated axon bundles at the most caudal level of the abdominal nerve cord, i.e. cA5/A6 (Chapter 3.1.1). By this, I was able to check if the stimulation evoked correlated activity of descending neurons that project their axons along all abdominal ganglia.

I recorded stimulus correlated activity during stimulations terminating, as well as stimulations initiating fictive locomotion of the swimmeret system, indicating the recruitment of descending neurons (Figure 3.3). I defined distinct triphasic activity as one unit and activities with four or more phases as an overlap of multiple units. Predominantly either one (Figure 3.3 Ai) or two distinct units (Figure 3.3 Aii) were recruited. If the activity of two units overlapped, I regarded this as only one unit being recruited. (Figure 3.3 Aiii). During both experimental conditions, i.e. inhibitory (termination) and excitatory (initiation or enhancement), either one or two neurons were recruited during the stimulations. Therefore, I compared the conduction velocities for both conditions independent of the number of units. Please note, that units that were recruited during enhancement are included in the dataset for initiation. These units were all recorded during stimulations that could both initiate and enhance fictive locomotion. The conduction velocities were faster (Wilcoxon rank-sum test, P = 0.026) for units recruited during termination (mdn = 2.60 m / s, iqr = 1.90 - 3.23 m / s, N = 27) than during initiation (mdn = 1.74 m / s, iqr = 1.24 - 2.57 m / s, N = 32) (Figure 3.3 B).
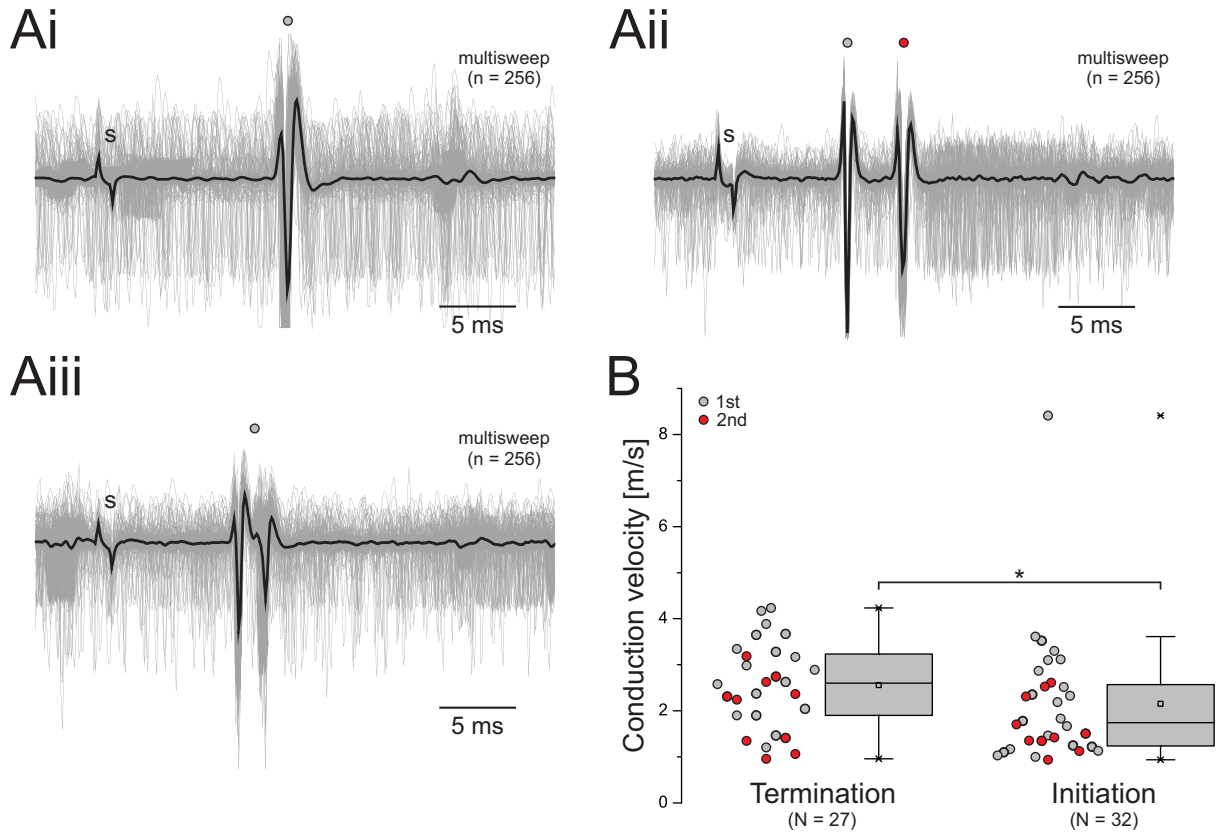
Figure 3.3: Stimulus correlated activity recorded at the most caudal level of the abdominal nervous system. **A:** Stimulus-triggered overdraws of extracellular recordings at the level of cA5/A6 revealed distinct neuronal activity that correlated with individual stimulation pulses (s). Figures show peri-stimulus overlays (n = 256) with averages depicted in black. If one (**Ai**) or two (**Aii**) distinguishable activity events were recorded they were regarded as two distinct units. If the activity of multiple units overlapped (**Aiii**), they were regarded as one. **B:** Conduction velocities of stimulus correlated activity during termination (mdn = 2.60, iqr = 1.90 - 3.23) and initiation (mdn = 1.74, iqr = 1.24 - 2.57) of fictive locomotion. Units recorded during termination showed faster conduction velocities then units recorded during initiation (Wilcoxon rank-sum test, P = 0.026). Grey and red data points indicate faster and slower units recorded in the same experiment, respectively. **cA5/A6** *connective between abdominal ganglia A5 and A6*.

Table 3.1: Conduction velocities of stimulus correlated activities recorded during termination or initiation of fictive locomotion. Data refers to figure 3.3. Conduction velocities were slower for neurons active during initiation of fictive locomotion (Wilcoxon rank-sum test).

[m/s]	N	mean ± SD	range	Q1	median	Q3	P
Termination	27	2.56 ± 0.94	0.96 - 4.24	1.90	2.60	3.23	**0.026**
Initiation	32	2.15 ± 1.40	0.94 - 8.41	1.24	1.74	2.57	

The conduction velocity of an action potential correlates with the diameter of the axon whereby larger axons enable faster conduction. This indicated that units recruited during terminations had larger axon diameters and can be recruited at lower stimulation amplitudes than units that were excited during initiation. The stimulation amplitudes were highly variable and provided no evidence for lower activation thresholds of inhibitory units. In two experiments, however, lower stimulation amplitudes terminated fictive locomotion while increased amplitudes evoked excitatory stimulation effects, i.e. enhancement. One of these experiments is presented in figure 3.4 and the stimulation initially terminated fictive locomotion (Figure 3.4 Ai). Rhythmic PS activity ceased and a subset of PS neurons, most likely PS inhibitory motor neurons, became tonically active. I recorded one unit recruited during the stimulation (Figure 3.4 Aii).
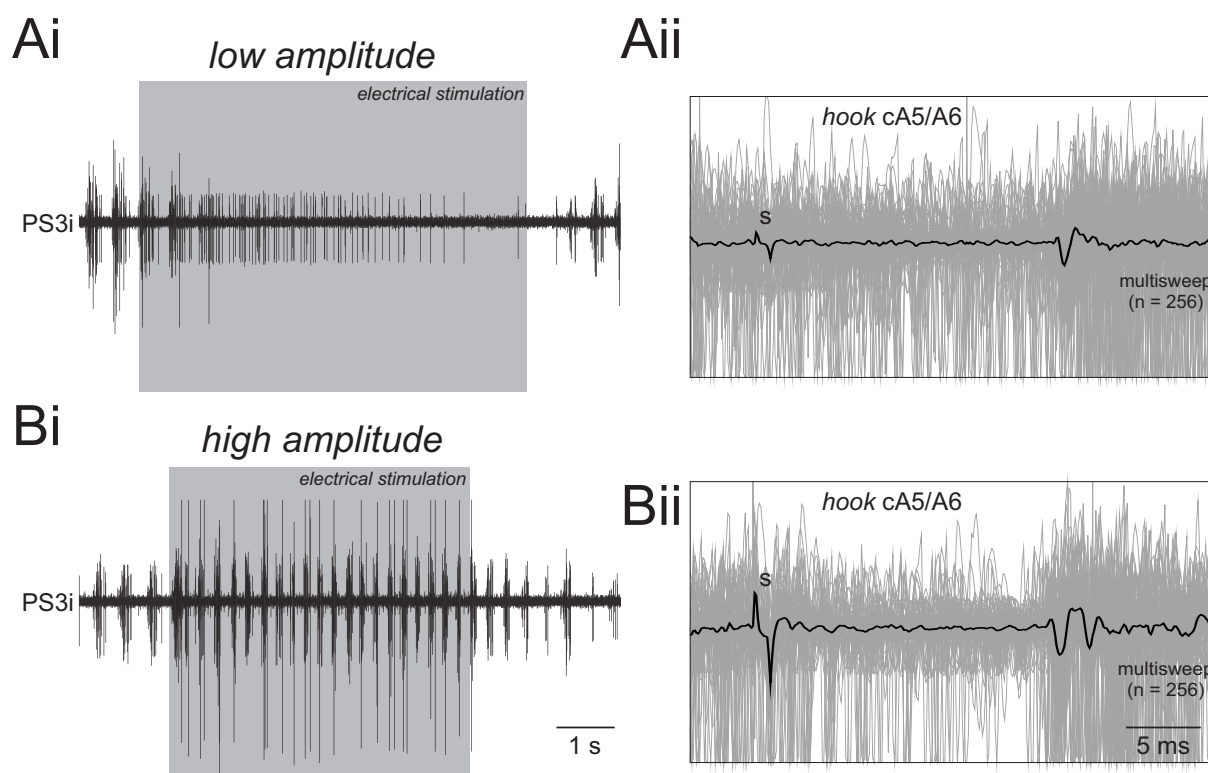
Figure 3.4: In one experiment, different stimulus amplitudes had opposing effects on PS activity. Extracellular recordings of PS in ganglia A3 (**Ai**, **Bi**) and stimulus-triggered overdraws (n = 256, averages depicted in black) of extracellular recordings at cA5/A6 (**Aii**, **Bii**). Stimulations are temporally depicted in gray. **A:** Stimulation terminated PS bursts in A3 and evoked stimulus-correlated activity of one descending neuron. Tonic discharge during stimulation most likely reflects the activity of PS inhibitor motor neurons. **B:** At a higher stimulation amplitude, the same stimulation enhanced PS3 and recruited an additional descending neuron. Please note, that the activities of both neurons overlapped. During stimulation, the period of PS3 decreased and additional, larger motor neurons discharged. **PS3i** *ipsilateral power stroke in ganglia A3*, **cA5**/**A6** *connective between abdominal ganglia A5 and A6.*

Later in the experiment, I increased the stimulation amplitude and observed enhancement of spontaneously expressed fictive locomotion (Figure 3.4 Bi). This enhancement was reflected by decreased periods (Pre-Stim: mdn = 0.41 s, iqr = 0.39 - 0.43 s; Stim: mdn = 0.23 s, iqr = 0.22 -

0.25 s; Wilcoxon signed rank test, P = 0.002) and increased burst strengths (normalized to Pre-Stim; Stim: mdn = 1.36, iqr = 1.24 - 1.45; Wilcoxon signed rank test, P = 0.002). During enhancement, one additional unit was recruited (Figure 3.4 Bii). Please note, that the conduction velocities of both neurons were similar and resulted in overlapping activities on the extracellular recordings. However, the opposite stimulation effects at different stimulation amplitudes indicate recruitment of two descending neurons and earlier recruitment of the neuron providing inhibitory input.

I also performed backfills of the extracellularly recorded axon bundles at the level of cA5/A6. Cross sections of the connective at the level of cA3/A4 not only revealed dye co-localization within the respective hemiconnective, but also double labeling of individual axons (Figure 3.5). I found double labeled axons in eight preparations both for terminating (N = 4) and initiating (N = 4) stimulations (Figure 3.5 Aii, Bii). Qualitatively, axon diameters for terminating stimulations were more diverse than for initiating stimulations. Please note, that several axons with comparably larger diameters were present for terminating stimulations, which is consistent with faster conduction velocities recorded for these neurons. However, tissue deformations during histological development and cross sectioning prevented detailed investigation of the double labeled axons, e.g. axon diameters. Therefore, I did not further address potential differences. Within a single preparation, one to three axons were double labeled. Due to the fact, that I recorded the stimulus-correlated activity of one or two distinct units within the respective experiments, these results indicate that these neurons were recruited during stimulations and provide descending input on the swimmeret system. In addition, the locations of the axons within the hemiconnectives were in line with the location of previously described command neurons [Wiersma and Ikeda, 1964; Acevedo et al., 1994], suggesting stimulation of corresponding axons.
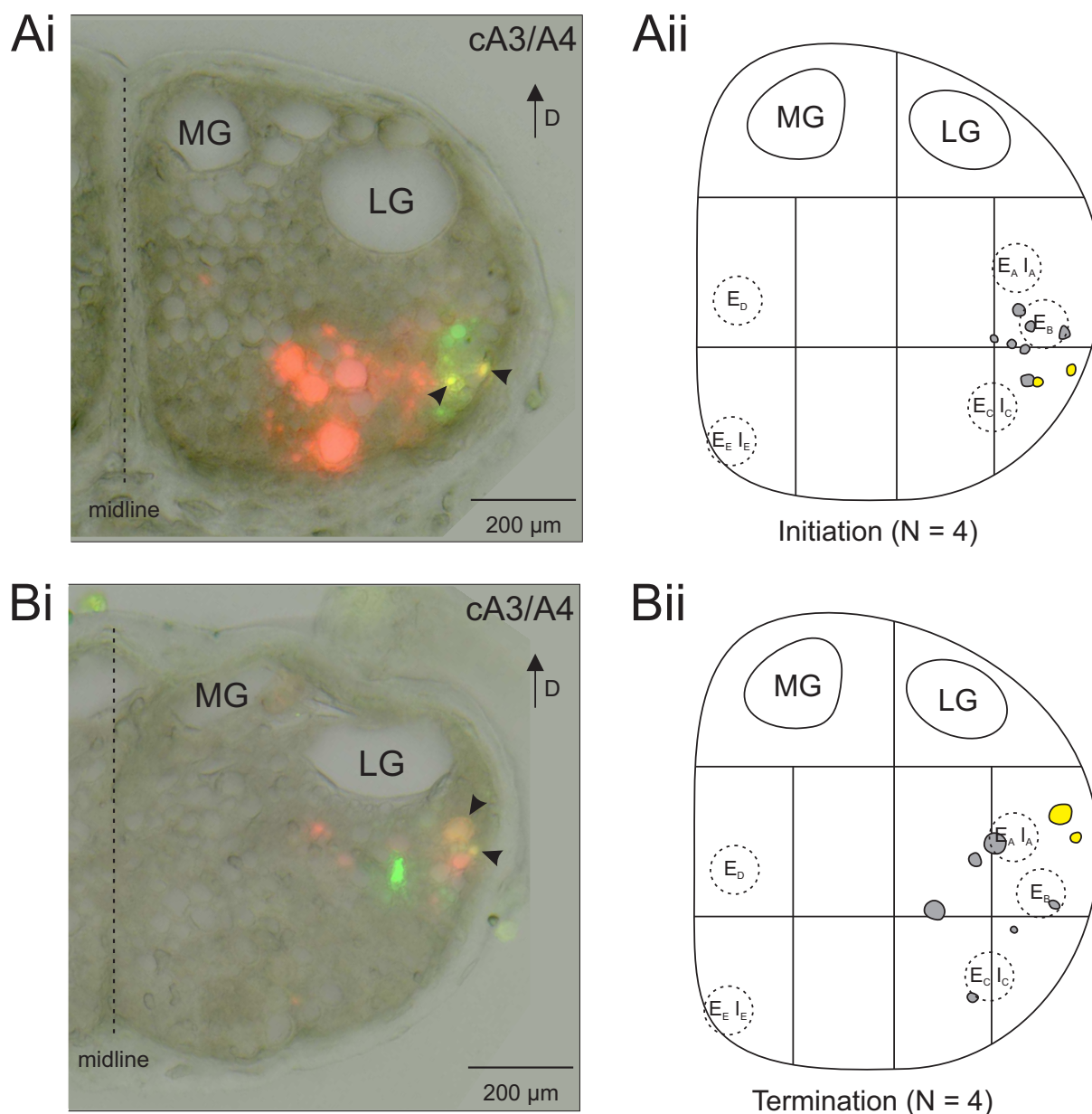
Figure 3.5: Double labeling of individual axons that showed stimulus-correlated activity. **Ai:** Cross section of one connective at the level of cA3/A4. Stimulation initiated fictive locomotion of the swimmeret system. Backfills of the stimulated (green, FITC) and recorded (red, TRDA) axon bundles revealed colocalization within the respective hemiconnective and double labeling of individual axons (arrow heads). **Aii:** Overview of double labeled axons from experiments where fictive locomotion was initiated. Axons from (**Ai**) are depicted in yellow. **Bi:** Backfills of the stimulated (FITC) and recorded (TRDA) axon bundles which terminated fictive locomotion. **Bii:** Overview of double labeled axons from experiments that terminated ficitve locomotion. Axons from (**Bi**) are depicted in yellow. **cA3/A4** *connective between ganglia A3 and A4*, **MG** *medial giant fiber*, **LG** *lateral giant fiber*, **E$_X$** *excitatory command neuron*, **I$_X$** *inhibitory command neuron*.

3.2 Stimulation effects on the swimmeret system

Electrical stimulations of separated axon bundles within the abdominal connectives were previously described to affect the motor output of the swimmeret system in terms of termination and initiation [Wiersma and Ikeda, 1964; Mulloney et al., 1987; Acevedo et al., 1994]. For my thesis, I focused on stimulating axons located in the lateral proportion of the connectives and evidence are given that descending command neurons were activated by these stimulations (Chapter 3.1). Please note, that stimulations without any consistent effect on the motor output are not comprised within this thesis. This includes stimulations that did not affect the motor output at all, had inconsistent effects on individual hemiganglia, or stimulations that evoked arrhythmic motor output of the swimmeret system, e.g. tonic activity of power stroke (PS) motor neurons. Therefore, the data presented here only reflects stimulations that terminated (Chapter 3.2.1), initiated (Chapter 3.2.2) or enhanced (Chapter 3.2.3) fictive locomotion of the swimmeret system. Generally, the stimulation sites of my experiments are in line with the locations of three excitatory (E_A, E_B, E_C) and two inhibitory (I_A, I_C) command neurons. I observed similar stimulation effects independent of the stimulation site and did not distinguish further between different inhibitory or excitatory command neurons. I already demonstrated that the projections of stimulated axons is predominantly restricted to ipsilateral hemiganglia and that individual axons project throughout the entire abdominal nervous system. Therefore, I generally analyzed PS activity expressed in ipsilateral hemiganglia and pooled data of different segments. However, I also investigated bilateral differences during enhancement (Chapter 3.2.4). In addition, I performed stimulations at different levels of the nervous system and describe the observed effects on the swimmeret and the walking system (Chapter 3.2.5).

3.2.1 Termination of fictive locomotion

The isolated swimmeret system can be spontaneously active, i.e. expressing coordinated cycles of PS activity. This fictive locomotion can also spontaneously terminate and restart without any external manipulation. I defined termination of fictive locomotion as the absence of PS activity on extracellular recordings of the posterior branch of the first nerve root, reflecting the activity of PS excitatory motor neurons (PSE). In this thesis, I could reproduce this termination by electrical stimulations (N = 38). In the experiment presented in figure 3.6, PS activity in the most posterior ganglion A5 (PS5i) ceased first and the other ganglia followed this termination in anterior direction (figure 3.6 A). In other words, spontaneous termination occurred after completion of one cycle of fictive locomotion. Vice versa, the PS activity restarted in A5

first. Please note that in the example presented here, ganglia A3 and A4 seem to express PS activity before A5 is active. This is most likely due to differences between the recording quality in these ganglia and earlier active units may not be reflected in PS5i. However, besides the individual units present in PS3i and PS4i, the first burst of PS activity appeared in A5 and was followed by bursts in A4 and A3. This was consistent across all experiments in which spontaneous termination occurred. In the same experiment, I also recorded ipsilateral return stroke (RS) activity from A3 and A4. Small action potentials reflect the activity of RS inhibitory motor neurons (RSI) and large action potentials indicate RS excitatory motor neurons' (RSE) activity. RSIs were not active when the swimmeret system was silent but resumed to their characteristic phasic discharge pattern afterwards. Interestingly, RSEs were tonically active when the system was in a silent state but did not discharge when fictive locomotion restarted. However, the characteristic phasic discharge pattern recovered after several seconds (data not shown). Figure 3.6 B illustrates the location of the axon bundle stimulated in figure 3.6 C.

In contrast to spontaneous termination, PS activity ceased in ganglion A3 first and ganglia A4 and A5 expressed two or three consecutive PS bursts, respectively. The preparation further remained silent during proceeding stimulation, in other experiments lasting up to several minutes (data not shown). In addition to the described differences in the beginning of termination, the restart of fictive locomotion was also different to the spontaneous termination. PS activity appeared in ganglion A3 first and showed a constant bursting pattern. PS activity of ganglia A4 and A5 followed in posterior direction and initially appeared to be tonic. It merged into a constant bursting pattern, eventually resulting in cycles of PS bursts propagating from posterior to anterior (PS5i to PS3i). As for spontaneous termination, the described observations were consistent across different experiments. In parallel to spontaneous termination, RSIs were silent and RSEs tonically active during termination. In contrast to RSIs, RSEs did not resume to their characteristic discharge pattern when fictive locomotion restarted. Instead, RSEs remained silent for several seconds (recovery not shown).

During my experiments, I occasionally observed tonically active units on PS recordings during both, spontaneous (Figure 3.6 A, PS4i) and stimulus-induced termination (Figure 3.7). Most likely, these units were power stroke inhibitors (PSI). Their axons also project through the anterior branch of N1 and they were shown to be active in antiphase with PSEs. Since PSIs inhibit PS muscles, these observations suggest that PSIs are tonically activated during termination of fictive locomotion to inhibit PS muscle activity.
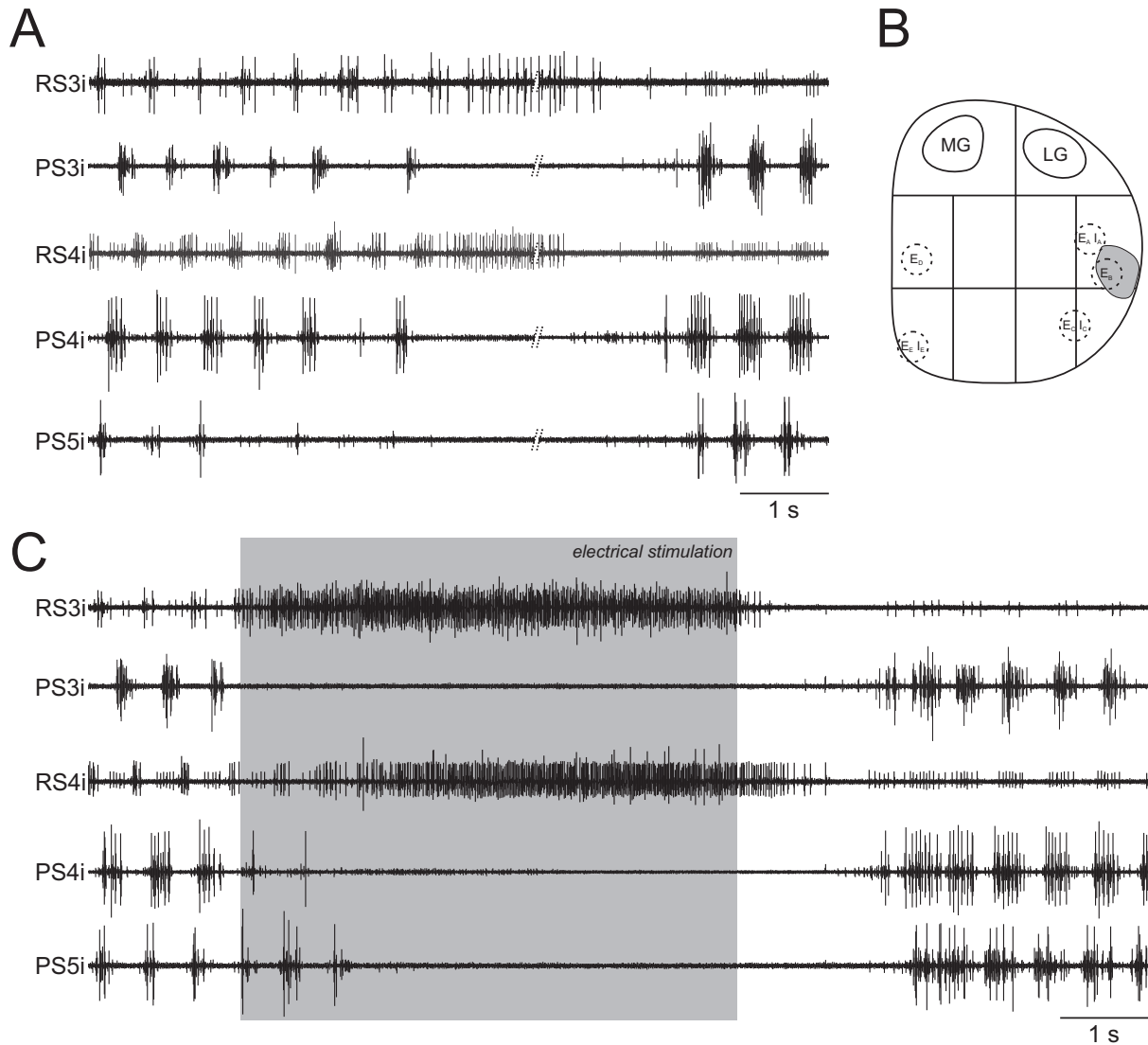
Figure 3.6: Terminating fictive locomotion of the swimmeret system. **A:** Fictive locomotion expressed by ganglia A3 to A5 spontaneously ceased. **B:** Schematic map of a hemiconnective, indicating the location of the stimulated axon bundle. **C:** Electrical stimulation of the axon bundle indicated in (**B**) terminated fictive locomotion to the same extent as spontaneous termination shown in (**A**). Please note that under both conditions, RS exciter motor neurons are tonically active during termination. Stimulation is depicted in gray. **RS3i-4i** *ipsilateral return stroke in ganglia A3 and A4*, **PS3i-5i** *ipsilateral power stroke in ganglia A3 - A5*, **cA2/A3** *connective between ganglia A2 and A3*, **MG** *medial giant fiber*, **LG** *lateral giant fiber*, **E$_X$** *excitatory command neuron*, **I$_X$** *inhibitory command neuron*.
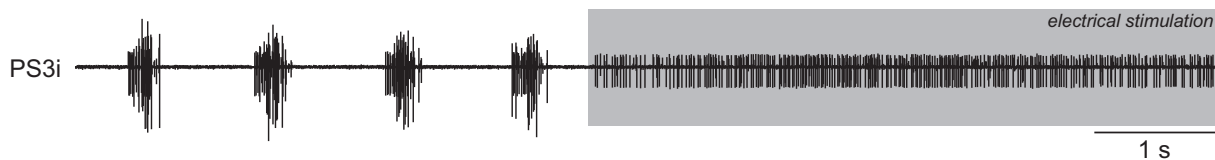
Figure 3.7: PS inhibitor motor neurons showed tonic activity during termination of fictive locomotion. Please note, that the activity PS excitatory motor neurons (larger units) was suppressed during termination. **PS3i** *ipsilateral power stroke in ganglion A3*.

3.2.2 Initiation of fictive locomotion

At a silent state of the swimmeret system, i.e. if no activity of PS motor neurons was recorded, fictive locomotion could be initiated by electrical stimulations. In this chapter I only include the data of experiments, in which a at least eleven consecutive cycles of PS activity were initiated (N = 22). In the experiment presented in figure 3.8, the preparation initially expressed coordinated PS activity (Figure 3.8 A). Severing of one individual axon bundle in the abdominal connective terminated PS activity (Figure 3.8 B, C). Afterwards, electrical stimulation of the severed bundle restored the initial PS activity. The initiated motor output had the same appearance as the spontaneous activity and was reflected by distinct PS bursts occurring in a metachronal wave within the abdominal chain of ganglia. The first PS burst was elicited in A5 and the other ganglia followed in anterior direction (Figure 3.8 D).
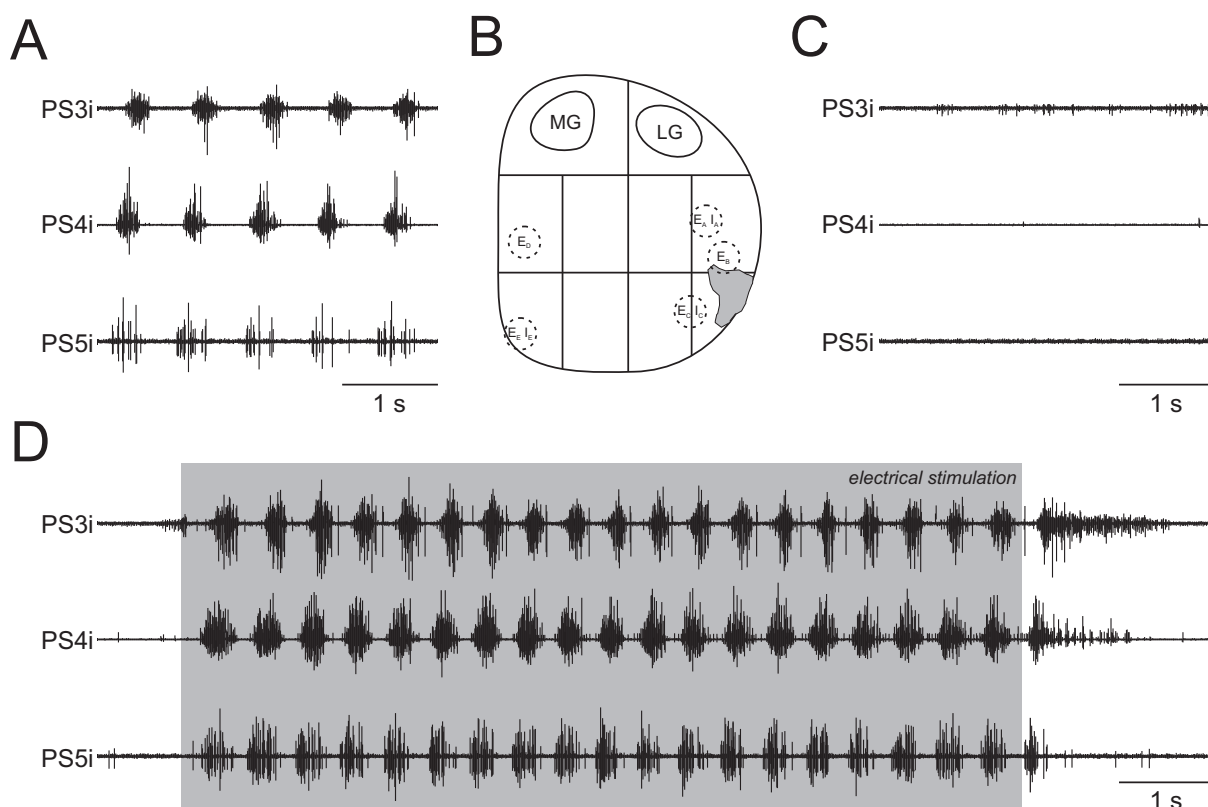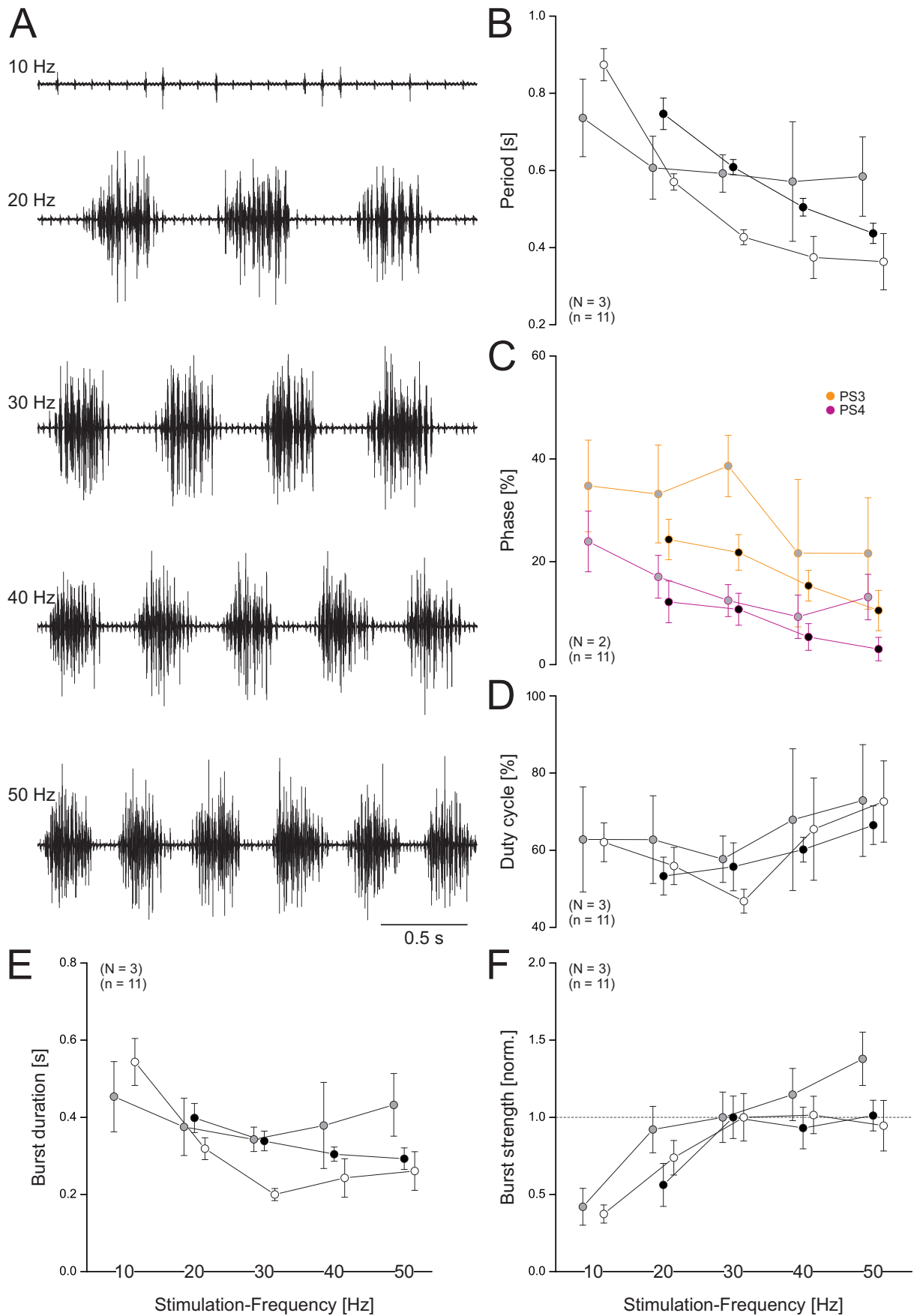

Figure 3.8: Initiation of fictive locomotion of the swimmeret system. **A:** Fictive locomotion spontaneously expressed by abdominal ganglia A3 to A5. **B:** Schematic map of a hemiconnective indicating the location of the stimulated axon bundle. **C:** Fictive locomotion ceased after severing the indicated axon bundle from (**B**). **D:** Electrical stimulation of the axon bundle shown in (**B**) initiated fictive locomotion of the swimmeret system. Stimulation is depicted in gray. **PS3i-5i** *ipsilateral power stroke in ganglia A3 to A5*, **cA2/A3** *connective between ganglia A2 and A3*, **MG** *medial giant fiber*, **LG** *lateral giant fiber*, **E$_X$** *excitatory command neuron*, **I$_X$** *inhibitory command neuron*.

In order to compare my experiments to previous descriptions of command neurons within the swimmeret system, I routinely stimulated at the same frequency as predominantly described in the literature (30 Hz, Wiersma and Ikeda [1964]; Acevedo et al. [1994]). In three experiments, I randomly tested a range of different frequencies (10 - 50 Hz) and observed varying stimulation effects regarding the initiation of fictive locomotion (Figure 3.9). Due to the small sampling size, I did not test the analyzed parameters for significance. Instead, all parameters of the experiments are presented in table 5.1 (appendix). Figure 3.9 A illustrates the PS activity of one representative PS (A3) in one of these experiments. Fictive locomotion was initiated at stimulation frequencies of 20 Hz and above. Please note that in the other experiments, stimulations with 10 Hz were sufficient for initiation. In all experiments, the period of fictive locomotion was highest at the lowest frequency and decreased with increasing frequency, independent of the initial period (Figure 3.9 B). I calculated the phases of PS3 and PS4 in two experiments where I also recorded PS5. Phase lags decreased with increasing frequency while the posterior-to-anterior progression of PS activity continued (Figure 3.9 C). Duty cycles were largest at high stimulation frequencies (40 and 50 Hz) while tending to be smallest at 30 Hz (Figure 3.9 D). Burst duration decreased with lower frequencies (10 - 30 Hz) and appeared to remain constant when the frequency further increased (30 - 50 Hz) (Figure 3.9 E). Burst strengths were normalized to the respective values at 30 Hz and were smaller at lower frequencies (10 - 20 Hz) (Figure 3.9 F). In parallel to the burst duration, burst strengths remained constant at higher frequencies (40 - 50 Hz) in two of three experiments. It is worth mentioning that standard deviations were comparably smallest at a stimulation frequency of 30 Hz, indicating the most stable pattern of fictive locomotion.

Figure 3.9: Fictive locomotion was expressed at different stimulation frequencies. **A:** PS activity of a representative PS (A3). Fictive locomotion was initiated at stimulation frequencies of 20 Hz and above. **B - F:** Analyzed parameters of three experiments (mean ± SD, n = 11). All parameters were influenced by the stimulation frequency and the standard deviations were comparably smallest at 30 Hz, indicating the most stable pattern of fictive locomotion. The complete dataset is given in table 5.1 (appendix). **PS3-4** *ipsilateral power stroke in ganglia A3 and A*4.

One of my aims in this thesis was to investigate if descending input, provided by previously described command neurons, reflects the potential source of spontaneous fictive locomotion in isolated preparations of the swimmeret system. Therefore, I compared the parameters of fictive locomotion that occurred spontaneously with fictive locomotion I initiated by electrical stimulations. I additionally compared the later condition to fictive locomotion elicited by bath application of carbachol (CCh). CCh acts on both muscarinic and nicotinic acetylcholine receptors and elicits fictive locomotion from previously silent preparations, suggesting a cholinergic pathway that excites the swimmeret system [Braun and Mulloney, 1993]. However, I mainly focus on the comparison of spontaneous and stimulus-induced fictive locomotion. The preparations in each experiment were initially silent. Fictive locomotion was then initiated by electrical stimulations and was recorded under at least one additional condition, i.e. elicited by CCh or expressed spontaneously. If possible, I tested all three conditions within a single experiment and the appearance of fictive locomotion revealed general similarities. Under all conditions, distinct bursts of PS activity were recorded from the abdominal ganglia and the metachronal wave of PS activity propagated from posterior to anterior segments (Figure 3.10).
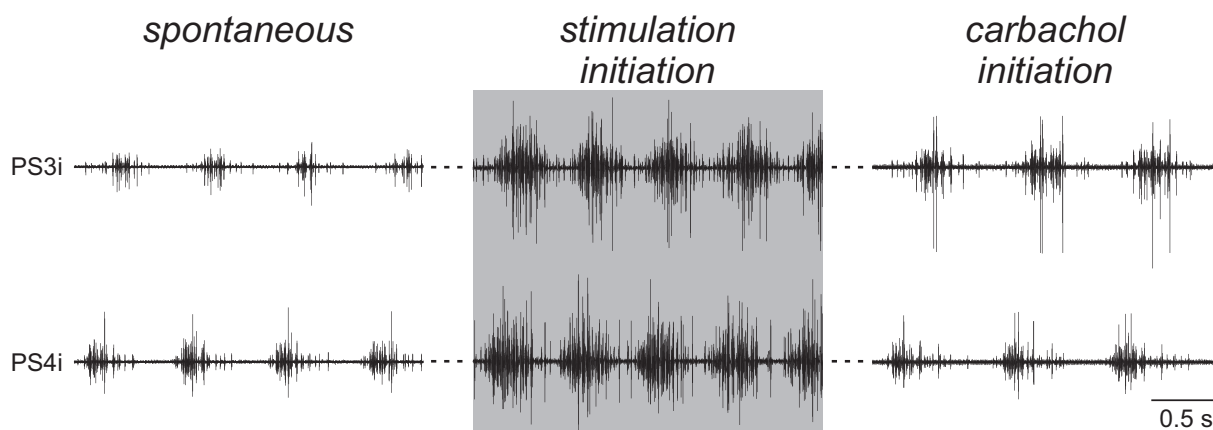
Figure 3.10: Fictive locomotion of the swimmeret system expressed under different conditions. Within one single experiment, fictive locomotion was expressed spontaneously, or initiated by electrical stimulation or bath application of carbachol. **PS3i-4i** *ipsilateral power stroke in ganglia A3 and A4*.

In the following, I will provide a more detailed description of the different parameters of fictive locomotion under the tested conditions. An overview about the analyzed parameters and the respective statistics is given in Table 3.2. Please note that data from experiments in which fictive locomotion was only recorded during stimulations is also included in the datasets regarding period and phase. However, I statistically tested only paired data (Wilcoxon signed rank test, $P \leq 0.025$, Bonferroni-corrected) and the results discussed in this chapter were significant, if not mentioned differently. I tested both spontaneous and CCh conditions against stimulation.

In general, the parameters varied within a wide range for all three conditions. This observation indicates that fictive locomotion was more variable between preparations and potential reasons will be discussed in more detail in chapter 4.

Period

Within single experiments, the period was different between the three conditions without any consistent trend between paired experiments. For example, in some experiments period was smaller during spontaneous fictive locomotion compared to during stimulation while in other experiments period was smaller under the later condition (Figure 3.11 A). However, across all experiments the period was not different for spontaneous (mdn = 0.57 s, iqr = 0.55 - 0.68 s, N = 10) or stimulus-induced fictive locomotion (mdn = 0.55 s, iqr = 0.43 - 0.62 s, N = 15) but higher during the application of CCh (mdn = 0.71 s, iqr = 0.68 - 0.79 s, N = 9).

Phase lag

The calculated phase lags are shown for PS3i and PS4i relative to PS5i (Figure 3.11 B). Within single experiments, the phase lags of PS4 were shorter than phase lags of PS3i, reflecting a stable posterior-to-anterior progression of PS activity under the three conditions. Due to the small sample size, I did not find any differences between the three conditions across all experiments. Therefore, I tested how the phase lags were affected in individual experiments (PS3i: N = 5, PS4i: N = 5). For five PSs, phase lags were smaller during stimulation compared to the spontaneous condition. Phase lag was higher for one PS and did not change for another PS. Phase lags of two PSs did not vary between stimulation and CCh conditions, whereas the phase lag of one PS was higher during stimulation.

Duty cycle

Duty cycles are presented for PS5i to PS2i and covered a wide range from 20 - 80 % without qualitative differences between different ganglia (Figure 3.11 C). Across all experiments, duty cycles were smaller under spontaneous condition (mdn = 42.2 %, iqr = 35.9 - 47.8 %, P = 0.001, N = 10, PSs = 21), but did not differ between stimulation (mdn = 56.8 %, iqr = 46.4 - 67.9 %, N = 15, PSs = 32) and CCh application (mdn = 41.0 %, iqr = 35.7 - 50.4 %, P = 0.057, N = 9, PSs = 16).

Burst duration

Burst durations are presented for PS5i to PS2i and normalized to the corresponding burst durations during stimulation (Figure 3.11 D). Qualitatively, the data range was not different between different ganglia. Burst durations did not differ between the three conditions but tended to be shorter during spontaneous fictive locomotion (normalized to Stim, N = 15, PSs = 32; Spontan: mdn = 0.84, iqr = 0.53 - 1.18, N = 10, PSs = 21; CCh: mdn = 1.02, iqr = 0.86 - 1.39, N = 9, PSs = 16).

Burst strength

Burst strengths are presented for PS5i to PS2i and normalized to the corresponding burst strengths during stimulation (Figure 3.11 E). Please note that calculated burst strengths are independent of the burst durations. Across all experiments, the data ranges were qualitatively not different between different ganglia. Burst strengths were weaker under spontaneous (mdn = 0.67, iqr = 0.55 - 0.93, N = 10, PSs = 21) or CCh conditions (mdn = 0.68, iqr = 0.58 - 0.81, N = 9, PSs = 16), compared to stimulations (N = 15, PSs = 32).

Table 3.2: Analyzed parameters of fictive locomotion initiated by stimulation, compared with fictive locomotion that occurred spontaneously or was elicited by carbachol in the same experiments. Periods were calculated for PS5 only and refer to individual experiments (N = number of experiments). The other parameters represent pooled datasets of abdominal ganglia A2 - A5 (Spontan: 21, Stim: 32, CCh: 16). Data depicts parameters presented in Figure 3.11. Spontaneous and carbachol conditions were tested against stimulation (Wilcoxon signed rank test, Bonferroni-corrected).

		N	mean ± SD	range	Q1	median	Q3	P
	Spontan	10	0.60 ± 0.07	0.52 - 0.69	0.55	0.57	0.68	0.322
Period [s]	*Stim*	15	0.55 ± 0.13	0.13 - 0.90	0.431	0.55	0.62	
	CCh	9	0.71 ± 0.10	0.51 - 0.86	0.68	0.71	0.79	**0.011**
	Spontan	10	44.2 ± 15.3	18.4 - 81.7	35.9	42.2	47.8	**0.001**
Duty cycle [%]	*Stim*	15	57.0 ± 13.3	26.4 - 79.3	46.4	56.8	67.9	
	CCh	9	42.1 ± 9.6	26.4 - 59.2	35.7	41.0	50.4	0.057
	Spontan	10	0.82 ± 0.36	0.29 - 1.37	0.53	0.84	1.18	0.050
Burst duration	*Stim*	15	(data normalized to stimulation)					
	CCh	9	1.22 ± 0.61	0.58 - 2.72	0.86	1.02	1.39	0.495
	Spontan	10	0.73 ± 0.33	0.22 - 1.47	0.55	0.67	0.93	**0.001**
Burst strength	*Stim*	15	(data normalized to stimulation)					
	CCh	9	0.69 ± 0.25	0.26 - 1.14	0.58	0.68	0.81	**0.001**
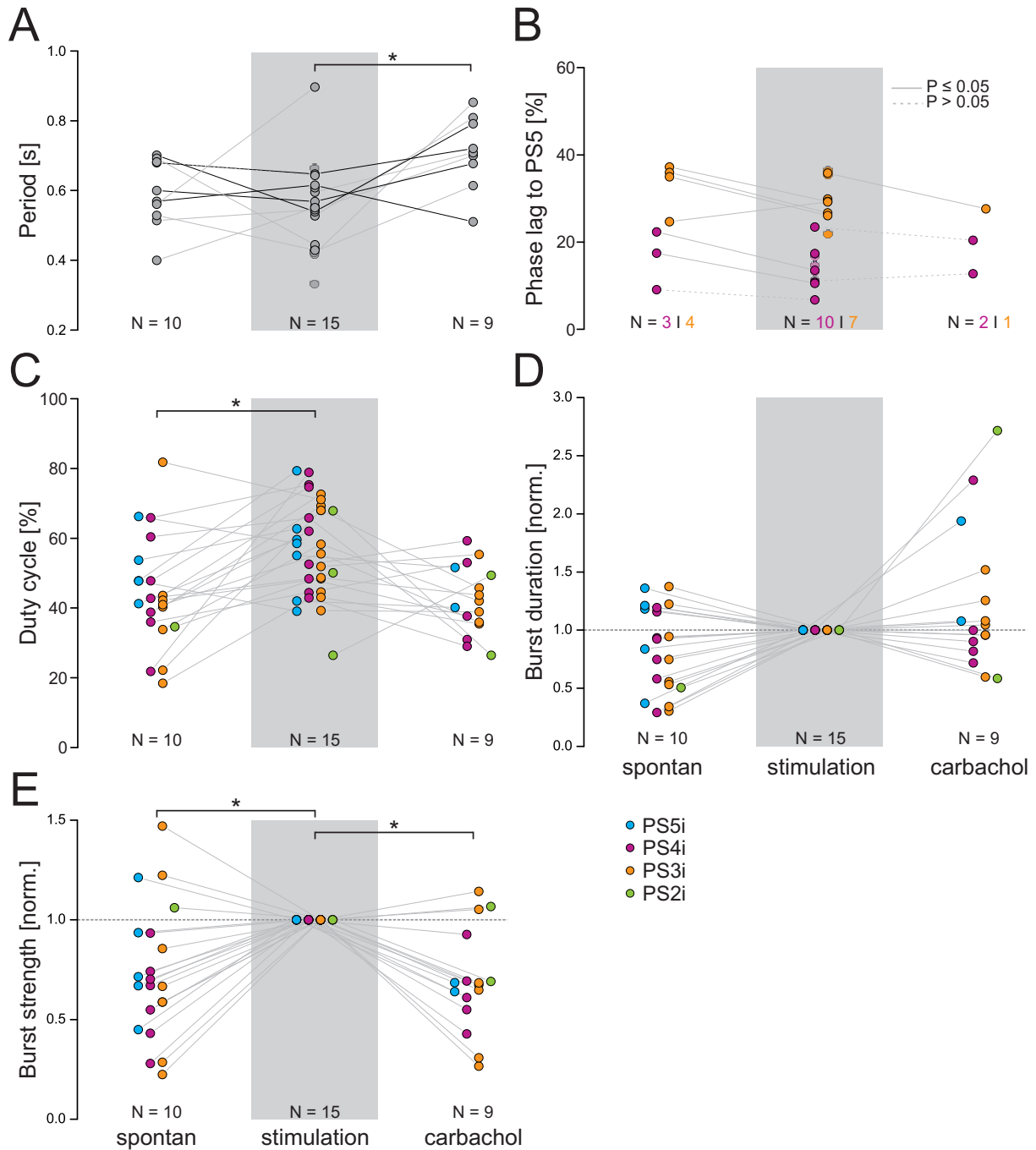
Figure 3.11: Analyzed parameters (means of cycles) of fictive locomotion initiated by stimulations, compared with fictive locomotion that occurred spontaneously or was elicited by carbachol. Either two (gray lines) or three conditions (indicated for periods; black lines) were tested in the same experiments . In some experiments, all three conditions were tested . Please note, that in (**A**) and (**B**) data is also shown for experiments in which fictive locomotion was solely initiated by stimulation. Statistical tests (Wilcoxon signed rank test, $P \leq 0.025$, Bonferroni-corrected) were performed with paired datasets only. Graphs in (**C**), (**D**) and (**E**) include PSs from different segments (spontan: 21, stimulation: 32, carbachol: 16). The complete datasets are given in table 3.2 **A:** Periods during carbachol application were higher than under spontaneous or stimulation conditions. **B:** Although phase lags changed within single experiments (solid lines), no differences across experiments were obtained. **C:** Duty cycles were smaller during spontaneous conditions than during stimulation or carbachol application. **D:** Burst durations were shorter during spontaneous fictive locomotion compared to stimulations or carbachol applications. **E:** Burst strengths were higher during stimulations compared to spontaneous or carbachol condition. **PS2i-5i** *ipsilateral power stroke in ganglia A2-A5*.

3.2.3 Enhancement of fictive locomotion

In addition to termination and initiation, I was also able to enhance fictive locomotion through electrical stimulation (N = 20). This applied for both spontaneous and CCh-elicited fictive locomotion. CCh not only elicits fictive locomotion from previously silent preparations but also decreases the period in a dose-dependent fashion [Mulloney, 1997]. The threshold for this decrease is approximately 1 µM and I only occasionally applied higher concentrations. Due to the fact that in experiments in which I used higher concentrations electrical stimulations further decreased the period, I did not differentiate between CCh-elicited and spontaneous fictive locomotion. Within a single experiment, all recorded PSs were affected by the stimulation and an example is illustrated in Figure 3.12. Immediately with begin of the stimulation, fictive locomotion was enhanced and after stimulation the initial PS activity was restored (Figure 3.12 A). I defined enhancement by either a decrease in period, an increase of burst strengths, or both instances in combination (Figure 3.12 B). The corresponding stimulation sites were already presented above (Chapter 3.1.1) and were in line with the previously described locations of excitatory command neurons. Interestingly, these locations were highly overlapping with the stimulation sites for initiations, suggesting that excitatory command neurons are able to initiate or enhance fictive locomotion, depending on the excitation level of the swimmeret system. This is further indicated by seven experiments, in which I was able to both initiate fictive locomotion in a silent preparation and enhance ongoing PS activity at a different time during experimental procedure.

In the experiments presented in this chapter, the parameters of fictive locomotion before the enhancement (pre-stimulus) were fully restored within varying time periods after the stimulation (post-stimulus, Figure 3.13). In Figure 3.14 A and B periods and phase lags are presented for the three conditions, i.e. pre-stimulation (pre-stim), stimulation (stim) and post-stimulation (post-stim). While the periods and phase lags returned to their initial states, also the other parameters recovered. For simplicity reasons, I solely show pre-stimulation (pre) and stimulation (stim) conditions for duty cycles, burst durations and burst strengths. The analyzed parameters and the respective statistics are given in Table 3.3. I statistically tested for differences between pre and stim conditions (Wilcoxon signed rank test, $P \leq 0.05$) and the results shown in this chapter are significant, if not mentioned differently.
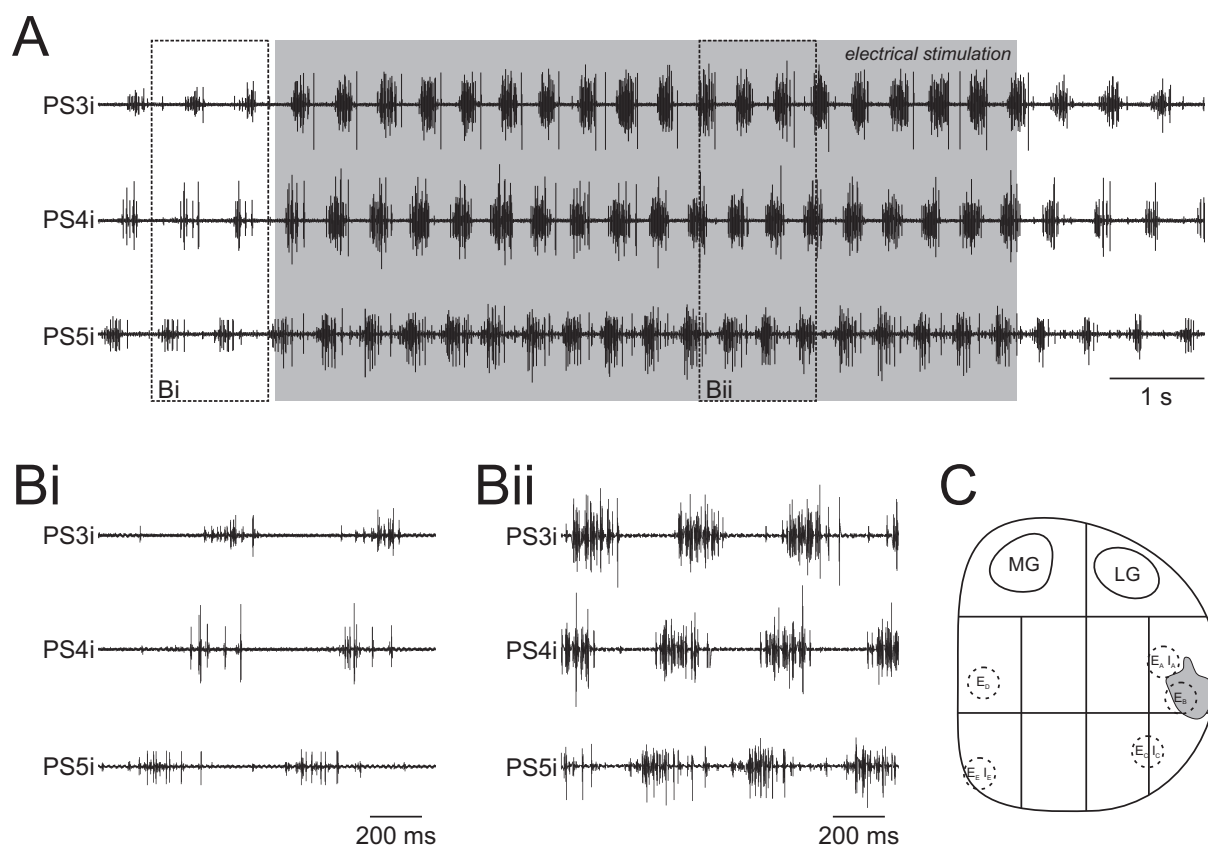
Figure 3.12: Enhancement of fictive locomotion in the swimmeret system. **A:** Fictive locomotion was enhanced during electrical stimulation (depicted in gray). **B:** Time windows indicated in (**A**), showing spontaneous (**Bi**) and enhanced (**Bii**) fictive locomotion. **D:** Schematic map of a hemiconnective, indicating the location of the stimulated axon bundle. **PS3i-5i** *ipsilateral power stroke in ganglia A3 to A5*, **cA2/A3** *connective between ganglia A2 and A3*, **MG** *medial giant fiber*, **LG** *lateral giant fiber*, **E$_X$** *excitatory command neuron*, **I$_X$** *inhibitory command neuron*.
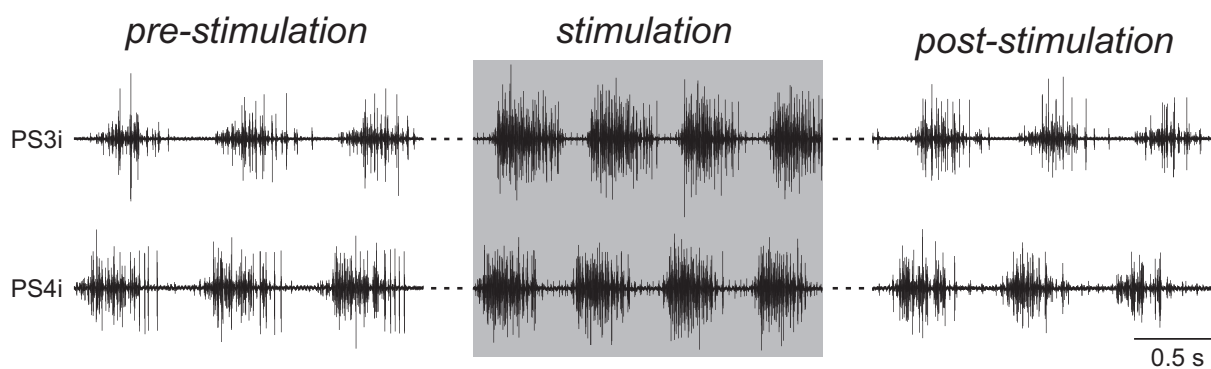
Figure 3.13: Fictive locomotion in the swimmeret system was enhanced during electrical stimulation but did not differ between pre- and post-stimulation conditions. **PS3i-4i** *ipsilateral power stroke in ganglia A3 and A4*.

Period

The decrease in period was a striking characteristic of enhancement and appeared in 17 out of 19 experiments (Pre: mdn = 0.62 s, iqr = 0.51 - 0.68 s; Stim: mdn = 0.46 s, iqr = 0.38 - 0.51 s, N = 19). The decrease was independent of the initial period which ranged from 0.41 to 0.71 s. Please note that in two experiments period remained unaltered and that enhancement in these experiments was reflected by increased burst strengths (Figure 3.14 A).

Phase lags

The calculated phase lags are shown for PS3i and PS4i relative to PS5i (Figure 3.14 B). Phase lags were only calculated if PS5 was recorded in the respective experiment. Within single experiments, the phase lags of PS4i were shorter than of PS3i, indicating that the posterior-to-anterior progression of PS activity remained stable. For 12 out of 18 PSs, individual phase lags advanced during stimulations but neither for PS3i (Pre: mdn = 43.6 %, iqr = 39.3 - 46.2 %, Stim: mdn = 37.5 %, iqr = 31.6 - 42.8 %, P = 0.232, N = 10) nor PS4i ([%], Pre: mdn = 21.3 %, iqr = 18.3 - 26.1 %, Stim: mdn = 17.9 %, iqr = 12.3 - 20.8 %, P = 0.078, N = 8) phase lags were significantly different.

Duty cycle

Duty cycles are shown for PS5i, PS4i and PS3i, and were normalized to the corresponding duty cycles before stimulation (Figure 3.14 C). Duty cycles increased during stimulations (Stim: mdn = 1.23, iqr = 1.11 - 1.61, N = 19, PSs = 36) and ranges were similar between different segments.

Burst duration

Burst durations are shown for PS5i, PS4i and PS3i, and were normalized to the corresponding burst durations before stimulation (Figure 3.14 D). Burst durations increased or decreased during enhancement without any consistency between segments. Burst durations were not affected during enhancement across all experiments (normalized to Pre-Stim; Stim: mdn = 0.96, iqr = 0.84 - 1.21, N = 19, PSs = 36).

Burst strength

Burst strengths are presented for PS5i, PS4i and P3i, and were normalized with respect to the corresponding burst strengths before stimulation (Figure 3.14 E). Please note that the calculated burst strengths are independent of the burst durations. Burst strengths of all analyzed PSs increased during enhancement (normalized to Pre-Stim; Stim: mdn = 2.04, iqr = 1.55 - 2.65, N = 19, PSs = 36).
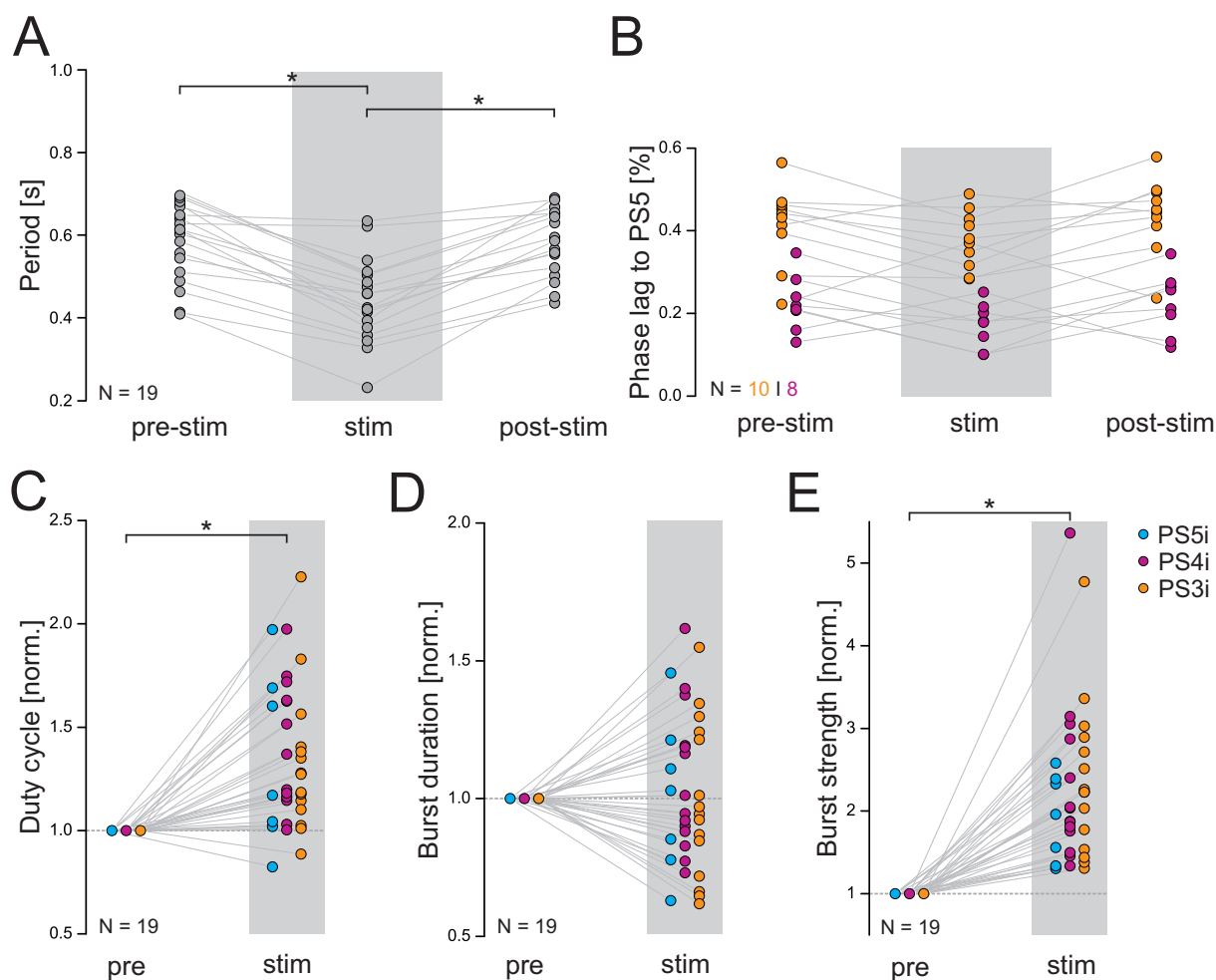
Figure 3.14: Analyzed parameters of fictive locomotion enhanced by stimulations, compared between pre-stimulation (pre) and stimulation (stim) (Wilcoxon signed rank test, P ≤ 0.05). Enhancement was defined by either decrease of the period, increase of the burst strength, or both. The complete dataset is given in table 3.3 **A:** Period decreased during stimulations and returned afterwards to the initial state. **B:** Phase lags of PS3i and PS4i calculated relative to PS5. The posterior to anterior progression was maintained during enhancement. **C:** Duty cycles increased during stimulations (PSs = 36). **D:** Burst durations of individual PSs increased and decreased without a predominant tendency (PSs = 36). **E:** Burst strengths increased during stimulations (PSs = 36). **PS2i-5i** *ipsilateral power stroke in ganglia A2-A5*.

Table 3.3: Analyzed parameters of fictive locomotion enhanced by stimulations, compared between pre-stimulation (pre) and stimulation (stim) conditions (Wilcoxon signed rank test, $P \leq 0.05$). Duty cycle, burst duration and burst strength represent pooled datasets of 36 abdominal ganglia (A3, A4, A5). Data depicts parameters presented in Figure 3.14.

		N	mean ± SD	range	Q1	median	Q3	P
Period [s]	*Pre*	19	0.59 ± 0.10	0.41 - 0.71	0.51	0.62	0.68	**0.001**
	Stim		0.45 ± 0.10	0.23 - 0.64	0.38	0.46	0.51	
Phase PS3 [%]	*Pre*	10	41.4 ± 9.5	22.2 - 56.4	39.3	43.6	46.2	0.232
	Stim		37.6 ± 7.0	28.3 - 48.9	31.6	37.5	42.8	
Phase PS4 [%]	*Pre*	8	22.4 ± 6.7	13.0 - 34.6	18.3	21.3	26.1	0.078
	Stim		17.1 ± 5.3	10.0 - 25.1	12.3	17.9	20.8	
Duty cycle	*Pre*	19	(data normalized to pre-stimulation)					**0.001**
	Stim		1.35 ± 0.34	0.82 - 2.23	1.11	1.23	1.61	
Burst duration	*Pre*	19	(data normalized to pre-stimulation)					0.785
	Stim		1.02 ± 0.27	0.62 - 1.62	0.84	0.96	1.21	
Burst strength	*Pre*	19	(data normalized to pre-stimulation)					**0.001**
	Stim		2.26 ± 0.91	1.30 - 5.36	1.55	2.04	2.65	

3.2.4 Side-specific stimulation effects during enhancement

Fictive activity of the isolated swimmeret system is expressed by both sides of the abdominal ganglia simultaneously. The bilateral chains of coupled oscillators, i.e. the neuronal micro circuits located in the hemiganglia, produce metachronal waves of PS activity with identical periods and constant phase shifts. Within a single ganglion the PS motor neurons of both hemiganglia are active at the same time. However, phase lags, duty cycles, burst durations and burst strengths strongly depend on the quality of extracellular recordings. Consequently, comparisons of these parameters between the hemiganglia of the same segment remain limited. Therefore, most studies focused on analyzing unilateral PS activity and we are still lacking detailed knowledge about how the bilateral coupling is maintained.

During enhancement of fictive locomotion I occasionally observed that the PS activities ipsilateral and contralateral to the stimulation electrode were affected differently. An example is given in Figure 3.15 A, illustrating the bilateral decrease of the period but additionally indicating a stronger enhancement of ipsilateral PS burst strengths. Therefore, I analyzed the contralateral PS activities and tested for side-specific effects during enhancement of fictive locomotion.

It is worthwhile to briefly explain the analysis and the illustration in figure 3.14 B - E. Parameters of PSs ipsi- and contralateral to the stimulation electrode were normalized to the pre-stimulation condition of the respective PS. The pre-stimulation condition is given as a reference

(Pre-Stim = 1). Please note that the graphs illustrate relative changes of the analyzed parameters. This means that data points > 1 represent increased parameters and data points < 1 decreased parameters. The relative changes from the same experiment and segment (ipsi and contra) are connected through gray lines, e.g. relative changes of burst durations in PS3i and PS3c.

I assumed bilateral periods to be constant, and confirmed this in selected experiments (data not shown). Therefore, I did not further analyze the periods on the contralateral side. The relative changes of each side were pooled for PS3, PS4 and PS5 and an overview including the respective statistics is given in Table 3.4. First, I statistically compared the parameters between pre-stimulation and stimulation for each side independently (not depicted in figure 3.14, Wilcoxon signed rank test, $P \leq 0.05$). In addition, I tested for significant differences between the relative changes of the two sides from one segment (e.g. PS3i and PS3c, Wilcoxon signed rank test, $P \leq 0.05$). The results described in this chapter were significant, if not mentioned differently.

As demonstrated before, ipsilateral phase lags of PS3 and PS4 relative to PS5 did not change during enhancement of fictive locomotion (Chapter 3.2.3). This is also reflected by the data presented in figure 3.15 B. Although the majority of phase lags decreased (ipsi: 9 out of 12, contra: 6 out of 12), significant differences were neither present between pre-stimulation and stimulation (see table 3.4), nor between ipsi- and contralateral sides (PS3: P = 0.562, PS4: P = 0.312). Please note that data is also presented for phase lags that were calculated solely unilaterally. However, statistics were performed only with paired datasets, when ipsi- and contralateral phase lags of the same ganglion were available. Taken together, this indicates that ipsi- and contralateral phases were equally affected during enhancement.

In contrast to phase lags, duty cycles (Figure 3.15 C), burst durations (Figure 3.15 D), and burst strengths (Figure 3.15 E) were affected side-specifically. Duty cycles increased bilaterally during enhancement , but the effect on the ipsilateral side was stronger (Ipsi: mdn = 1.24, iqr = 1.11 - 1.61; Contra: mdn = 1.08, iqr = 0.99 - 1.17, N = 19, PSs = 36). Burst durations ipsilateral to the stimulations were not affected during enhancement but decreased on the contralateral side (Ipsi: mdn = 0.96, iqr = 0.87 - 1.21; Contra: mdn = 0.86, iqr = 0.68 - 0.94, N = 19, PSs = 36). Finally, burst strengths increased bilaterally with a stronger increase on the ipsilateral side (Ipsi: mdn = 2.04, iqr = 1.55 - 2.65; Contra: mdn = 1.44, iqr = 1.17 - 1.71, N = 19, PSs = 36).
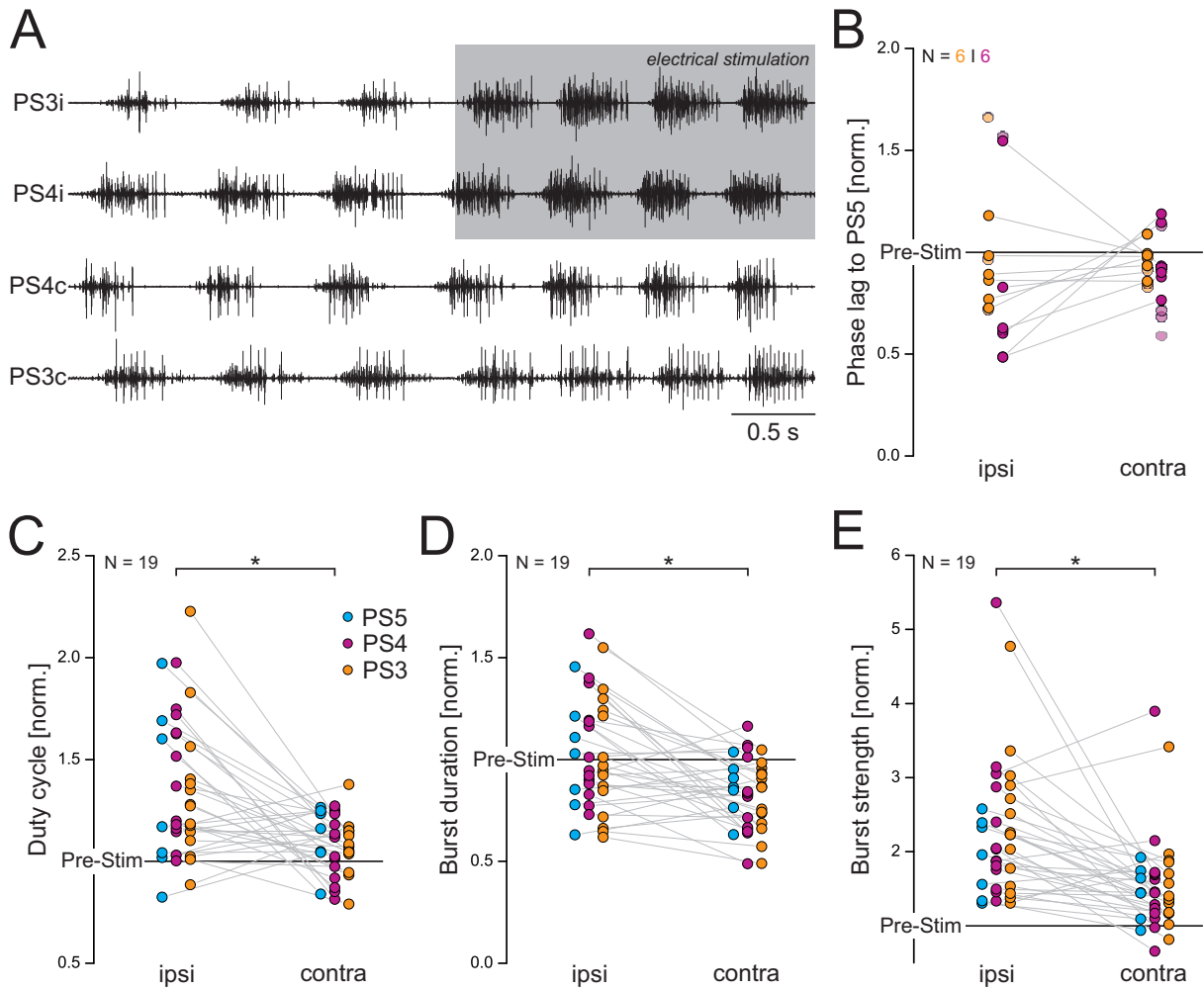
Figure 3.15: Enhancement of fictive locomotion is side specific. Relative changes in the analyzed parameters of enhanced fictive locomotion compared between ipsi- and contralateral side to the stimulation electrode (Wilcoxon signed rank test, P ≤ 0.05). *Ipsi* and *contra* refer to the stimulation electrode. Parameters of individual hemiganglia were normalized to pre-stimulus condition (Pre-Stim) and data illustrate relative changes. Graphs in (**C**), (**D**) and (**E**) include PSs from 36 abdominal segments. **A:** Example of side specific enhancement during stimulation. Stimulation is depicted in gray. **B:** Although the majority of phase lags advanced (ipsi: 9 out of 12, contra: 6 out of 12), they were not significantly different to the pre-stimulation condition and relative changes did not differ between both sides. **C:** Duty cycles increased on both sides and the effect was stronger on the ipsilateral side. **D:** Burst durations were not affected on the ipsilateral side but decreased contralateral to the stimulation. **E:** Burst strengths increased on both sides and were stronger affected ipsilateral to the stimulation. **PS3-4** *power strokes in ganglia A3 and A4.*

Table 3.4: Analyzed parameters of fictive locomotion enhanced through stimulation. Parameters were normalized to pre-stimulation conditions. A detailed description is given in the text. Effects on both sides of the preparation were tested for significant differences to the respective pre-stimulation conditions (*) and between each other (Wilcoxon signed rank test, P ≤ 0.05). Duty cycle, burst duration and burst strength represent pooled datasets of 36 abdominal ganglia (A3, A4, A5). Data depicts parameters presented in Figure 3.14.

		N	mean ± SD	range	Q1	median	Q3	P*	P
Phase PS3	*Ipsi*	6	0.90 ± 0.16	0.72 - 1.18	0.77	0.88	0.98	0.218	0.562
	Contra		0.97 ± 0.08	0.86 - 1.09	0.93	0.98	0.99	0.312	
Phase PS4	*Ipsi*	6	0.76 ± 0.40	0.49 - 1.55	0.49	0.61	0.83	0.437	0.312
	Contra		0.97 ± 0.16	0.76 - 1.19	0.88	0.92	1.15	0.843	
Duty cycle	*Ipsi*	19	1.35 ± 0.34	0.82 - 2.23	1.11	1.24	1.61	**0.001**	**0.001**
	Contra		1.08 ± 0.14	0.79 - 1.38	0.99	1.08	1.17	**0.004**	
Burst duration	*Ipsi*	19	1.02 ± 0.27	0.62 - 1.62	0.84	0.96	1.21	0.785	**0.001**
	Contra		0.82 ± 0.15	0.49 - 1.05	0.68	0.86	0.94	**0.001**	
Burst strength	*Ipsi*	19	2.26 ± 0.91	1.30 - 5.36	1.55	2.04	2.65	**0.001**	**0.001**
	Contra		1.54 ± 0.63	0.66 - 3.90	1.17	1.44	1.71	**0.001**	

3.2.5 Similar effects evoked at different levels of the CNS

Since stimulation of descending axons within the abdominal part of the nervous system modulates the activity of the swimmeret system two questions arose: (1) Where does this descending input originates within the CNS and (2) does it also affect the motor output of the walking legs?

Therefore, I tested if it is possible to reproduce the observed stimulation effects with electrical stimulations at different levels upstream of the swimmeret system. I tested three different levels for stimulation. I stimulated between the first and second thoracic ganglia (cT1/T2), between the subesophageal and the first thoracic ganglion (cSOG/T1), or between the brain and the subesophageal ganglion (cBrain/SOG). All successful experiments are presented here and data was not further analyzed. Please note that the results are only presented for PS3i and PS4i but PS2i and PS5i were also affected if recorded.

I terminated fictive locomotion at all tested levels (Figure 3.16). In contrast, fictive locomotion was solely initiated at the levels of cBrain/SOG and cT1/T2 (Figure 3.17). However, one stimulation at the level of cSOG/T1 initiated tonic activity in PS3i and PS4i, revealing an excitatory effect on the swimmeret system (Figure 3.17 Bii). The preparations shown in figure 3.17 Bi and Bii further indicate that enhancement of fictive activity might also be possible by stimulations at the tested levels of the CNS. Individual PS recordings showed weak rhythmic activity before stimulation, potentially being enhanced during the stimulation.
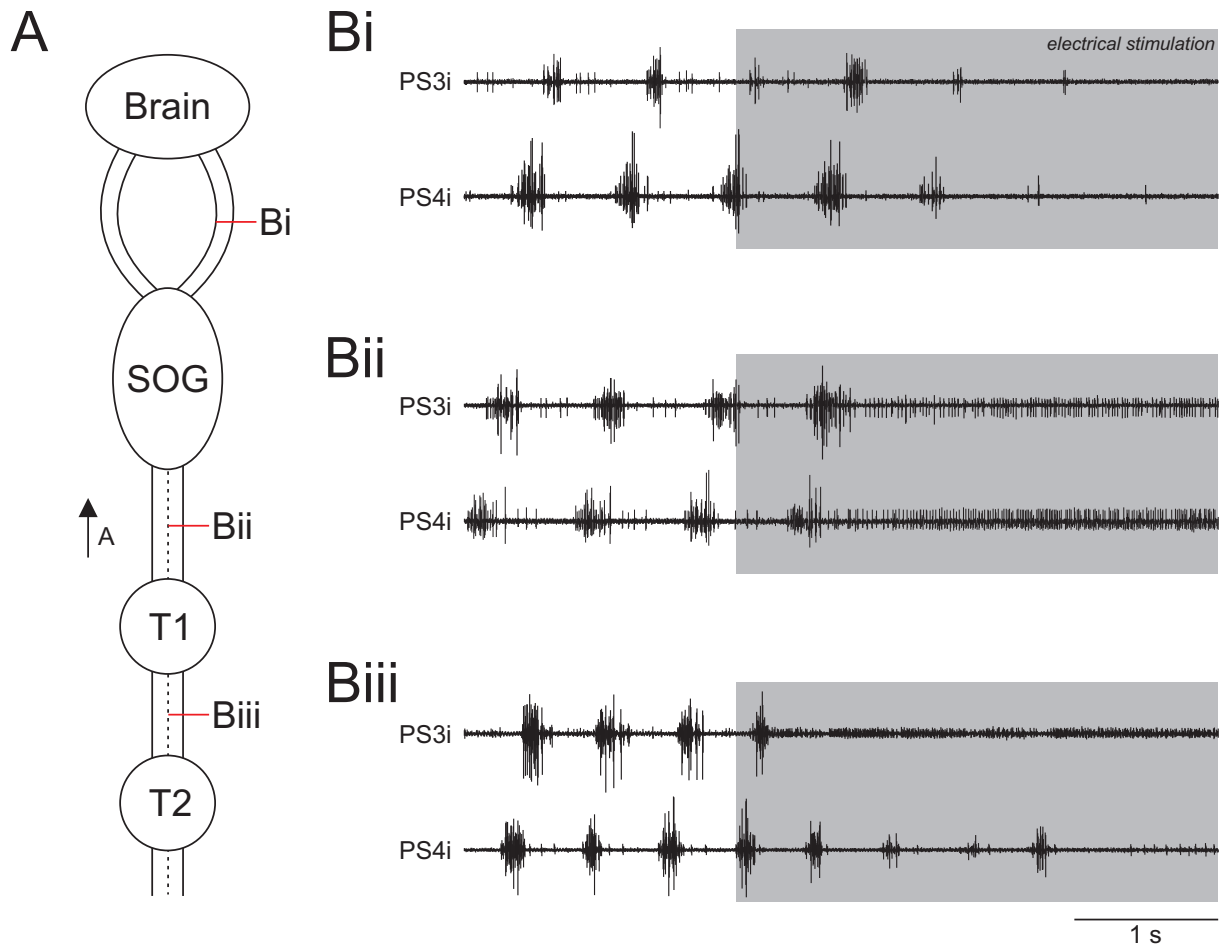
Figure 3.16: Fictive locomotion was terminated anterior of the swimmeret system. **A:** In three different preparations axon bundles in similar portions of the connectives were stimulated anterior to the swimmeret system. **B:** Power stroke recordings of abdominal ganglia A3 and A4 showing termination of fictive locomotion during electrical stimulations. Stimulations were performed at positions indicated in (**A**) and are depicted in gray. **SOG** *subesophageal ganglion*, **T1, T2** *thoracic ganglia*, **PS3i-4i** *ipsilateral power stroke in ganglia A3 and A4*.
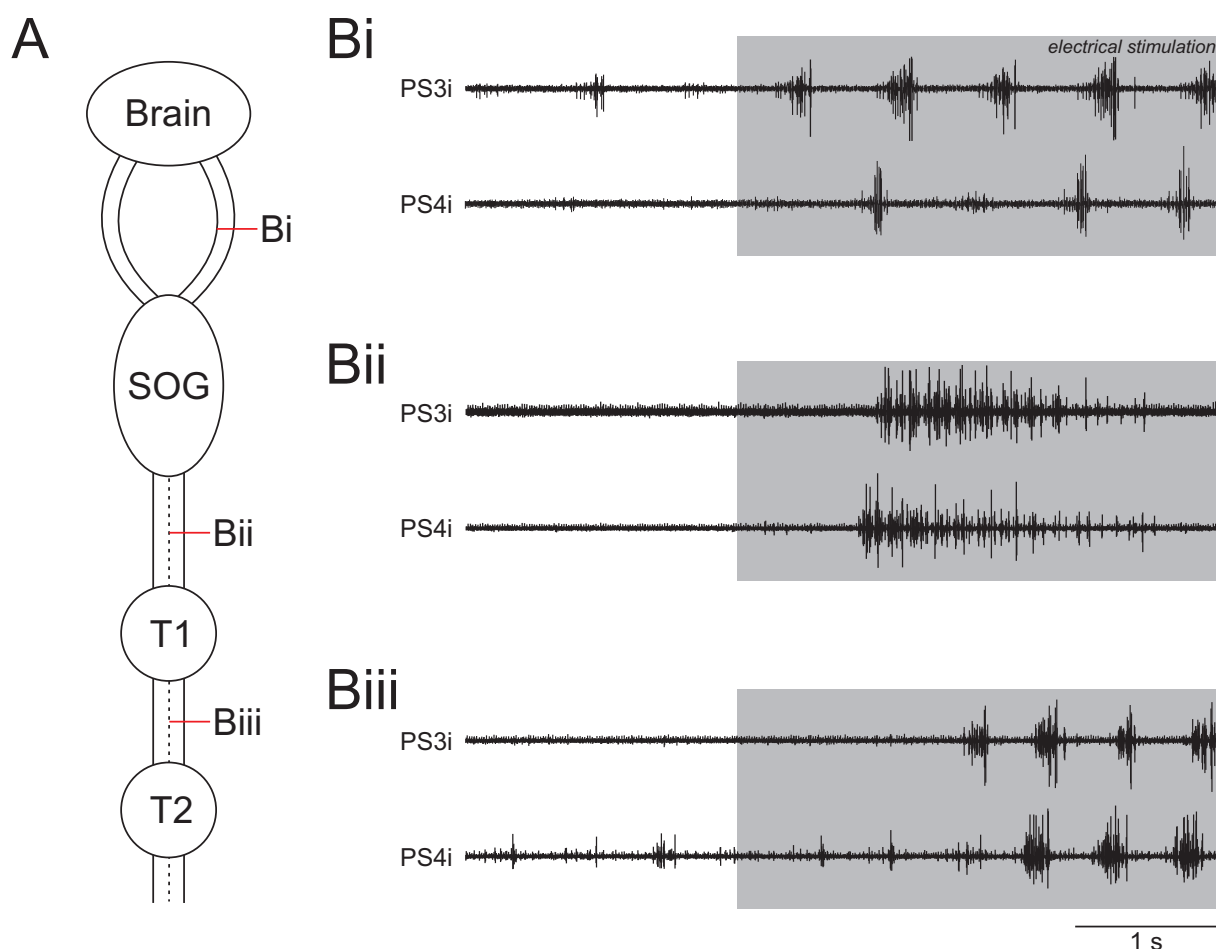
Figure 3.17: Fictive locomotion was initiated anterior of the swimmeret system. **A:** In three different preparations axon bundles in similar portions of the connectives were stimulated anterior to the swimmeret system. **B:** Power stroke recordings of abdominal ganglia A3 and A4 during electrical stimulations, performed at positions indicated in (**A**). PS motor neurons were excited or fictive locomotion was initiated. Stimulations are depicted in gray. **SOG** *subesophageal ganglion*, **T1, T2** *thoracic ganglia*, **PS3i-4i** *ipsilateral power stroke in ganglia A3 and A4*.

The motor output of the swimmeret system is coupled to the activity of the walking legs [Cattaert and Clarac, 1983; Barthe et al., 1991; Cattaert et al., 1992]. Therefore, I additionally recorded from the thoracic nerves innervating the muscles of the third ipsilateral walking leg during stimulations at cT1/T2. These nerves are very delicate and the preparations require a lot of practice. Due to the preliminarity of these experiments, I did not record continuously from the same nerves and the observed motor activity was mostly tonic. However, in two experiments rhythmic motor activity was initiated by the stimulations and I observed simultaneous effects on the swimmeret system (Figure 3.18). In the experiment presented in figure 3.18 C the stimulation evoked bursts of action potentials in the depressor and protractor nerves, indicating backward walking [Barthe et al., 1991]. At the same time, rhythmic PS activity in abdominal ganglia A4 (PS4) was suppressed, indicating termination of the swimmeret system during backward walking. In another experiment, I recorded bursts of action potentials in the levator and protractor nerves during a stimulation (Figure 3.18 D). This pattern indicates the initiation of

forward walking. During this elicited forward walking, the period of the swimmeret system increased (Pre-Stim: mdn = 0.52 s, iqr = 0.49 - 0.54 s; Walking: mdn = 0.53 s, iqr = 0.51 - 0.55 s; Wilcoxon signed rank test, P = 0.029) and burst strength decreased (normalized to Pre-Stim; Walking: mdn = 0.69 s, iqr = 0.60 - 0.79 s; Wilcoxon signed rank test, P = 0.001).
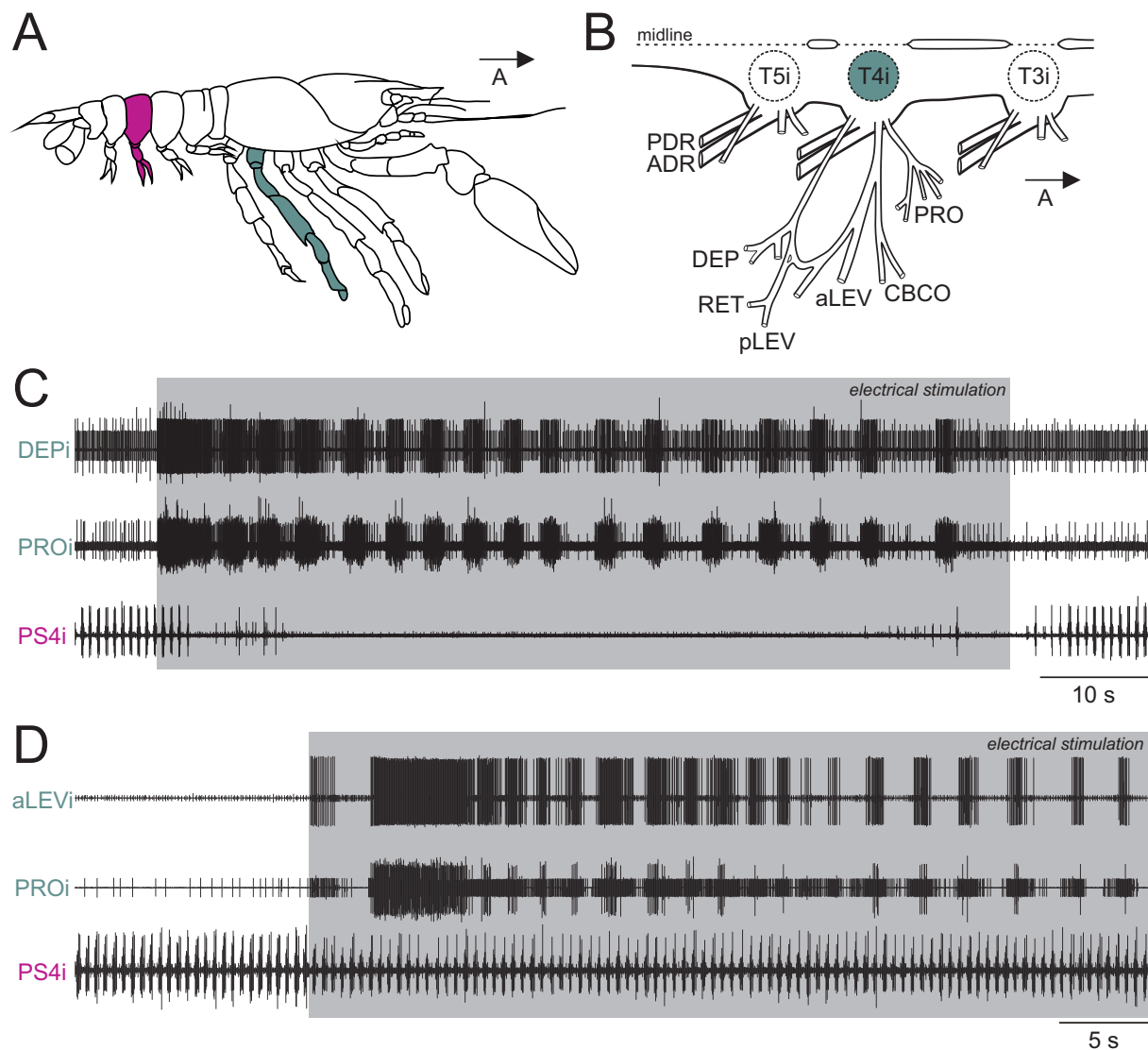
Figure 3.18: Electrical stimulations at the level of cT1/T2 affected the motor activity of both the walking and the swimmeret system. **A:** Schematic drawing of a crayfish. I recorded ipsilateral motor activities of the fourth abdominal (A4i, purple) and forth thoracic (T4i, gray) ganglia. **B:** Schematic drawing of thoracic hemiganglia T3i to T5i, illustrating the nerves recorded in (**C**) and (**D**). **C:** In one experiment, stimulation induced bursts of motor activity in the depressor (DEPi) and protractor (PROi) nerves of T4, indicating backward walking. Simultaneously, PS activity in A4i was terminated. **C:** In another experiment, stimulation induced bursts of motor activity in the anterior levator (aLEVi) and PROi nerves of T4i, indicating forward walking. At the same time, periods of PS4i increased while the burst strengths decreased (see text). **PDR** *posterior distal root*, **ADR** *anterior distal root*, **DEP** *depressor*, **RET** *retractor*, **pLEV** *posterior levator*, **aLEV** *anterior levator*, **CBCO** *coxo-basipodite chordotonal organ*, **PRO** *protractor*, **PS4i** *ipsilateral power stroke in ganglia A4*.

3.3 Stimulation effects on individual neurons of the swimmeret microcircuits

I successfully showed that electrical stimulations of descending pathways affected the motor output of the swimmeret system in terms of termination, initiation, and enhancement of fictive locomotion. In general, the parameters of PS activity are mainly determined by the activity of the neurons forming the central pattern generator (CPG) in each individual hemiganglion, i.e. periods, phase lags, duty cycles and burst durations. As an exception, the burst strengths solely reflect the activity of PSE motor neurons [Mulloney, 2005]. The CPGs comprise two groups of interneurons, Inhibitors of PS (IPS) and Inhibitors of RS (IRS). The groups of IPS and IRS neurons reciprocally inhibit each other and form inhibitory synapses on PS and RS excitatory motor neurons (PSE, RSE), respectively. To this date, no information are available about any additional synaptic input these neurons receive, e.g. if they are directly targeted by descending input. Therefore, I intracellularly recorded from individual neurons and analyzed how stimulations affected their membrane potentials (V_m) (Chapter 3.3.1). During enhancement, the analyzed parameters of fictive locomotion were affected differently and revealed side-specific stimulation effects. Therefore, I investigated the V_m of individual neurons during enhancement (Chapter 3.3.2). In addition, I tested the idea that CPG neurons are directly targeted by descending pathways that excite the swimmeret system (Chapter 3.3.3).

3.3.1 Shifts in membrane potential during activity transitions

During fictive locomotion, the V_m of both, motor neurons and CPG neurons oscillated between the peak (PP) and trough potential (TP), representing the most depolarized and hyperpolarized phases of oscillation, respectively. These oscillations were absent if the swimmeret system was at a silent state, i.e. no rhythmic PS activity was expressed. Transitions between active and silent states appeared spontaneously or were evoked by electrical stimulations (termination and initiation). Please note that fictive locomotion both started and stopped spontaneously and I do not differentiate between spontaneous inactivation or activation. I defined the stable V_m at a silent state as the non-oscillating potential (NOP) and compared it to the corresponding PP and TP before or after transitions. On the one hand, these shifts in V_m provide data to compare between different types of transition and between different types of neurons. On the other hand, the NOPs describe the silent state of the neuronal micro circuits, i.e. of the CPG neurons and motor neurons.

In principle, shifts in V_m and the corresponding NOPs of individual neurons were potentially caused by three distinct mechanisms: (1) Direct input from the stimulated pathways, (2) passive V_m properties of the recorded neuron, and (3) synaptic interactions within the neuronal microcircuits. Direct inputs and passive properties may be investigated when the swimmeret neurons are synaptically isolated between each other. However, I performed my recordings in the intact network. Under this condition the previously discovered circuitry of the swimmeret microcircuits is sufficient to describe the activity of CPG neurons and motor neurons while the system is active (see Mulloney and Smarandache-Wellmann [2012] for a review). Therefore, I predominantly describe the results with respect to the known circuitry and correlated activities of different neuron groups. Under this simplified condition the V_m of a PSE is determined by the inhibition from the group of IPS neurons, while inhibitory input from IRS neurons determines the V_m of a RSE. The groups of IPSs and IRSs reciprocally inhibit each other. These graded synaptic connections are possible explanations for the during activity transitions. In contrast, additional excitatory inputs on CPG neurons or motor neurons are not known but may arise from descending pathways. Possible contributions of direct input or passive membrane properties are discussed in a later section (Chapter 4).

Motor neurons

Independent of the type of transition, intracellularly recorded PSEs showed consistent shifts in V_m (Figure 3.19). I did not observe any differences regarding the recording side, i.e. between PSEs ipsilateral or contralateral to the stimulated axon bundle. NOPs were at the level of TPs, suggesting either tonic inhibition during a silent state or phasic excitation in an active state. Please note that the PSE shown in Figure 3.19 Ai and Bi did not reach the threshold for the generation of action potentials during PS activity. However, strong depolarization of the V_m evoked tonic discharge in this neuron. The action potentials were also present on extracellular PS recordings of the corresponding hemiganglion, clearly demonstrating the recording of one PSE (data not shown). However, these action potentials were smaller and the initial V_m more hyperpolarized than in the two other PSEs. This might be due to damaging the neuron through impaling the membrane with the intracellular microelectrode.
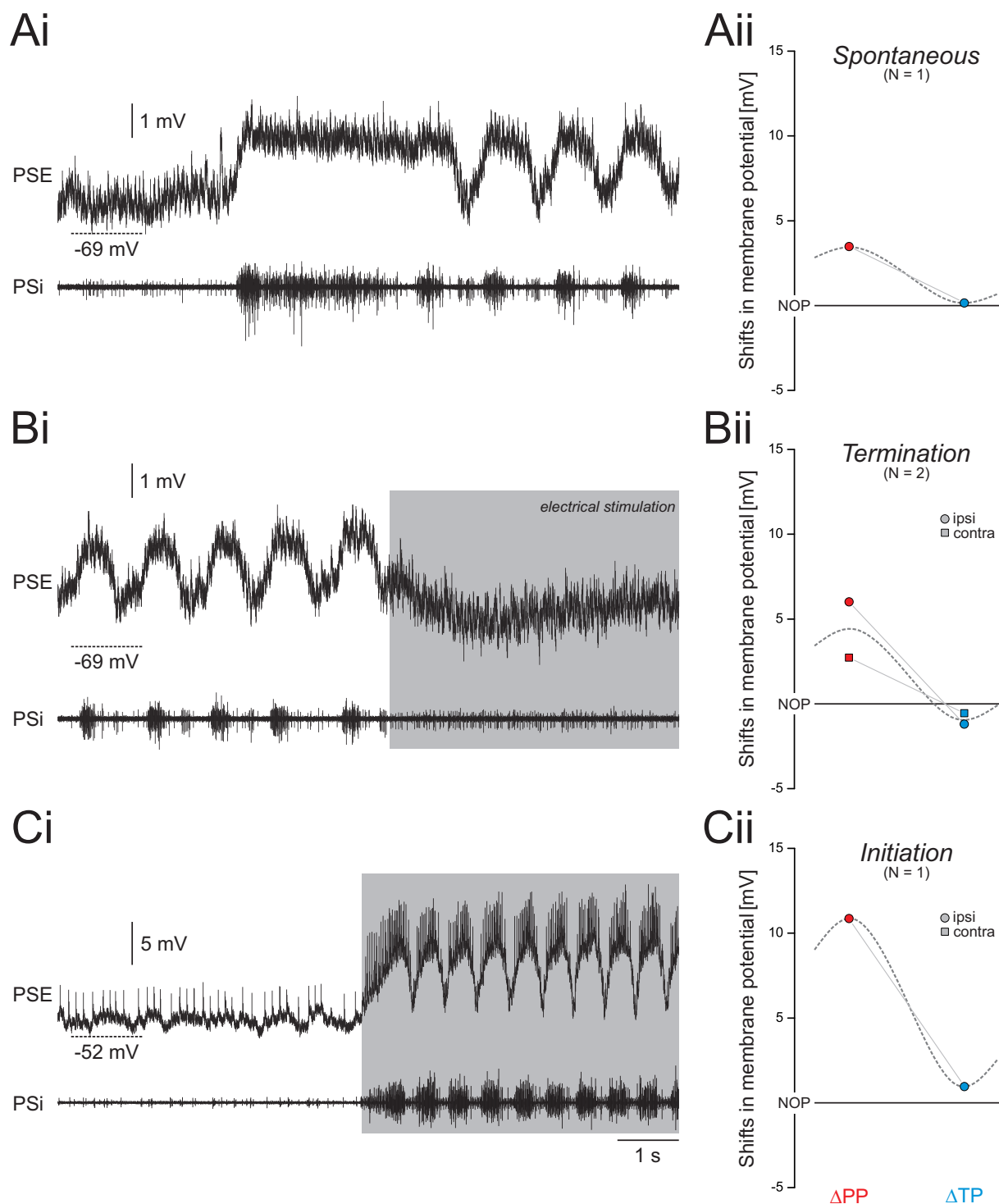
Figure 3.19: Activity transitions of PSE (N = 3), induced through stimulations or spontaneously, showed consistent shifts in the membrane potential. Examples and analyzed parameters (ΔPP (red) and ΔTP (blue) relative to the NOP) for all recorded neurons are presented for each kind of transition, i.e. spontaneous (**A**), termination (**B**), and initiation (**C**). Stimulations are depicted in gray. Dashed lines in (**A**ii), (**B**ii) and (**C**ii) indicate suggested V_m oscillations derived from mean values. **A:** Intracellular recording of one PSE during spontaneous transition revealed a more depolarized V_m during PS activity of the corresponding hemiganglion. TP during oscillations was at the level of the NOP, suggesting phasic release from inhibition during PS activity. **B:** During termination, the V_m of the PSE shown in (**A**i) was more hyperpolarized without showing any oscillations. The NOP was at the level of TP during oscillations. **C:** During initiation, the V_m of a PSE was depolarized and oscillated in phase with the PS. The TP during oscillations was at the same level as the NOP, suggesting phasic release from inhibition during PS activity. **PSE** *power stroke exciter*, **PSi** *ipsilateral power stroke*, **V_m** *membrane potential*, **NOP** *non-oscillating potential*, **PP** *peak potential*, **TP** *trough potential*.

RSEs showed divergent shifts in V_m, depending on the type of transition but not depending on the recording side. (Figure 3.20). On the one hand, spontaneous transitions and transitions during termination revealed consistent shifts in RSEs, that were opposite to shifts observed in PSEs. NOPs were at the level of PPs, suggesting either tonic excitation during a silent state or phasic inhibition during an active state. Please note that the RSE shown in Figure 3.20 Ai and Bi fired action potentials at the level of NOP, indicating tonic excitatory input on RS muscles at a silent state of the swimmeret system. On the other hand, transitions during initiation showed inconsistent shifts in V_m for different RSEs. NOPs were either at the level of the PPs or the TPs, at a even more depolarized or hyperpolarized level, or at a level in between the PP and the TP. However, the pooled data for all three types of transition revealed significant differences between the values of the NOPs (mdn = - 53.3 mV, iqr = - 48.0 - - 58.2 mV, 20 transitions) and TPs (mdn = - 59.9 mV, iqr = - 57.4 - - 62.7 mV, P = 0.001, 20 transitions) but not between NOPs and PPs (mdn = - 51.7 mV, iqr = - 48.2 - - 57.1 mV, P = 0.348, 20 transitions) (Wilcoxon signed rank test, P $\leq$ 0.05).

During normal forward swimming in intact crayfish, both swimmerets of one segment are active in phase [Davis, 1968b]. In addition, stimulations of command neurons were described to affect the motor activity of both sides of the isolated nervous system similarly [Wiersma and Ikeda, 1964]. I assumed that the basic principles of transitions between different states of activity are also similar in ipsi- and contralateral motor neurons. Therefore, I present pooled data for PSE and RSE, independent of the recording sites (Table 3.5). Neither NOPs, PPs, nor TPs were significantly different between PSEs and RSEs (Wilcoxon rank-sum test, P $\leq$ 0.05). However, PSEs tended to have more hyperpolarized NOPs (mdn = - 59.3 mV, iqr = - 49.4 - - 68.2 mV, four transitions) compared to RSEs (mdn = - 53.3 mV, iqr = - 48.0 - - 58.2 mV, 20 transitions), indicating absent excitation of PS muscles and tonic excitation of RS muscles at a silent state.
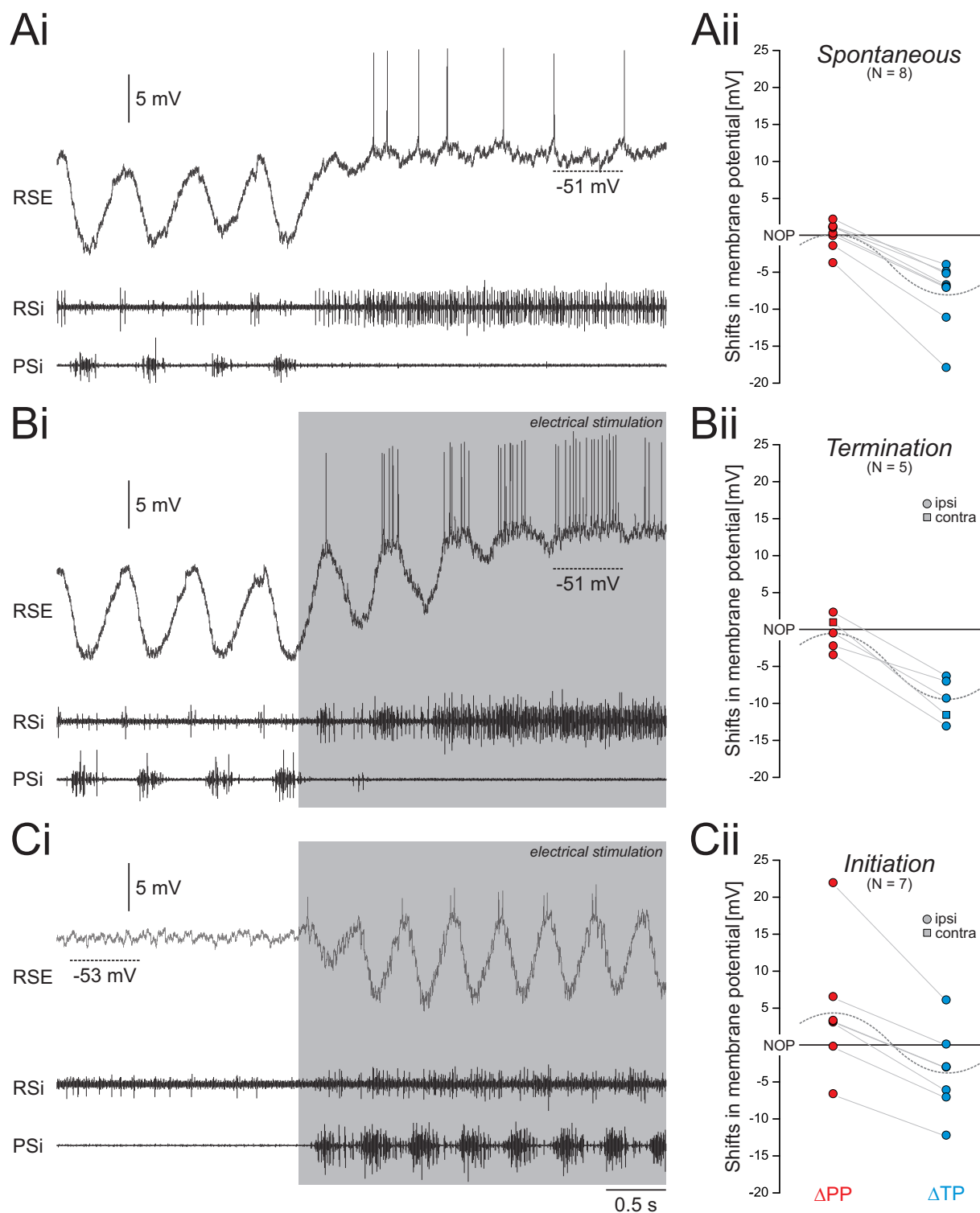
Figure 3.20: Activity transitions of RSE (N = 14), induced through stimulations or spontaneously, showed consistent shifts in the membrane potential. Examples and analyzed parameters (ΔPP (red) and ΔTP (blue) relative to the NOP) for all recorded neurons are presented for each kind of transition, i.e. spontaneous (**A**), termination (**B**), and initiation (**C**). Stimulations are depicted in gray. Dashed lines in (**A**ii), (**B**ii) and (**C**ii) indicate suggested V_m oscillations derived from mean values. **A:** Intracellular recordings of RSEs during spontaneous transition revealed a more depolarized V_m at a silent state and tonic RS activity of the corresponding hemiganglion. The NOP was at the level of PP during oscillations, suggesting absent inhibition of RSEs and tonic excitement of RS muscles at a silent state. **B:** During termination, the RSE shown in (**A**i) and additional RSEs showed similar shifts in V_m as described for spontaneous transition. **C:** During initiation, the V_m of RSE oscillated in antiphase with the PS. However, individual neurons showed variable shifts in their V_m, including the PP or the TP being at the level of the NOP. **RSE** *power stroke exciter*, **RSi** *ipsilateral return stroke*, **PSi** *ipsilateral power stroke*, **V_m** *membrane potential*, **NOP** *non-oscillating potential*, **PP** *peak potential*, **TP** *trough potential*.
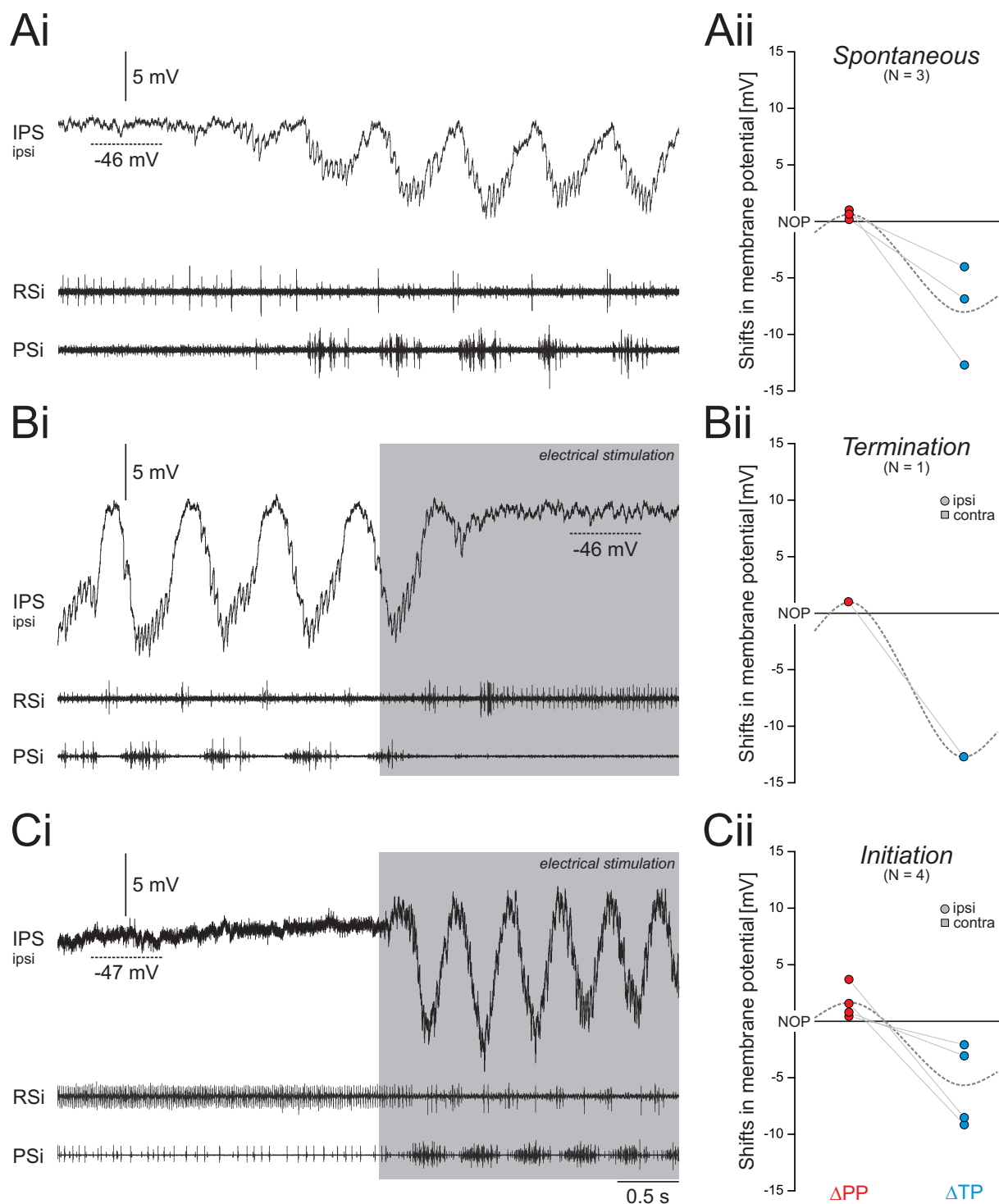
Table 3.5: Analyzed parameters of activity transitions in motor neurons. Data was pooled for the three types of transition (spontaneous, termination, initiation) and refers to parameters presented in figures 3.19 (Power stroke exciters, PSE) and 3.20 (Return stroke exciters, RSE). For RSEs, peak potentials (PP) and trough potentials (TP) were tested against the non-oscillating potential (NOP, Wilcoxon signed rank test). PSE were not tested due to the small sampling size. **T** *number of transitions*.

	[mV]	T	mean ± SD	range	Q1	median	Q3	P
	NOP		- 58.8 ± 10.9	(- 48.1) - (- 68.6)	- 49.4	- 59.3	- 68.2	
PSE (N = 3)	*PP*	4	- 53.9 ± 13.1	(- 40.0) - (- 65.1)	- 42.7	- 55.2	- 65.1	
	TP		- 59.0 ± 10.9	(- 49.2) - (- 68.4)	- 49.6	- 59.1	- 68.4	
	NOP		- 53.0 ± 6.5	(- 41.3) - (- 65.9)	- 48.0	- 53.3	- 58.2	
RSE (N = 14)	*PP*	20	- 51.6 ± 6.6	(- 36.9) - (- 62.9)	- 48.2	- 51.7	- 57.1	0.348
	TP		- 59.9 ± 4.5	(- 50.0) - (- 69.1)	- 57.4	- 59.9	- 62.7	**0.001**

CPG neurons

I recorded from seven IPSs that were characterized as either IPS *tangent* or IPS *orthogonal* by their morphology. The third type, IPS *wedge*, was not recorded. In parallel to PSEs, shifts in V_m were consistent across individual IPSs, with no differences between the types of transition (Figure 3.21). In contrast to PSEs, NOPs were at the level of PPs, suggesting either tonic excitation during a silent state or phasic inhibition during an active state. During oscillations at an active state, depolarizations in IPSs V_m causes inhibition of PSEs. Consequently, NOPs at the level of PPs in IPSs suggest tonic inhibition of PS muscles at a silent state. In contrast to those observations, pooled datasets, including each type of transition, revealed significant differences both between the NOPs and PPs, and between the NOPs and TPs (Wilcoxon signed rank test, $P \leq 0.05$, eight transitions). However, NOPs (mdn = - 45.4 mV, iqr = - 44.3 - - 50.1 mV, eight transitions) were only slightly more depolarized compared to PPs (mdn = - 44.4 mV, iqr = - 42.9 - - 49.2 mV, eight transitions).

Figure 3.21: Activity transitions of IPS (N = 7), induced through stimulations or spontaneously, showed consistent shifts in the membrane potential. Examples and analyzed parameters (ΔPP (red) and ΔTP (blue) relative to the NOP) for all recorded neurons are presented for each kind of transition, i.e. spontaneous (**A**), termination (**B**), and initiation (**C**). Stimulations are depicted in gray. Dashed lines in (**A**ii), (**B**ii) and (**C**ii) indicate suggested V_m oscillations derived from mean values. **A:** Intracellular recordings of IPS during spontaneous transition revealed a more hyperpolarized V_m during PS activity of the corresponding hemiganglion. The NOP was at the level of PP during oscillations, suggesting absent inhibition in a silent state of the system. **B:** During termination, the MV of the IPS shown in (**A**i) depolarized. The NOP was at the level of PP during oscillations. **C:** During initiation, the V_m of IPSs revealed similar shifts in V_m as described for spontaneous transition or termination. **IPS** *inhibitor of power stroke*, **RSi** *ipsilateral return stroke*, **PSi** *ipsilateral power stroke*, V_m *membrane potential*, **NOP** *non-oscillating potential*, **PP** *peak potential*, **TP** *trough potential*.

I recorded from four IRSs that were characterized as IRS *nohook* by their morphology. The second type, IPS *hook*, was not recorded. IRSs revealed the most diverse shifts in V_m, both in terms of the type of transition as well as regarding the recording side with respect to stimulation electrode (Figure 3.22). The NOP of one contralateral IRS was at the level of the PP, both during spontaneous transition and initiation. In contrast to that, NOPs of ipsilateral IRSs were at the level of TPs during termination (N = 1) and initiation (N = 1). In another ipsilaterally recorded IRS, the NOP was at the level of the PP during initiation. Across all experiments, NOPs were neither significantly different to the PPs (P = 0.062), nor to the TPs (P = 0.125) (Wilcoxon signed rank test, P $\leq$ 0.05, five transitions). Instead, NOPs (mdn = - 53.2 mV, iqr = - 47.8 - - 56.4 mV, five transitions) tended to be in between PPs (mdn = - 49.9 mV, iqr = - 45.6 - - 52.1 mV, five transitions) and TPs (mdn = - 60.9 mV, iqr = - 60.4 - - 61.4 mV, five transitions).

The absolute values of NOPs, PPs and TPs are presented as pooled data for IPS and IRS in table 3.5, independent of the type of transition or the recording sites with respect to the stimulation electrode.

Table 3.6: Analyzed parameters of activity transitions in CPG neurons. Data was pooled for the three types of transition (spontaneous, termination, initiation) and refers to parameters presented in figures 3.21 (Inhibitors of power stroke, IPS, N = 7) and 3.22 (Inhibitors of return stroke, IRS, N = 4). Peak potentials (PP) and trough potentials (TP) were tested against the non-oscillating potential (NOP, Wilcoxon signed rank test). **T** *number of transitions*.

	[mV]	T	mean ± SD	range	Q1	median	Q3	P
	NOP		- 47.4 ± 4.7	(- 42.9) - (- 57.0)	- 44.3	- 45.4	- 50.1	
IPS (N = 7)	*PP*	8	- 46.3 ± 5.1	(- 40.9) - (- 56.2)	- 42.9	- 44.4	- 49.2	**0.001**
	TP		- 54.5 ± 5.0	(- 45.0) - (- 60.1)	- 51.6	- 55.8	- 58.1	**0.001**
	NOP		- 52.8 ± 7.1	(- 44.3) - (- 62.4)	- 47.8	- 53.2	- 56.4	
IRS (N = 4)	*PP*	5	- 48.5 ± 6.3	(- 39.2) - (- 55.6)	- 45.6	- 49.9	- 52.1	0.062
	TP		- 58.1 ± 6.7	(- 46.1) - (- 61.6)	- 60.4	- 60.9	- 61.4	0.125
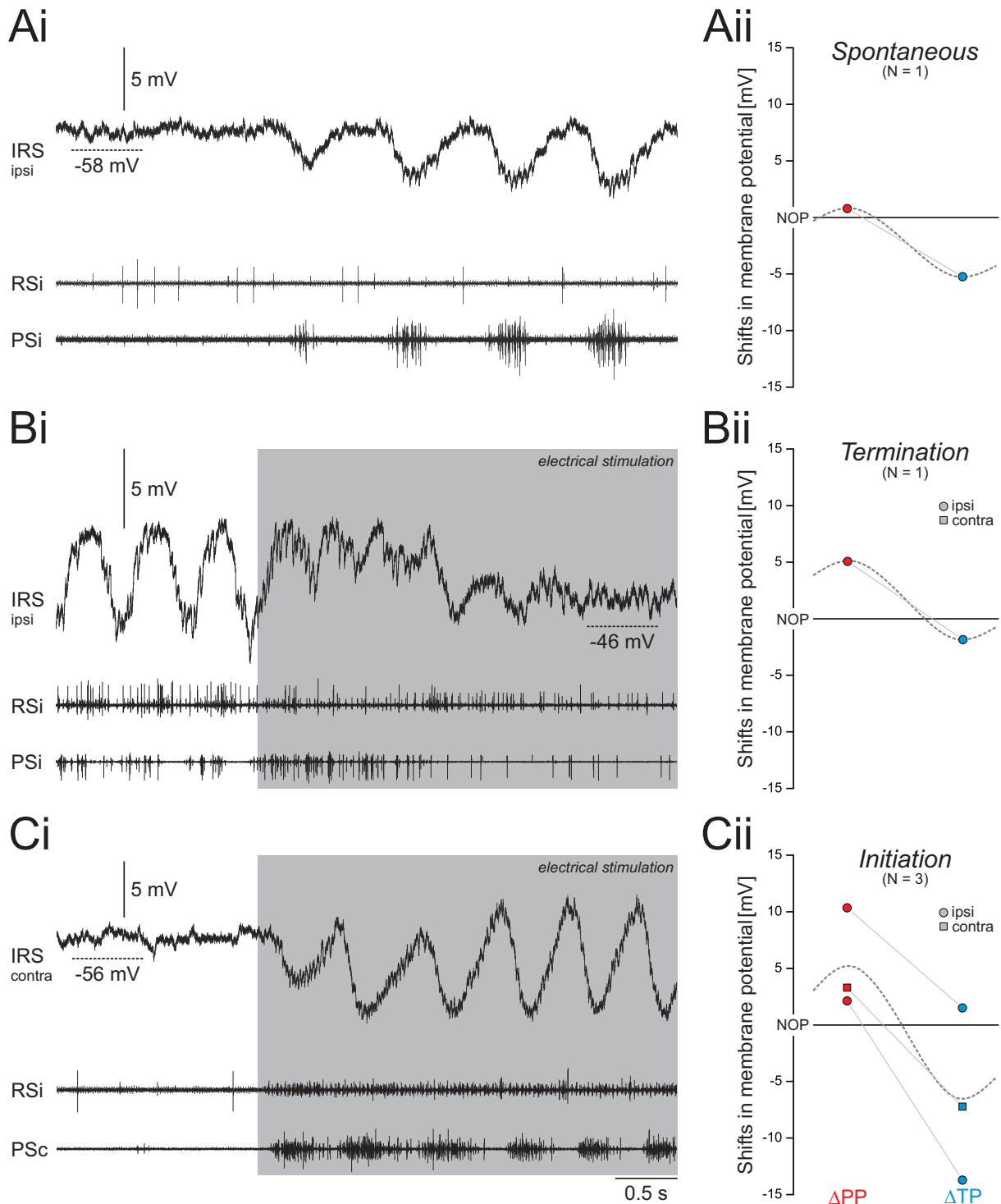
Figure 3.22: Activity transitions of IRS (N = 4), induced through stimulations or spontaneously, showed variable shifts in the membrane potential. Examples and analyzed parameters (ΔPP (red) and ΔTP (blue) relative to the NOP) for all recorded neurons are presented for each kind of transition, i.e. spontaneous (**A**), termination (**B**), and initiation (**C**). Stimulations are depicted in gray. Dashed lines in (**A**ii), (**B**ii) and (**C**ii) indicate suggested V_m oscillations derived from mean values. **A:** Intracellular recording of one IRS during spontaneous transition revealed a hyperpolarized V_m during PS activity of the corresponding hemiganglion. The NOP was at the level of PP during oscillations, suggesting absent inhibition in a silent state of the system. **B:** During termination, the V_m of one IRS hyperpolarized. The NOP was at the level of TP during oscillations. **C:** During initiation, the V_m of IRSs oscillated during PS activity. However, individual neurons showed variable shifts in their V_m, including the PP or the TP being at the level of the NOP. **IPS** *inhibitor of power stroke*, **RSi** *ipsilateral return stroke*, **PSi** *ipsilateral power stroke*, **PSc** *contralateral power stroke*, **V_m** *membrane potential*, **NOP** *non-oscillating potential*, **PP** *peak potential*, **TP** *trough potential*.

3.3.2 Enhancement on a cellular level

In a subset of experiments, I intracellularly recorded both, motor neurons and CPG neurons during enhancement of fictive locomotion. Enhancement was reflected by decreased periods and increased burst strengths (Chapter 3.2.3). I further demonstrated that the increase in burst strength included a side specific component (Chapter 3.2.4) and assumed that ipsi- and contralateral neurons are differently affected during enhancement. Therefore, I did not pool the data and will describe my observations qualitatively. Analyzed parameters (means ± SD) of individual motor neurons (Table 5.2) and CPG neurons (Table 5.3) are given in the appendix.

Motor neurons

Periods of V_m oscillations of both PSEs (N = 3 / 3, Figure 3.23) and RSEs (N = 5 / 5, Figure 3.24) decreased during enhancement, independent of the recording site. In contrast, amplitudes of V_m oscillations increased in ipsilateral motor neurons (PSE: N = 2 / 2, RSE: N = 3 / 4) but decreased in contralateral motor neurons (PSE: N = 1 / 1, RSE: N = 1 / 1). This is in line with the side specific effect of enhancement, observed on the system's level. PS bursts ipsilateral to the stimulation electrode were more strengthened than PS bursts on the contralateral side, indicating stronger excitation of the respective PS motor neuron pools.

Figure 3.23 A illustrates the enhancement of V_m oscillations in one representative PSE recorded ipsilateral to the stimulation electrode. During the electrical stimulation of an axon bundle, the V_m depolarized and oscillation period decreased (Pre-Stim: 0.71 ± 0.05 s; Stim: 0.49 ± 0.01 s). Simultaneously, the oscillation amplitude (Pre-Stim: 6.4 ± 0.6 mV; Stim: 10.8 ± 0.3 mV) and the number of spikes per burst increased (Pre-Stim: 8.7 ± 1.0; Stim: 14.5 ± 1.0).
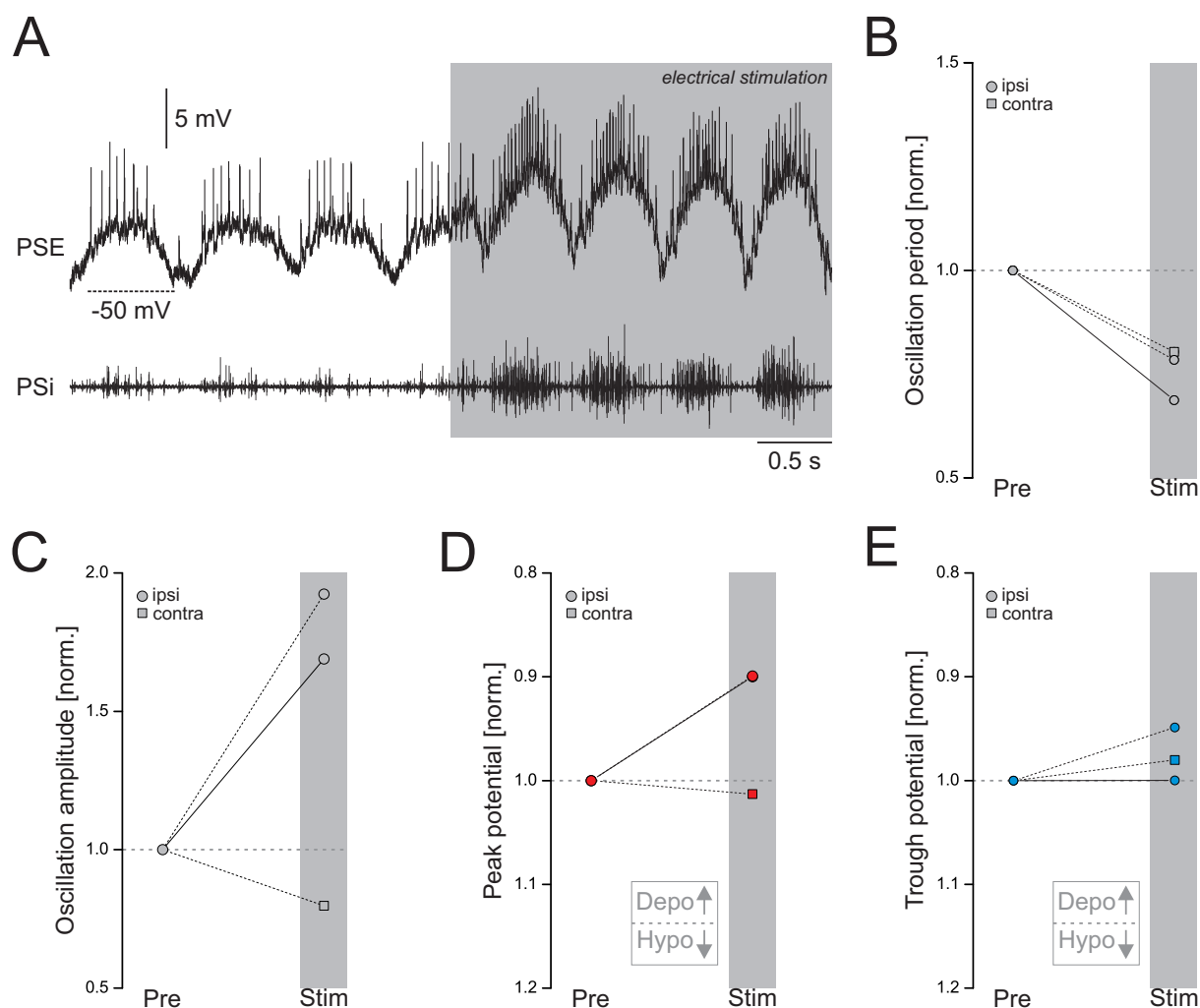
Figure 3.23: Effects on PSE membrane potential oscillations during enhancement of fictive locomotion. **A:** Intracellular recording of one PSE during enhancement of fictive locomotion. The stimulation is depicted in gray. **B-E:** Oscillation period, oscillation amplitude, peak potential (red), and trough potential (blue) of three PSEs normalized to pre-stimulus condition. The analyzed parameters of the PSE presented in (**A**) are depicted by solid lines in the graphs. The oscillation period of all PSEs decreased during enhancement. Oscillation amplitude increased in PSEs recorded ipsilateral to the stimulation electrode, but decreased in one PSE recorded on the contralateral side. The decrease was reflected by a more hyperpolarized PP and a more depolarized TP. **PSE** *power stroke exciter*, **PSi** *ipsilateral power stroke*, **V_m** *membrane potential*, **NOP** *non-oscillating potential* **PP** *peak potential*, **TP** *trough potential*.

Figure 3.24 A illustrates the enhancement of one representative RSE recorded ipsilateral to the stimulation electrode. During the electrical stimulation of an axon bundle, the oscillation period decreased (Pre-Stim: 0.58 ± 0.03 s; Stim: 0.39 ± 0.01 s). Simultaneously, the oscillation amplitude increased (Pre-Stim: 5.3 ± 0.5 mV; Stim: 16.2 ± 0.9 mV) and the V_m was depolarized above the spiking threshold (5.9 ± 0.7 Spikes / burst).
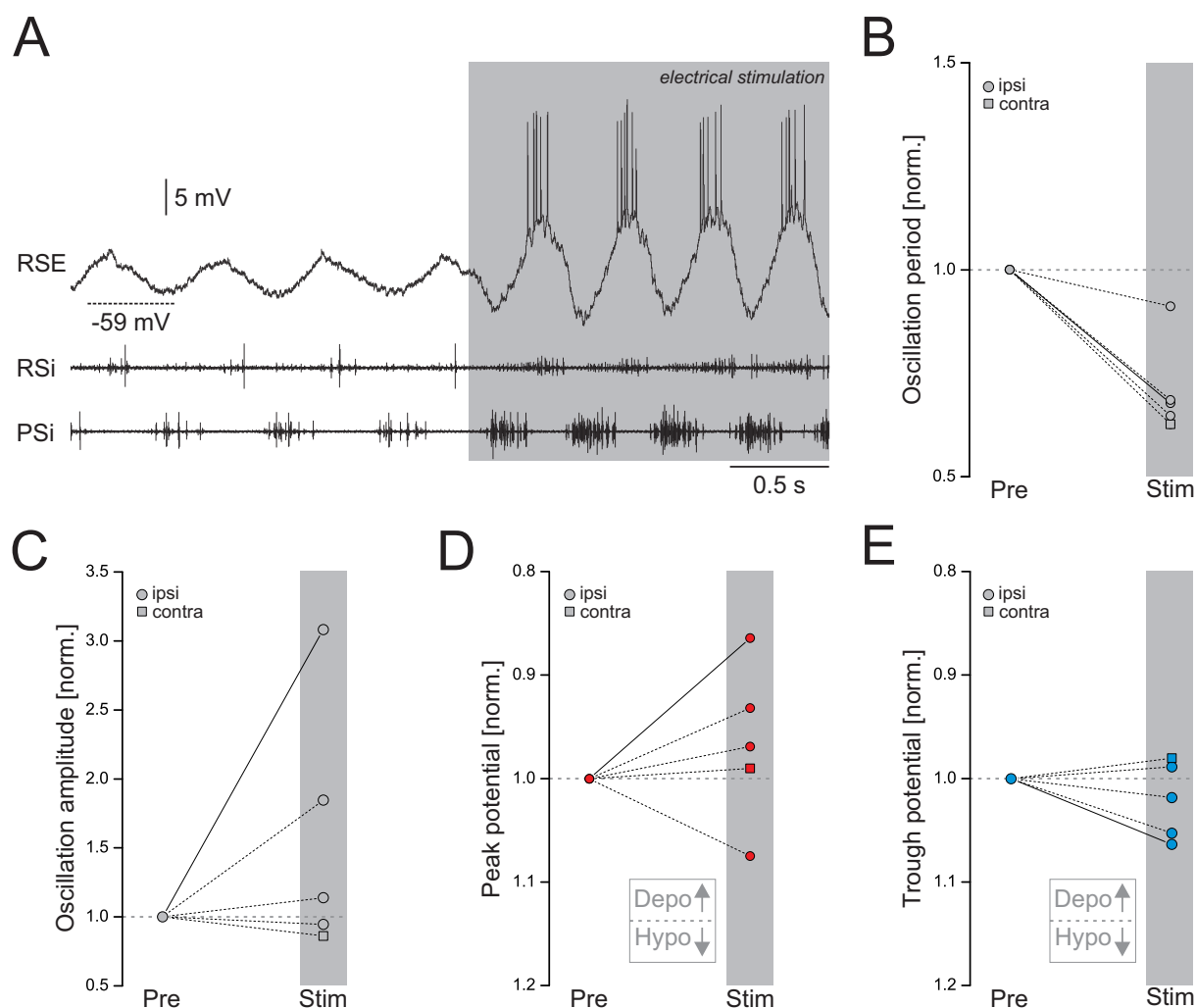
Figure 3.24: Effects on RSE membrane potential oscillations during enhancement of fictive locomotion. **A:** Intracellular recording of a RSE during enhancement of fictive locomotion. The stimulation is depicted in gray. **B-E:** Oscillation period, oscillation amplitude, peak potential (red), and trough potential (blue) of five RSEs normalized to pre-stimulus condition. The analyzed parameters of the RSE presented in (**A**) are depicted by solid lines in the graphs. The oscillation period of all RSEs decreased during enhancement. Oscillation amplitude increased in 3 out of 4 PSEs recorded ipsilateral to the stimulation, but decreased in one PSE recorded on the contralateral side. Both PP and TP were more depolarized in this PSE during enhancement. **PSE** *power stroke exciter*, **RSi** *ipsilateral return stroke*, **PSi** *ipsilateral power stroke*, **V_m** *membrane potential*, **NOP** *non-oscillating potential*, **PP** *peak potential*, **TP** *trough potential*.

CPG neurons

In parallel to motor neurons, periods of V_m oscillations of IPSs (N = 2 / 2, figure 3.25) and IRSs (N = 3 / 3, figure 3.26) decreased during enhancement. I recorded two IPSs ipsilateral to the stimulation electrode, one showed increased and the other decreased amplitudes of V_m oscillations. One ipsilateral IRS increased its amplitude of V_m oscillations during enhancement while amplitudes in two contralateral IRSs increased and decreased, respectively. Figure 3.25 A illustrates the increase of V_m oscillations in one representative IPS recorded ipsilateral to the stimulation electrode. During stimulation, the PP slightly depolarized and the oscillation period decreased (Pre-Stim: 0.75 ± 0.10 s; Stim: 0.44 ± 0.04 s). Simultaneously, the oscillation amplitude increased (Pre-Stim: 6.4 ± 0.8 mV; Stim: 13.7 ± 0.5 mV).
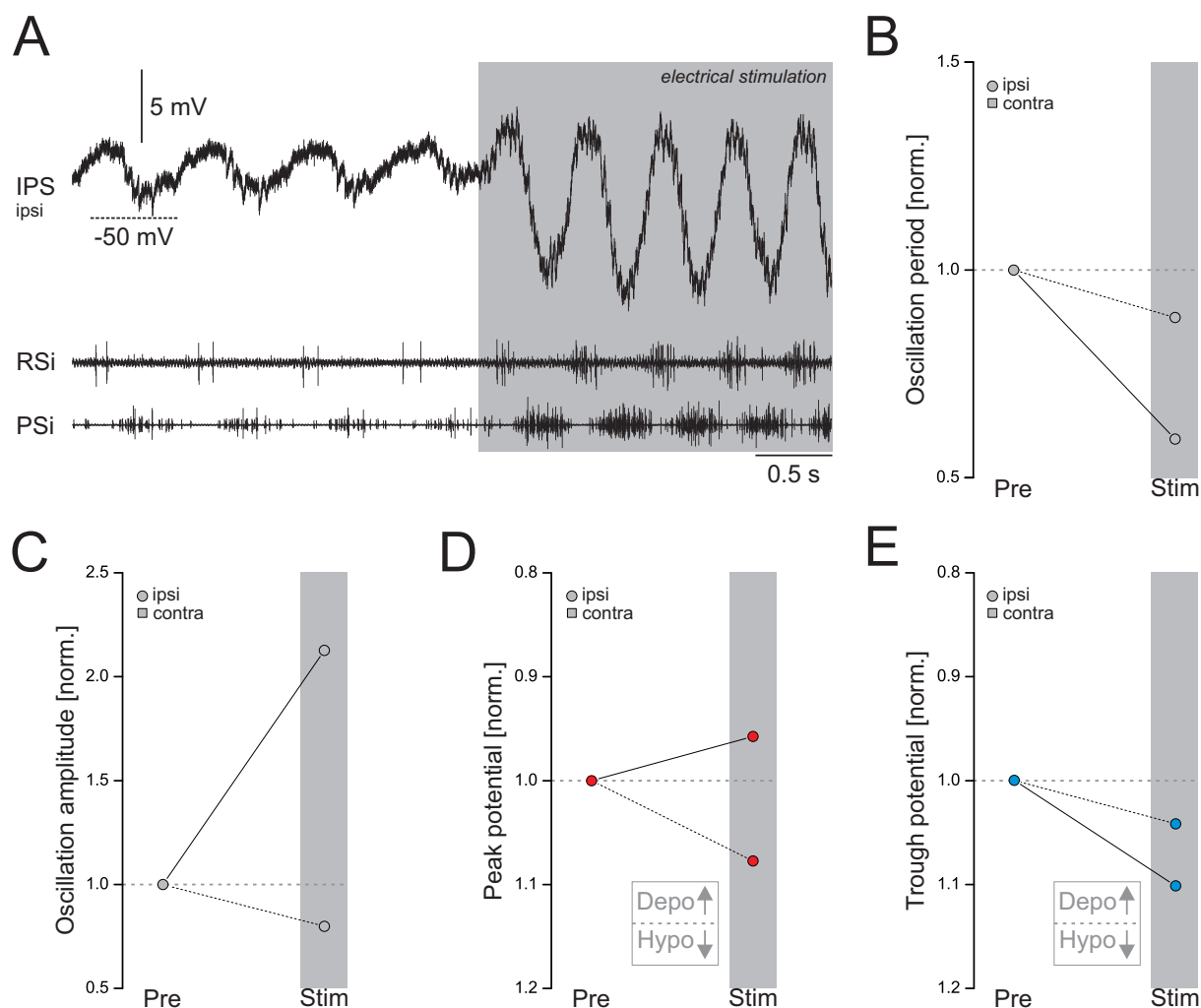
Figure 3.25: Effects on IPS membrane potential oscillations during enhancement of fictive locomotion. **A:** Intracellular recording of one IPS during enhancement of fictive locomotion. The stimulation is depicted in gray. **B-E:** Oscillation period, oscillation amplitude, peak potential (red), and trough potential (blue) of two IPSs normalized to pre-stimulus condition. The parameters of the IPS presented in (**A**) are depicted by solid lines in the graphs. The oscillation period of both IPSs decreased during enhancement. Oscillation amplitude increased in one IPS and decreased in the other one. **PSE** *power stroke exciter*, **RSi** *ipsilateral return stroke*, **PSi** *ipsilateral power stroke*, **V$_m$** *membrane potential*, **NOP** *non-oscillating potential*, **PP** *peak potential*, **TP** *trough potential*.

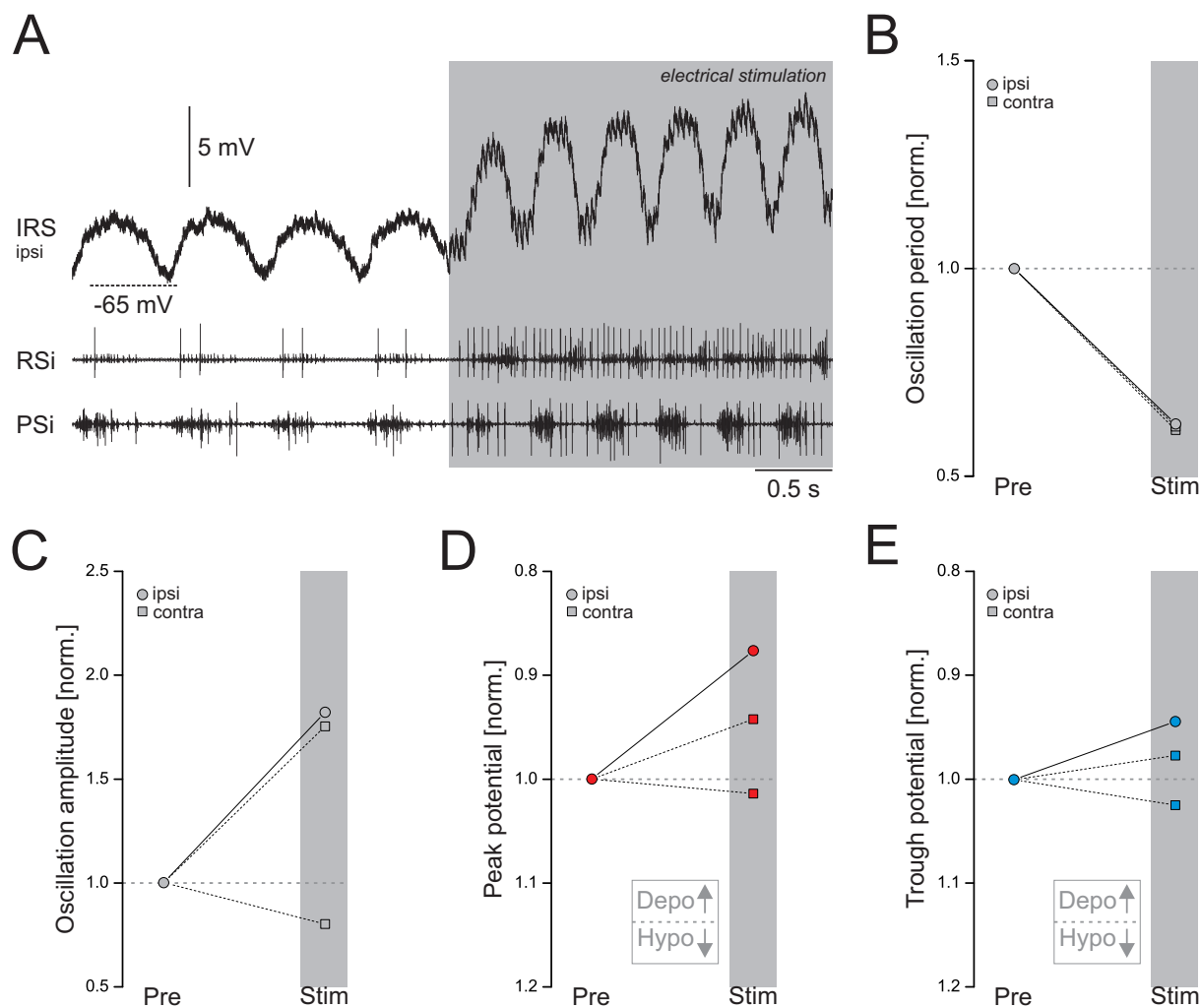Figure 3.26 A illustrates the enhancement of one representative IRS recorded ipsilateral to the stimulation electrode. During stimulation, the V_m depolarized and the oscillation period decreased (Pre-Stim: 0.60 ± 0.02 s; Stim: 0.37 ± 0.01 s). Simultaneously, the oscillation amplitude increased (Pre-Stim: 4.7 ± 0.2 mV; Stim: 8.5 ± 0.3 mV).

Figure 3.26: Effects on IRS membrane potential oscillations during enhancement of fictive locomotion. **A:** Intracellular recording of one IRS during enhancement of fictive locomotion. The stimulation is depicted in gray. **B-E:** Oscillation period, oscillation amplitude, peak potential (red), and trough potential (blue) of three IRSs normalized to pre-stimulus condition. The parameters of the IRS presented in (**A**) are depicted by solid lines in the graphs. The oscillation period of all IRSs decreased during enhancement. Oscillation amplitude increased in two and decreased in one IRS. **PSE** *power stroke exciter*, **RSi** *ipsilateral return stroke*, **PSi** *ipsilateral power stroke*, **NOP** *non-oscillating potential*, **PP** *peak potential*, **TP** *trough potential*.

3.3.3 IRS is directly targeted by descending pathways

The alternating activity of PS and RS motor neurons drives the periodic muscle activity of the swimmeret system. Since this neuronal activity is solely achieved by graduated inhibition from the CPG neurons, IPS and IRS are likely targets of descending control without any additional input on the motor neurons as a prerequisite. In addition, the bilateral stimulation effects observed during initiation suggested the possibility that descending pathways affect the swimmeret microcircuits in a unilateral fashion, i.e. CPGs ipsilateral and contralateral to the stimulation being affected differently.

In contrast to indirect targeting of neurons, e.g. by unspecific transmitter release within the lateral neuropil, direct input is carried out by direct synaptic contact which can generate postsynaptic potentials (PSP) in the targeted neurons. During intracellular recordings, I observed PSPs during initiation or enhancement of fictive locomotion in IPSs (N = 5 / 5). However, these PSPs were not correlated with the stimulation and therefore did not further suggest direct synaptic input on IPS (data not shown). Since both groups of CPG interneurons are reciprocally inhibiting each other's activity, affecting the activity of one group consequently modulates the activity of the other group as well. I intracellularly recorded from three IRS during the initiation of fictive locomotion through electrical stimulation. All three neurons were characterized as IRS *nohook* by their morphology. The second type, IPS *hook*, was not recorded. Indeed, stimulus-correlated PSPs were present in IRSs but only when recorded ipsilateral to the stimulation (N = 2 / 2).

Figure 3.27 illustrates this unilateral targeting by showing intracellular recordings of one ipsilateral (Figure 3.27 A) and one contralateral IRS (Figure 3.27 B). Both neurons were recorded in the same ganglion and fictive locomotion was initiated by identical stimulation parameters. I made overdraws of the intracellular recordings, triggered to individual stimulation pulses (n = 256) and found stimulus-triggered PSPs. Please note that during the initiation of fictive locomotion the V_m of IRS showed large oscillations. Therefore, the stimulus-triggered PSPs seem to be masked by the V_m fluctuations. However, a distinct PSP is depicted by the average of the overdraw in the ipsilateral IRS (latency: 8.8 ms, amplitude: 0.6 mV at - 54.3 mV, figure 3.27 Aiii), but no such stimulus-triggered PSP can be seen in the contralateral IRS (Figure 3.27 Biii).
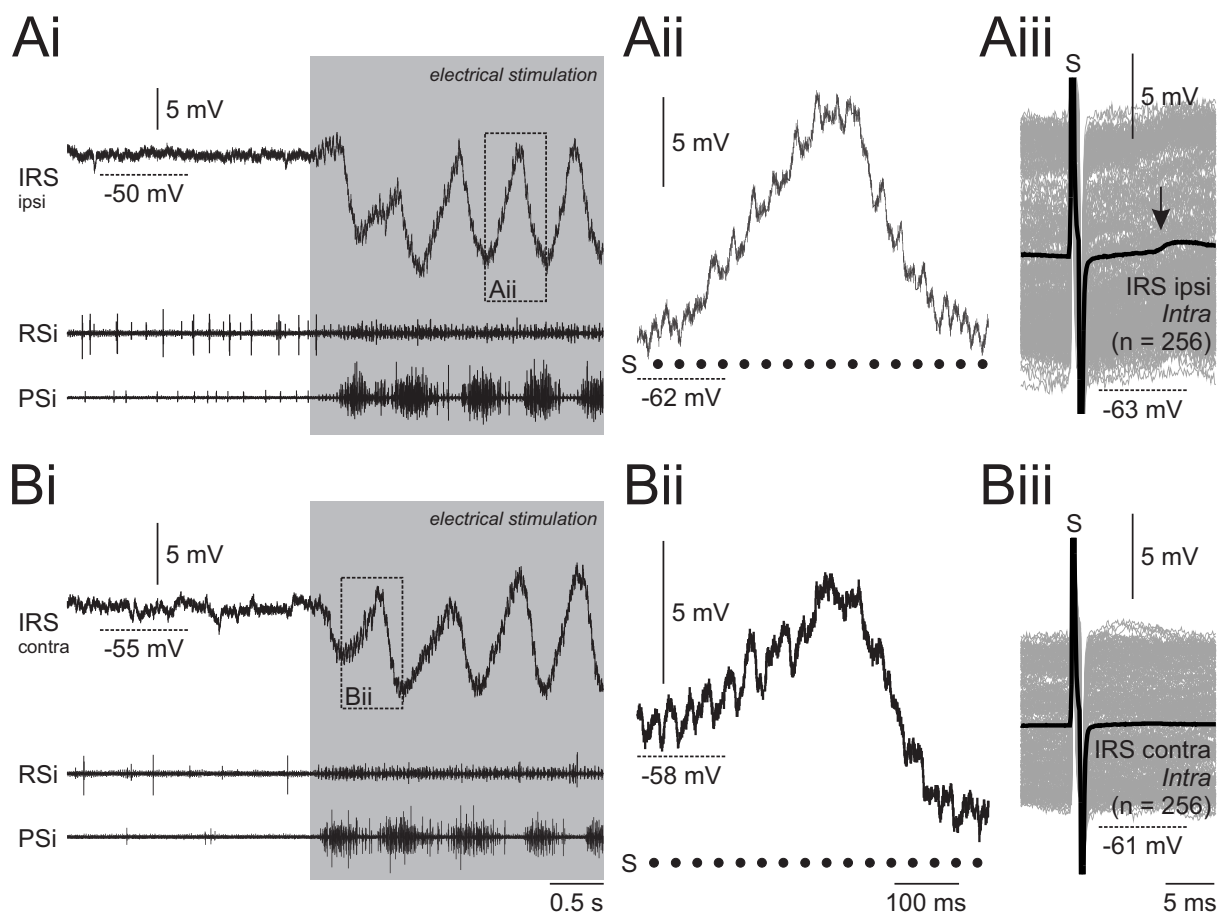
Figure 3.27: Individual stimulation pulses evoked postsynaptic potentials (PSP) only in IRS recorded ipsilateral to the stimulation. Stimulations are depicted in gray. Please note that both IRS were recorded in the same ganglion and experiment. **A:** Intracellular recording of one ipsilateral IRS during initiation of fictive locomotion, illustrating PSPs during V_m oscillations (**Aii**). An stimulus-triggered overdraw (**Aiii**, n = 256, black line indicates the average) demonstrating the correlation of individual stimulation pulses (s) with PSPs (arrow, latency: 8.8 ms, amplitude: 0.6 mV). **B:** Within the same ganglion, one IRS recorded contralateral also revealed PSPs during V_m oscillations (**Bii**). However, these PSPs were not correlated with the stimulation (**Biii**). **IRS** *inhibitor of return stroke*, **RSi** *ipsilateral return stroke*, **PSi** *ipsilateral power stroke*, **S** *stimulus artifact*, **PSP** *postsynaptic potential*, V_m *membrane potential*.

Another IRS recorded ipsilateral to the stimulation is shown in Figure 3.28. During stimulation with a low amplitude, the V_m was tonically depolarized but did not oscillate. The stimulus amplitude was below the threshold for the initiation of fictive locomotion but increased the spiking activity of both RS and PS motor neurons (Figure 3.28 Ai). During this stimulation, I recorded stimulus-correlated action potentials at the level of cA5/A6, indicating the recruitment of one descending neuron (Figure 3.28 Aii). I further detected stimulus-correlated PSPs in IRS (Aiii, latency: 9.2 ms, amplitude: 0.9 mV at - 61.0 mV). In the same experiment, a higher stimulation amplitude initiated fictive locomotion in the swimmeret system and V_m oscillations in IRS (Figure 3.28 B). The increased stimulation amplitude recruited one additional descending neuron (Figure 3.28 Bii). Analogously, one additional PSP was evoked in IRS (3.28 Biii, latency: 4.1 ms, amplitude: 1.4 mV at - 57.6 mV). I additionally recorded from the same neuron during

enhancement of fictive locomotion through stimulation of the same axon bundle. This stimulation also evoked both PSPs and is illustrated in figure 5.2 (appendix). On the one hand, this experiment further demonstrated direct targeting of one ipsilateral IRS by descending input. On the other hand, the results indicate that the increased stimulation amplitude activated a second descending pathway and that both pathways may be necessary to initiate fictive locomotion.
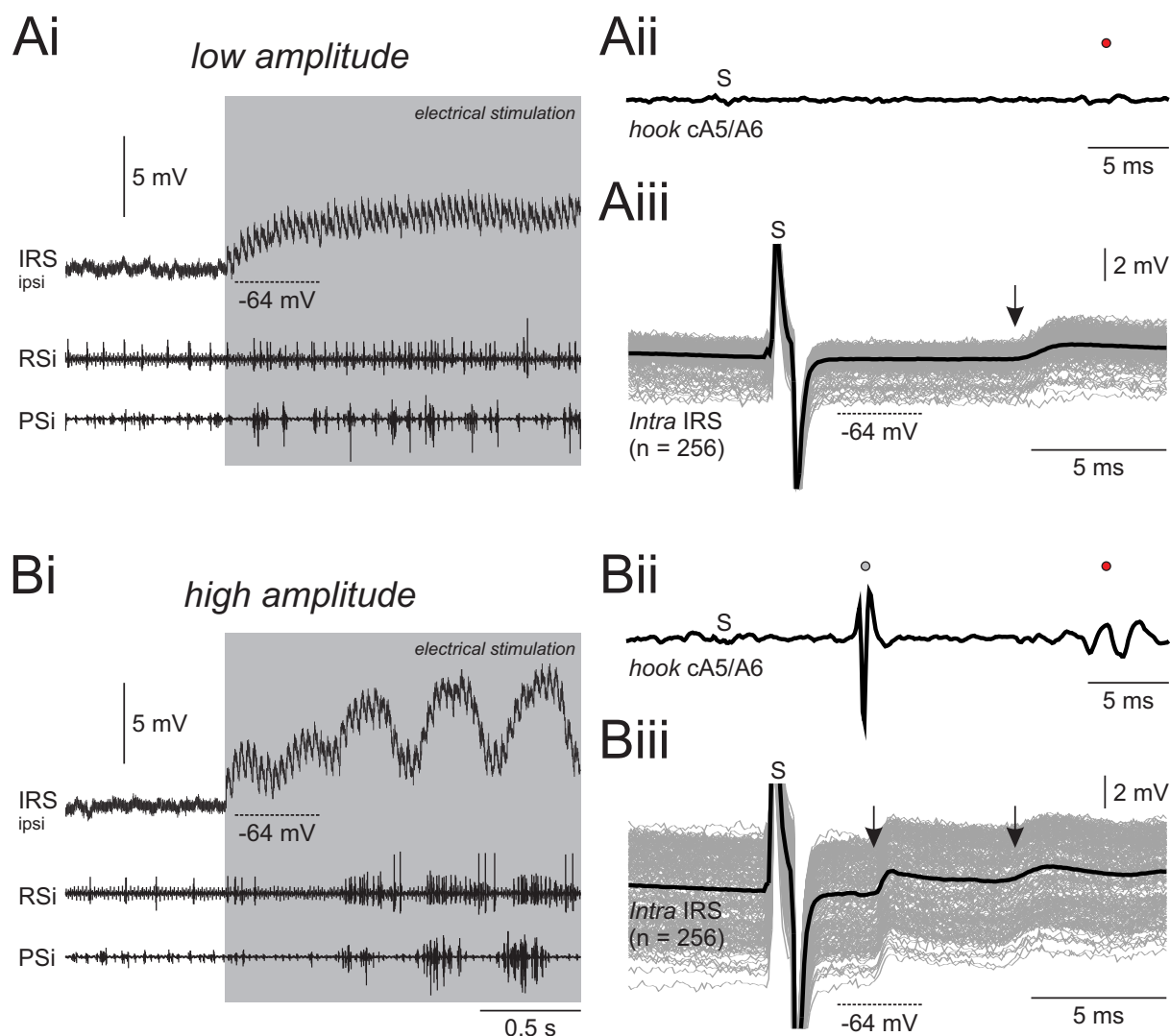
Figure 3.28: Generation of two distinct postsynaptic potentials (PSP), elicited by the stimulation of the same axon bundle. Stimulations are depicted in gray. **A:** Intracellular recording of one ipsilateral IRS during subthreshold stimulation. Neither fictive locomotion nor V_m oscillations in IRS were present but the V_m depolarized. One single descending neuron was activated by the stimulation (red dot, **Aii**). An stimulus-triggered overdraw (n = 256, black line illustrates the average), illustrating the generation of a stimulus-triggered PSPs (arrow, latency: 9.2 ms, amplitude: 0.9 mV) in IRS (**Aiii**). **B:** Within the same experiment, a higher stimulation amplitude initiated fictive locomotion and V_m oscillations in IRS. This stimulation activated an additional descending neuron (gray dot**, Bii**). Analogously, one additional stimulus-triggered PSP (left arrow, latency: 4.1 ms, amplitude: 1.4 mV) was evoked in IRS (**Biii**). Please note the different time bars in (**Aii** / **Bii**) and (**Aiii** / **Biii**). **IRS** *inhibitor of return stroke*, **RSi** *ipsilateral return stroke*, **PSi** *ipsilateral power stroke*, **S** *stimulus artifact*, **PSP** *postsynaptic potential*.

## 3.4 Neuromodulators mimic the stimulation effects - to some extent

I successfully showed, that the activation of descending neurons modulates the motor output of the swimmeret system and strong indications are given that one group of CPG interneurons is directly targeted by this input. In order to better understand the mechanisms of this targeting, as well as possible effects on other neurons within the micro circuits, I performed further experiments addressing the question of potential neurotransmitters released by descending neurons. Previous studies suggested the release of proctolin (PR) and octopamine (OA), mainly since these substances were shown to initiate and terminate fictive locomotion, respectively [Mulloney et al., 1987; Acevedo et al., 1994]. However, further research showed that during initiation through electrical stimulation PR is released within the nervous tissue and that a subset of excitatory command neurons, i.e. E_A, E_C and E_E, contain PR [Acevedo, 1990]. In parallel to that, the effect of stimulations terminating fictive locomotion was strongly decreased by bath application of the OA antagonist phenylalanin [Mulloney et al., 1987]. Here, I present preliminary data, illustrating the effect of PR (Chapter 3.4.1) and OA (Chapter 3.4.2) on the swimmeret motor output and individual neurons. I performed both bath application to the entire chain of abdominal ganglia and focal application within single hemiganglia. Due to the small number of experiments and a low repetition rate, I qualitatively describe the effects within single experiments and present individual parameters (mean ± SD) to highlight important observations. Nevertheless, the results further contribute to both the clarification of potential neurotransmitters released by descending neurons and to the comparison with the effects of electrical stimulations.

3.4.1 Proctolin

The experiment presented in figure 3.29 illustrates the initiation of fictive locomotion by PR. The preparation initially expressed fictive locomotion that was absent at a later point of experimental procedure. Bath application of PR reactivated the preparation and initiated bursts of PS activity, propagating from posterior to anterior. Period (Spontan: 0.82 ± 0.07 s; PR: 0.75 ± 0.02 s) and burst strengths (PS3: normalized to Spontan; PR: 0.82 ± 0.04) decreased compared to spontaneous fictive locomotion. Within the same experiment, I intracellularly recorded one PS exciter (PSE) motor neuron. At a silent state of the swimmeret system, V_m oscillations were absent and the non-oscillating potential (NOP) at a comparatively hyperpolarized level around

the TP. PR application reinduced V_m oscillations at a more depolarized V_m (TP: Spontan: -74.4 ± 0.3 mV; PR: - 69.8 ± 0.3 mV) compared to spontaneous condition.
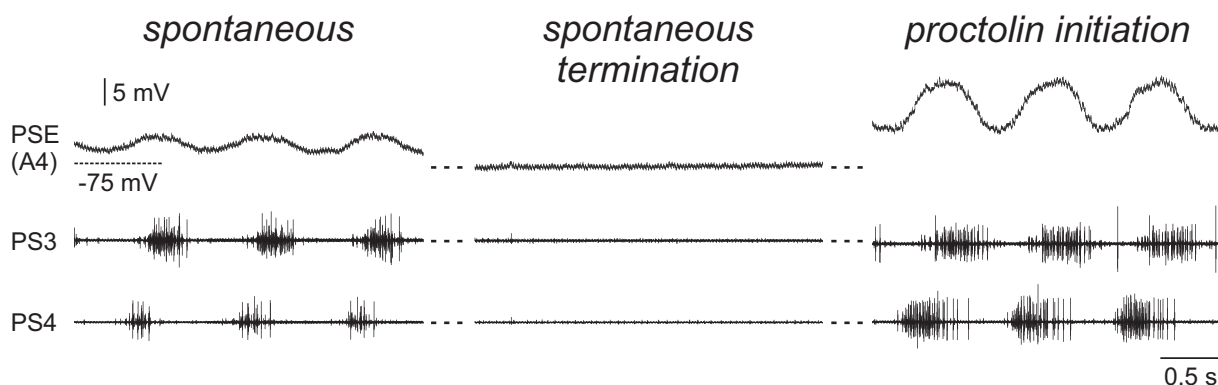
Figure 3.29: Intracellular recording of one PSE in A4 and extracellular recordings of PS activity in abdominal ganglia A3 and A4. Initially, the preparation spontaneously expressed fictive locomotion but was silent at a later point of experimental procedure. Bath application of proctolin reinduced fictive locomotion and membrane potential oscillations in PSE. **PSE** *power stroke exciter*, **PS3-4** *power stroke in ganglia A3 and A4.*

The experiment presented in figure 3.30 illustrates the enhancement of fictive locomotion by PR. The preparation initially expressed fictive locomotion that was enhanced by an electrical stimulation, reflected by decreased period (Spontan: 0.68 ± 0.03 s; Stim: 0.39 ± 0.01 s) and increased burst strengths by a factor of four (normalized to Spontan, Stim: 4.79 ± 0.44). At a later point of the experiment, bath application of PR increased burst strengths twofold (normalized to Spontan, PR: 2.37 ± 0.25) but increased period (PR: 0.75 ± 0.04 s).
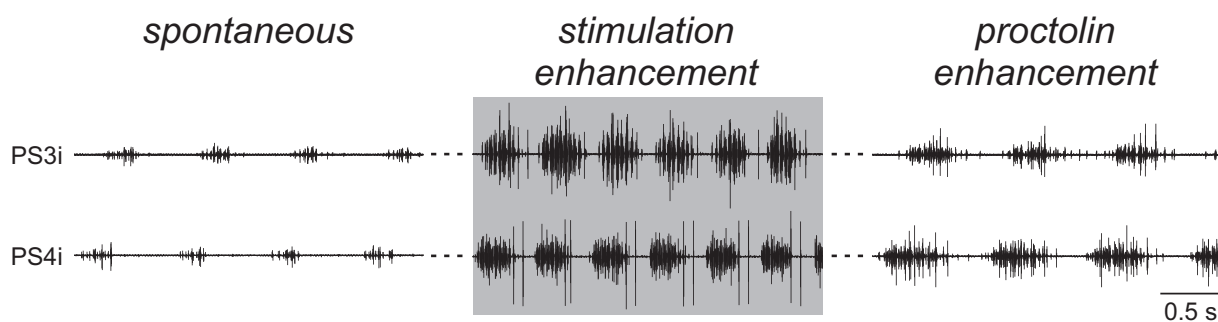
Figure 3.30: Extracellular recordings of PS activity in A3 and A4. The preparation was spontaneously active and both stimulation and bath application of proctolin enhanced fictive locomotion. **PS3i-4i** *ipsilateral power stroke in ganglia A3 and A4.*

Figure 3.31 illustrates focal application of PR within the lateral neuropil in a single hemiganglion. Application excited local PS motor neurons without effecting the other segments. Motor neurons were tonically active but I did not observe any bursts of PS activity after focal PR application. Fictive locomotion was not initiated by focal PR application.
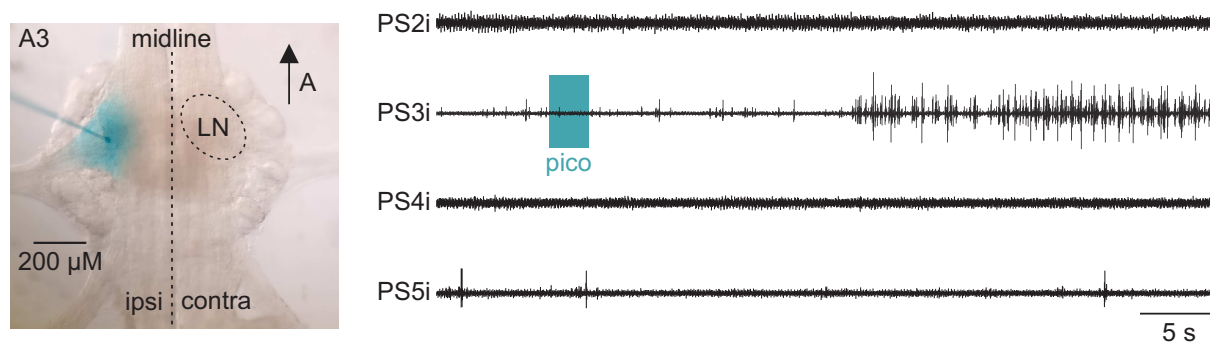
Figure 3.31: Focal application of proctolin within the LN excited PS motor neurons of the specific hemiganglion but neither PS bursting nor fictive locomotion was initiated. Please note that no excitation was present in other hemiganglia. **LN** *lateral neuropil*, **PS2i-5i** *ipsilateral power stroke in ganglia A2 to A5*.

Bath applications of PR and electrical stimulations evoked similar modulations of the swimmeret system's motor output in terms of initiation and enhancement of fictive locomotion. Therefore, I wanted to know if individual neurons within the stimulated axon bundles contain PR that might be released during stimulations. In three experiments, I successfully performed antibody labeling against PR and simultaneously labeled the stimulated axons (Figure 3.32). Stimulations in these experiments initiated fictive locomotion and cross sections of the connectives at the level of cA2/A3 revealed distinct, proctolinergic axons within the stimulation sites (Figure 3.32 Ai and B) or in close distance (Figure 3.32 C). Additional axons were occasionally labeled in different portions of the connectives. Further investigation of the axon locations was prevented due to strong tissue deformation within the histological development. The location indicated in figure 3.32 Aii should be handled with caution.
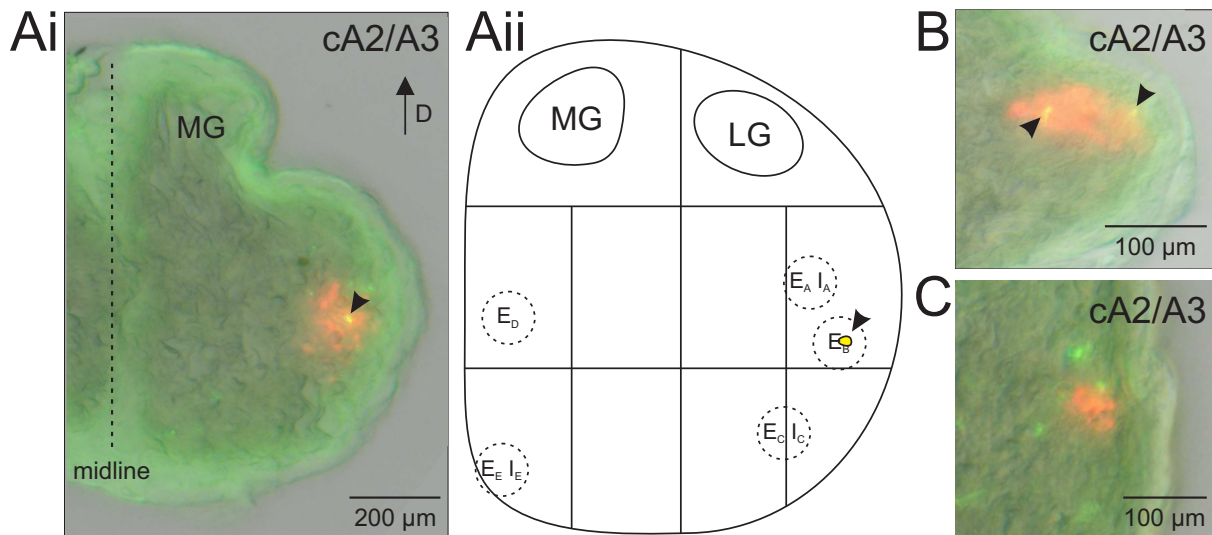
Figure 3.32: Proctolinergic axons were located within the stimulated axon bundles. **A:** Cross section of a connective at the level of cA2/A3. Antibody labeling against proctolin (green, Alexa Fluor 488) revealed double labeling with one axon (arrow head) in the stimulated and backfilled axon bundle (red, TRDA). Note, that additional proctolinergic axons are present within the ipsilateral hemiconnective. Stimulation initiated fictive activity and the stimulation site was in line with the location of command neurons introduced by Wiersma and Ikeda [1964] (**Aii**, dashed circles). **B, C:** Proctolinergic axons were present in two more preparations, either located within or close to the stimulation sites. **cA2/A3** *connective between ganglia A2 and A3*, **MG** *medial giant fiber*, **LG** *lateral giant fiber*, **E$_X$** *excitatory command neuron*, **I$_X$** *inhibitory command neuron*.

In one experiment, I additionally prepared whole mounts of the abdominal ganglia A1, A2, A3 and A6 (Figure 3.33). Distinct proctolinergic fibers were present in the abdominal connectives (Figure 3.33 A). Dense PR-labeling was present in all hemiganglia, including the lateral neuropil (LN) (Figure 3.33 B and C). Within the LN, motor neurons and CPG interneurons project their dendritic processes and perform synaptic interactions and reflect potential targets of PR. In addition, I observed one medial pair of proctolinergic axons projecting until A6 (Figure 3.33 D). These results prove that during initiation, stimulated axon bundles contained distinct proctolinergic axons that potentially projected throughout the entire abdominal nervous system. During stimulations, the terminals of these axons may released PR within the abdominal ganglia as indicated by Acevedo [1990].
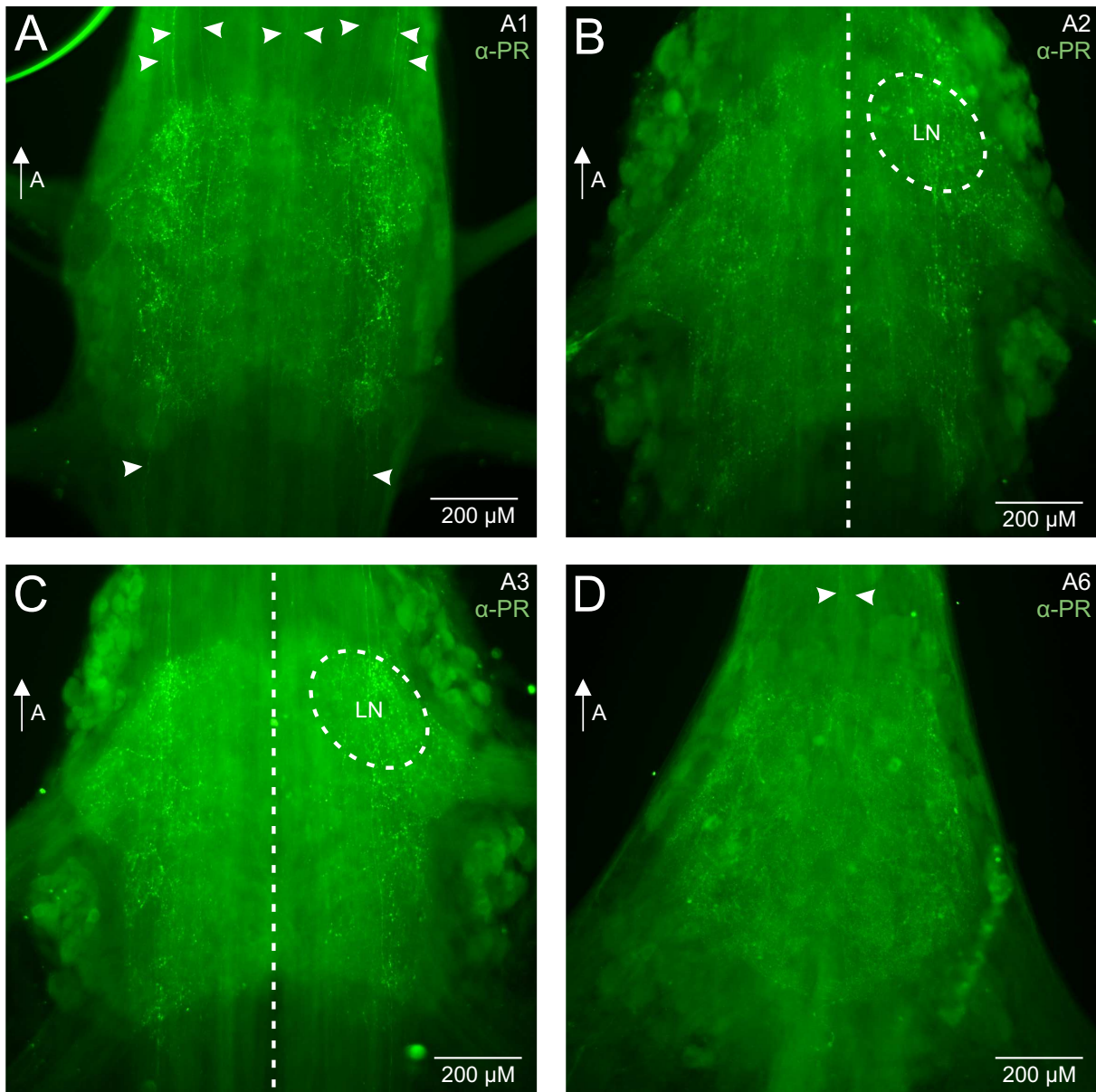
Figure 3.33: Whole mounts of abdominal ganglia. Dorsal views. Dashed lines indicate midline. **A-D**: Antibody labeling against proctolin (green, Alexa Fluor 488) revealed proctolinergic axons (arrowheads), projecting throughout the entire abdominal nervous system (highlighted in A1 and A6). In addition, dense labeling was present in all abdominal ganglia, including the lateral neuropil (highlighted in A2 and A3). **A1-6** *abdominal ganglia*, **LN** *lateral neuropil*.

3.4.2 Octopamine

The experiment presented in figure 3.34 illustrates the termination of fictive locomotion by OA. The preparation initially expressed fictive locomotion and bath application of OA silenced the swimmeret system. Simultaneous application of epinastine, a specific antagonist of OA, restored the initial motor output (Figure 3.34).
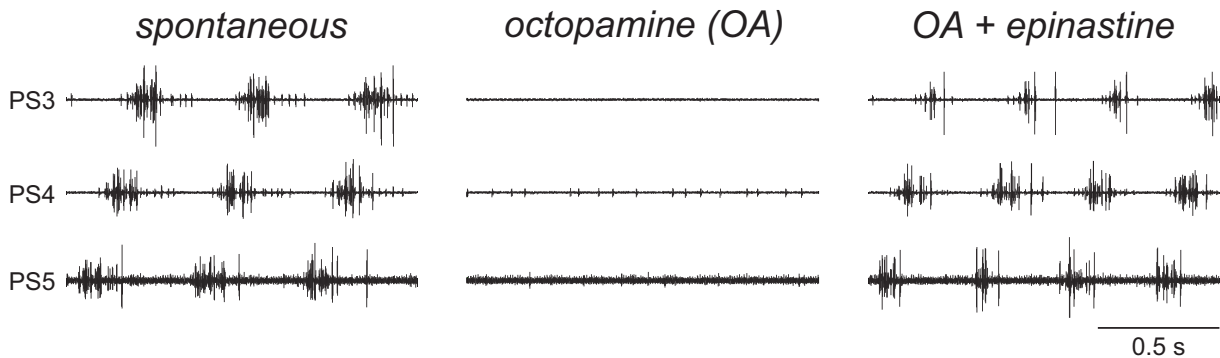
Figure 3.34: Extracellular recordings of PS activity in A3 to A5. Spontaneous fictive locomotion was terminated by bath application of octopamine (OA). Simultaneous application of epinastine, a specific OA antagonist, restored fictive locomotion. **PS3-5** *power stroke in ganglia A3 to A5*.

I intracellularly recorded from CPG neurons during bath application of OA in two experiments. OA completely terminated fictive locomotion and V_m oscillations of both neurons, i.e. one Inhibitor of PS (IPS, Figure 3.35 A) and one Inhibitor of RS (IRS, Figure 3.35 B), stopped at the depolarized phase. The non-oscillating potentials (NOP) were at the level of the peak potentials (PP) during oscillations, as also observed for spontaneous and stimulus-evoked transitions in IPS and IRS. In both experiments, I was able to bypass the termination induced by OA. Hyperpolarization of IPS reactivated rhythmic PS activity and V_m oscillations in the corresponding ganglion. In parallel, electrical stimulation of an axon bundle in the presence of OA still initiated fictive locomotion and associated V_m oscillations in IRS.
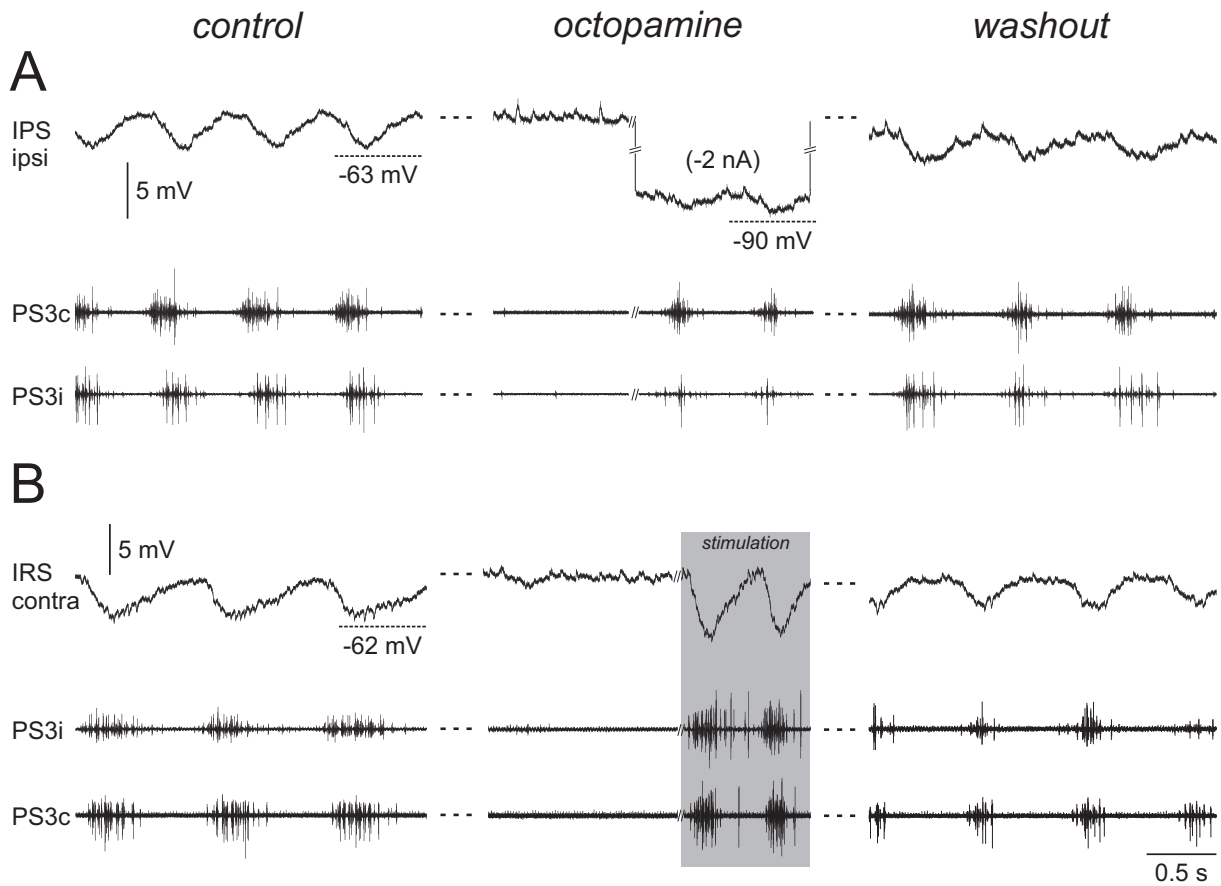
Figure 3.35: Intracellular recordings of CPG neurons and extracellular recordings of corresponding ipsilateral and contralateral PS activity in A3. Spontaneous fictive locomotion was terminated by bath application of octopamine (OA). **A:** The NOP of IPS during OA application was at the PP as also observed for transitions during spontaneous or stimulus-evoked terminations. Hyperpolarization of IPS induced V_m oscillations and PS activity in A3, even in the presence of OA. **B:** In parallel to spontaneous transitions, the NOP of IRS was at the PP. Electrical stimulation bypassed the termination induced by OA and initiated fictive locomotion and V_m oscillations in IRS. **IPS** *Inhibitor of power stroke*, **IRS** *Inhibitor of return stroke*, **PS3i** *ipsilateral power stroke in ganglia A3*, **PS3c** *contralateral power stroke in ganglia A3*, V_m *membrane potential*, **PP** *peak potential*.

The effect of OA on fictive locomotion strongly varied between different experiments, ranging from complete termination to not affecting the motor output at all. In my experiments, this variations seemed to be independent of the applied concentration and I also observed enhancement due to OA application. In the experiment presented in figure 3.36, period decreased (Spontan: 0.57 ± 0.02 s; OA: 0.43 ± 0.02 s) similar to enhancement during electrical stimulations. In contrast to enhancement through stimulation, burst strengths decreased while OA was applied to the preparation (normalized to Spontan; OA: 0.79 ± 0.18). In the same experiment, I intracellularly recorded one return stroke exciter (RSE) motor neuron. Due to bath application of OA, V_m depolarized (TP: Spontan: $- 60.4 \pm 0.4$ mV; OA: $- 56.7 \pm 0.3$ mV) and spiking rate increased (Spontan: 7.2 ± 1.1 spikes / burst; OA: 11.9 ± 1.3 spikes / burst).

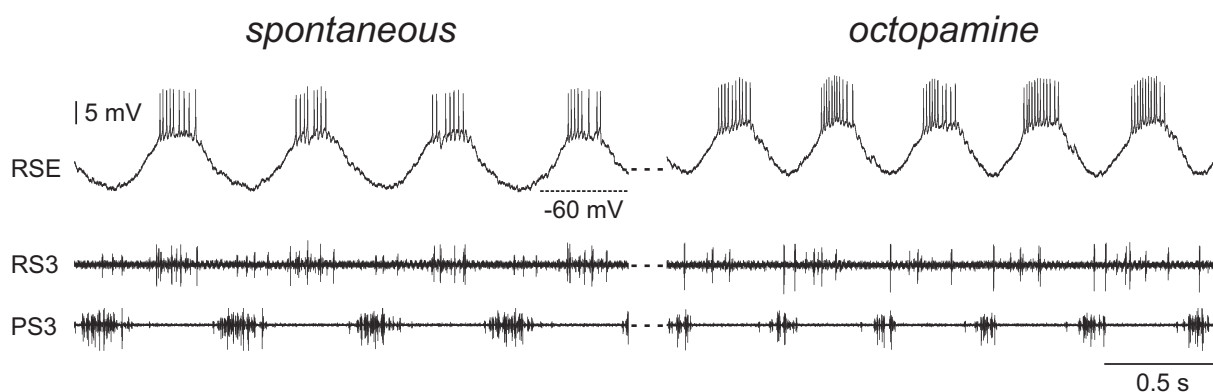**Figure 3.36:** Intracellular recording of one RSE in A3 and extracellular recordings of RS and PS activity in A3. Spontaneous fictive locomotion was enhanced by bath application of octopamine, i.e. period decreased. RSE V_m oscillation period decreased according to that. The V_m polarized and spiking activity increased. **RSE** *return stroke exciter*, **RS3** *return stroke in ganglia A3*, **PS3** *power stroke in ganglia A3*, **V_m** *membrane potential*.

Figure 3.37 illustrates focal application of OA within the lateral neuropil in single hemiganglia. Applications either terminated the PS activity exclusively within the respective hemiganglion (Figure 3.37 A), or terminated fictive locomotion in the entire swimmeret system (Figure 3.37 B).
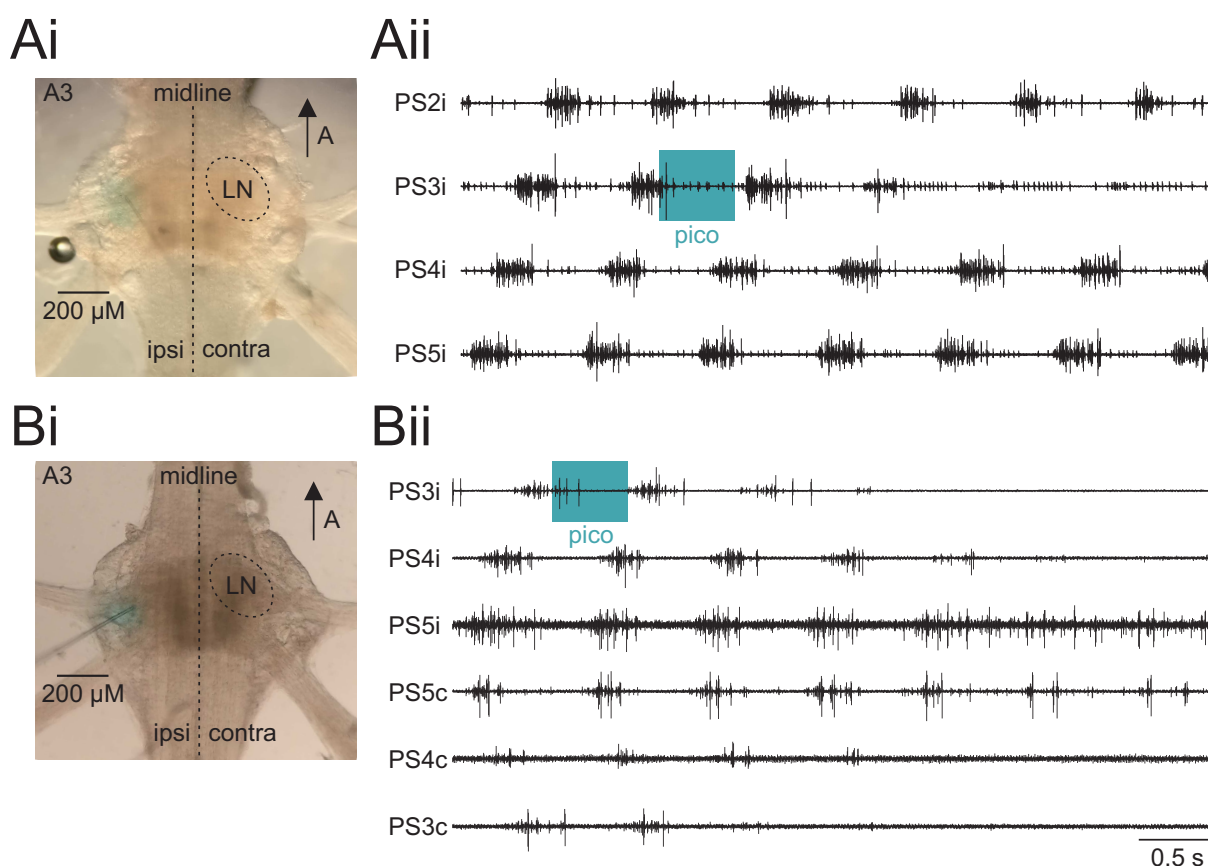
Figure 3.37: Focal application of octopamine within the LN of a single hemiganglion in abdominal ganglion A3. **A:** In one experiment, focal application of OA terminated PS activity exclusively within the corresponding hemiganglion. **B:** In another experiment, focal application of OA terminated fictive locomotion of the entire swimmeret system. **LN** *lateral neuropil*, **PS2-5i** *ipsilateral power stroke in ganglia A2 to A5*, **PS3c-5c** *contralateral power stroke in ganglia A3 to A5*.

4 Discussion

The general question of my thesis was how descending input is able to modulate the activity of a locomotor system. More precisely, I wanted to know how this modulation is achieved on a cellular level, i.e. how descending neurons affect a neuronal network to generate transitions between different states of activity. To address this question, I used the swimmeret system of the crayfish *Pacifastacus leniusculus*. The swimmeret system consists of paired limbs that are used during forward swimming and offers several experimental advantages. First of all, isolated preparations of the swimmeret system can express the same precisely coordinated motor output as observed *in vivo*. Furthermore, the system offers detailed knowledge of the neuronal microcircuits and the synaptic interactions which enabled me to investigate which neurons are affected by descending input. Finally, previous studies described inhibitory and excitatory command neurons that provide descending input to the swimmeret system and can terminate or initiate fictive locomotion. I was able to both revise the presence of these neurons and to extend the description of their axonal locations and physiological properties (Chapter 4.1). During electrical stimulations of inhibitory and excitatory axons, I observed consistent stimulation effects both on the level of the motor output and on a cellular level. I further provide evidence that during these stimulations, the neurons of the microcircuits show similar activity transitions to that occurring spontaneously in isolated preparations (Chapter 4.2). In addition to termination and initiation, I demonstrated for the first time that excitatory command neurons may account for side-specific enhancement of fictive locomotion (Chapter 4.2.4). Eventually, my results describe activity transitions and corresponding changes in the activity of single identified neurons. I revealed that a subset of ipsilateral interneurons of the central pattern generators (CPG) is directly targeted by excitatory descending input. Therefore, I will discuss the silent state of the swimmeret system's micro circuits and speculate on how descending pathways modulate the motor output in terms of termination, initiation and enhancement (Chapter 4.3).

4.1 Stimulation of command neurons

Detailed investigations of descending input and how it modulates a neuronal network requires reproducible and unvarying activation of the involved neurons, e.g. command neurons. On the one hand, the swimmeret system fulfills this requirement since distinct command neurons and their axonal locations were repeatedly described [Wiersma and Ikeda, 1964; Atwood and Wiersma, 1967; Mulloney et al., 1987; Acevedo et al., 1994]. On the other hand, the method used to excite these neurons contains some restrictions that limit it's repeatability. I addressed these limitations in my thesis and will discuss how reliable the results can be assigned to the previously described command neurons of the swimmeret system.

Limited repeatability when stimulating individual command neurons

The locations of command neurons were previously defined only by visual estimation [Wiersma and Ikeda, 1964; Acevedo, 1990]. This methodological approach limits not only the anatomical comparison between different studies, but also comparable descriptions between individual preparations. Therefore, I introduced a more standardized method to examine stimulation sites. I histologically labeled the stimulated axons, performed cross sections of the connectives and compared the stimulation sites with the previously described locations of command neurons. In order to narrow down the number of command neurons I performed electrical stimulations only in the lateral proportion of the connectives. Lateral axons are easier accessible and my goal was to reduce the impact of the preparation, ensuring optimal conditions of the swimmeret system. I particularly wanted to preclude additional axonal damage within the connectives that possibly affect the motor activity of the system in general. Referring to the command neurons described in the literature [Wiersma and Ikeda, 1964; Mulloney et al., 1987; Acevedo et al., 1994], lateral stimulation sites potentially activated two inhibitory (I_A, I_C) and three excitatory (E_A, E_B, E_C) command neurons. In each experiment, labeling was restricted to a small subset of axons in the lateral portion of the hemiconnective but did not allow to verify the stimulation of one specific command neuron. I terminated fictive locomotion using varying stimulation sites within the lateral proportions of the hemiconnectives without any obvious differences. This indicates that inhibitory command neurons I_A and I_C are not distinguishable only by the observed stimulation effect as also mentioned previously [Wiersma and Ikeda, 1964; Acevedo, 1990]. This also applies for the stimulation of excitatory command neurons. Acevedo et al. [1994] stated that the five excitatory command neurons initiate comparable fictive locomotion and I generally observed the same extent of initiation while stimulating in the axonal region of

E_A, E_B or E_C. This is further in line with the initial description by [Wiersma and Ikeda, 1964], who particularly stated that stimulations of excitatory command neurons E_A, E_B and E_C initiate similar motor outputs of the swimmeret system.

Taken together, the evoked terminations or initiations themselves do not enable to differentiate between individual command neurons which are located in the lateral portions of the connective. I did not demonstrate the existence of I_A and I_C , or E_A, E_B and E_C within the same preparations which further reduces possible differentiation. In addition, the stimulations sites provided only limited validity. By performing extracellular recordings from the connectives, however, I showed that individual command neurons were recruited during stimulations.

Recruitment of individual command neurons

I physiologically and histologically demonstrated distinct units that were recruited during stimulations and it is reasonable to assume that these units are consistent with inhibitory and excitatory command neurons (Chapter 3.1.2). Within my experiments, not more than two command neurons were recruited both during terminations or initiations. I cannot completely exclude the possibility that signals of more than two neurons were not distinguishable or that recruited axons did not project as far as to the extracellular recording. In the vast majority of experiments, however, multiple signals showed clear temporal separation and only occasionally overlapped. It is also possible that additional neurons were recruited during stimulations but were not comprised in the recorded axon bundles. Therefore I should mention that within each experiment I additionally recorded from adjacent axon bundles and did not observe any neurons recruited by the stimulations. In parallel to physiological indications, I histologically demonstrated that distinct axons (1 to 3) were comprised in both the stimulated and the recorded axon bundles. By visual estimation, the axons of inhibitory neurons appeared to be larger compared to excitatory neurons but technical reasons limited a more detailed investigation. However, additional results also indicate larger axon diameters for inhibitory neurons. On the one hand, conduction velocities of inhibitory neurons were faster. On the other hand, in one experiment the same stimulation had both an inhibitory and excitatory effect on locomotion that depended on the strength of stimulation (Figure 3.4). One inhibitory command neuron was recruited at a comparably lower threshold and terminated fictive locomotion. One simultaneously stimulated excitatory neuron was exclusively recruited when the stimulation strength increased, indicating a smaller axon diameter. Lower thresholds for the recruitment of inhibitory command neurons were also briefly mentioned by Acevedo et al. [1994]. However, further histological investigations are necessary to clarify if the axon diameters are consistently different between inhibitory

and excitatory command neurons.

Taken together, my results strongly suggest that I stimulated individual command neurons, i.e. I_A, I_C , or E_A, E_B, E_C, but further discrimination was not possible. Even though the effectiveness of inhibitory and excitatory command neurons was similar under experimental conditions, the existence of two inhibitory and three excitatory pathways with the same impact on the swimmeret system would be inefficient and is rather unlikely. Individual command neurons may have specific roles within certain behaviors or are simultaneously activated to evoke the desired movements of the swimmerets. This is indicated by the experiment presented in figure 3.28. Within the stimulation of one axon bundles, two excitatory pathways were recruited at different thresholds and when both pathways were simultaneous activated fictive locomotion was initiated.

Possible co-stimulation of additional descending pathways

Another limitation that comes with the method I used is that the stimulated axon bundles consisted of a variety of additional axons different to command neurons. The abdominal connective of the virile crayfish, *Orconectes virilis*, contains about 2,600 pairs of axons [Sutherland and Nunnemacher, 1968]. Assuming a similar number in *P. leniusculus* and a homogeneous distribution within the connectives, each area introduced by Wiersma and Hughes [1961] contains about 260 axons. Within this still large number of axons, distinct command neurons were described in individual areas. The presence of only five excitatory (E_A to E_E) and three inhibitory (I_A, I_C, I_E) command neurons points out the difficulty to specifically, and preferable exclusively, excite one of these neurons. Parallel descending pathways, e.g. from the statocysts system or the walking legs, may be also excited through the stimulations and contributed to the modulation of fictive locomotion. Furthermore, E_A and E_B were found in the same division and, to make it even more difficult, the axons of inhibitory command neurons were described as close neighbors of excitatory neurons. Even though Acevedo et al. [1994] repeatedly confirmed five different excitatory command neurons in individual preparations, simultaneous activation of more than one command neuron is not generally excluded. This constraint depends on the number of stimulated axons, i.e. the dimension of the stimulation site, and applies especially for simultaneous recruitment of inhibitory and excitatory command neurons. Consequently, it is difficult to rule out that termination or initiation were influenced, or maybe even entirely evoked by simultaneous activation of additional descending pathways.

Parallel descending pathways

Although individual command neurons were most likely recruited during my experiments, stimulation of additional descending pathways other than command neurons potentially account for the observed modulation of fictive locomotion. I want to highlight two other motor systems and one sensory input that were shown to interact with the swimmeret system and I discuss the possibility that these interactions may influenced the stimulation effects.

The tail-flip system generates the fast escape response and is activated by single action potentials in the giant fibers [Wiersma, 1947; Edwards et al., 1999]. On a behavioral level, tail-flips are generated by flexion of the abdomen and simultaneous termination of the swimmeret system's activity. The inhibitory mechanism underlying the termination of the swimmerets remains unclear but the behavior suggests an inhibitory input provided by the giant fibers. However, I removed the giant fibers in the part of the connectives where I stimulated. Therefore, stimulation of these neuron was precluded in my preparations.

In parallel, walking leg activity was shown to both terminate and initiate fictive locomotion of the swimmeret system under certain conditions. In the experiments of Barthe et al. [1991] swimmeret activity was phasically inhibited during the activity of depressor motor neurons while the crayfish was walking backwards, indicating an inhibitory input from the walking system. The same is true regarding a possible excitatory input from the walking system. Phasic stimulation of the coxo-basipodite chordotonal organ (CBCO) in a single walking leg is able to initiate fictive locomotion of the swimmeret system [Cattaert et al., 1992]. Since projections of primary sensory neurons of the CBCO are restricted to the hemiganglion that innervates the respective walking leg, this suggests an excitatory descending pathway from the walking legs to the swimmeret system. Unfortunately, no information about the axonal locations these inhibitory or excitatory pathways are available and it is subsequently difficult to discuss their potential stimulation in my experiments. However, in one of my experiments fictive locomotion of the swimmeret system was continuously terminated during the entire period of potential backward walking. In contrast to Barthe et al. [1991], I initiated backward walking by an electrical stimulation between the first and second thoracic ganglia. This might indicate the activation of an descending pathway that affects both locomotor systems simultaneously. In addition, I both terminated and initiated fictive locomotion of the swimmeret system by stimulations at additional levels anterior to the walking legs. Therefore, I assume that at least certain command neurons affect both locomotor systems. The described interactions between these systems may be explained by modulatory inputs on the activity of command neurons within the walking leg

system. However, additional inhibitory and excitatory inputs that arise from the walking system remain possible.

The main known sensory input that affects the activity of the swimmerets arises from the statocysts system. Behavioral experiments clearly demonstrated the effect of changes in the animal's body orientation on the swimmerets' activity [Davis, 1968a]. Four types of statocyst-driven interneurons (SDI) were described to project from the brain to the most posterior abdominal ganglion A6 [Takahata and Hisada, 1982]. These SDIs control for the uropod movements during righting responses and it is reasonable to assume that they interact with the swimmeret system [Yoshino et al., 1980]. However, possible targets of SDIs within the swimmeret system are unknown. Takahata and Hisada [1982] visually examined the locations of SDIs within the abdominal nerve cord and described three of them (C_2, I_1, and I_2) within the lateral portions of the connectives. These locations are simliar to the stimulation sites in my experiments while the fourth type of SDIs, C_1, was located in the medial portions of the connectives. Takahata and Hisada [1982] measured the conduction velocity of C_1 (3.8 ± 1.3 m / s) and assumed simliar conduction velocities of the lateral SDIs. In my experiments I obtained conduction velocities of 2.56 ± 0.9 m / s for inhibitory command neurons and 2.15 ± 1.4 m / s for excitatory command neurons, suggesting that both groups were generally different to SDIs. However, SDIs might have been simultaneously stimulated within single experiments and influenced the stimulation effects. During both terminations and initiations individual units with conduction velocities of up to 4 m / s were recruited. Moreover, Takahata and Hisada [1982] performed their experiments in *Procambarus clarkii* and SDIs in *P. leniusculus* may have different conduction velocities. Due to their potential role within righting responses, recruitment of SDIs may partially explain the side-specific enhancement during stimulations.

Taken together, I assume that the stimulation effects during my experiments are predominantly due to the activation of inhibitory and excitatory command neurons. Future studies are necessary to clarify potential influences of additional descending pathways, e.g. from the walking legs or the statocysts system. Additional activation of these pathways may alter termination or initiation and might account for the variability of initiated fictive locomotion. Moreover, activation of SDIs offers an explanatory approach regarding side-specific enhancement during stimulations.

4.2 Activity transitions of the swimmeret system

4.2.1 Spontaneous activity transitions

Isolated preparations of the swimmeret system tend to spontaneously express the same motor output as it is observed during swimming behavior in intact crayfishes. This fictive locomotion brings important experimental advantages and enabled detailed investigations of the swimmeret system's neuronal circuitry. However, not all preparations express fictive locomotion but remain silent instead. In addition, transitions from a silent state to fictive locomotion and vice versa can occur spontaneously. To this date, the reasons why isolated preparations of the swimmeret system can be spontaneously active, silent, or switch between active and silent states are unknown.

Since motor activity of the walking legs can both terminate and initiate fictive locomotion of the swimmeret system, descending input from the walking system may provide a possible explanation for spontaneous activity transitions in the swimmeret system [Barthe et al., 1991; Cattaert et al., 1992]. In my preparations, the two most posterior thoracic ganglia T4 and T5 were isolated together with the abdominal ganglia. Consequently, spontaneous network activity in T4 or T5 could terminate or initiate the swimmeret system's activity. In this case we would have to address the question of why the walking system generates spontaneous activity transitions, pushing the gap of knowledge in anterior direction. In contrast, isolated preparations without the thoracic ganglia, and even individual, isolated abdominal ganglia are capable of expressing rhythmic PS activity. A subset of my experiments suggest the presence of descending pathways that simultaneously modulate the activity of both locomotor systems i.e. the walking and the swimmeret system. The descending neurons within these pathways are most likely inhibitory and excitatory command neurons which unfold another explanation for spontaneous activity transitions. Mulloney et al. [1987] suggested that inhibitory and excitatory command neurons contain octopamine (OA) and proctolin (PR), respectively, and that these neuromodulators are locally released to terminate or initiate swimming. However, the presynaptic input that command neurons receive, e.g. from sensory systems, and that consequently triggers the release of OA or PR within the swimmeret system is unknown.

Octopamine and proctolin in descending neurons

Evidence regarding the central projection of inhibitory command neurons derives from OA-antibody labeling in the lobster, *Homarus americanus* [Schneider et al., 1993]. Two pairs of

intensively labeled neurons have their somata located at the midline of the subesophageal ganglion (SOG). They posteriorly project their axons in a dorsolateral portion of the abdominal hemiconnectives (presumably area 81), eventually reaching abdominal ganglion A6. Schneider et al. [1993] described bilateral ramifications within both the thoracic and abdominal ganglia and stated the possibility of terminal varicosities within the neuropils. Therefore, these descending, OA-ergic neurons may reflect some of the inhibitory command neurons of the swimmeret system, most likely I_A. During a set of preliminary experiments, I was able to terminate fictive locomotion while stimulating one lateral axon bundle from the connectives between the SOG and the first thoracic ganglia T1. This finding further emphasizes the assumption that the somata of inhibitory command neurons are located in the SOG and I stimulated the respective axons both between the SOG and T1 (cSOG/T1) and between A1 and A2 (cA1/A2).

In lobster (*H. americanus*) and crayfish (*Procambarus clarkii*), comparable axons were found to contain PR [Siwicki and Bishop, 1986]. Continuous proctolinergic axons are present between the SOG and A6, although no related somata were found in the SOG. However, I initiated fictive locomotion at a level of the CNS anterior to the swimmeret system, i.e. cT1/T2, suggesting stimulation of some of these axons. In addition, insights from other arthropod systems also suggest that the SOG contains neurons that are related to the initiation of locomotion (e.g.: flying in locust, Ramirez [1988]; crawling in fruit fly larvae, Schoofs et al. [2014]). Interestingly, I terminated and initiated fictive locomotion of the swimmeret system by stimulations anterior to the SOG, i.e. between the brain and the SOG. These results either indicate the presence of additional descending pathways from the brain that work in parallel to pathways originating in the SOG, or the stimulations elicited descending input that activated the command neurons in the SOG.

Spontaneous release of octopamine and proctolin

As already mentioned, the input command neurons receive is unknown. However, in preparations of the isolated abdominal nerve cord command neurons are lacking any potential source of excitation, either from sensory input or from proprioception. How can these neurons still modulate the activity of the swimmeret system? One possible explanation is that OA and PR are released without excitation of the respective command neurons. This is based on previous research, describing that synaptic neurotransmitter release can occur in the absence of presynaptic action potentials [Fatt and Katz, 1952]. Spontaneous neurotransmitter release differs from evoked release in the dependency on extracellular Ca^{2+} concentrations and was initially considered to appear as stochastic events (see Kavalali [2014] for a review). In crayfishes (*O.*

virilis), spontaneous neurotransmitter release was reported at the neuromuscular junction in the walking legs [Dudel and Orkand, 1960; Dudel and Kuffler, 1961; Finger and Stettmeier, 1981]. Cohen et al. [1974] provided evidence that this release may not be entirely randomly distributed but can also appear in temporal clusters. If this is true for terminals of command neurons in the swimmeret system, OA or PR may be spontaneously released within the neuronal microcircuits at concentrations sufficient to terminate or initiate fictive locomotion. Therefore, I speculate that spontaneously active terminals of command neurons account for spontaneous activity transitions in isolated preparations of the swimmeret system. I base this assumption on the results of this thesis, showing that the general appearance of termination is equal during spontaneous termination or termination through activation of inhibitory command neurons. Vice versa, this is true for spontaneous initiation and initiation through stimulations of excitatory command neurons. In addition, I found these similarities also on a cellular level, both for motor neurons and CPG neurons of the swimmeret microcircuits. In the following sections I will discuss these transitions during active and silent states in more detail.

4.2.2 Termination through inhibitory command neurons

Wiersma and Ikeda [1964] were the first to describe three pairs of inhibitory command neurons of the swimmeret system at the level of the abdominal nerve cord. Acevedo [1990] repeated their experiments in *P. leniusculus* and named these neurons I_A, I_C and I_E referring to excitatory command neurons located in the same portion of the connectives. Analog to these descriptions, I repeatedly terminated fictive locomotion by stimulating inhibitory command neurons I_A or I_C. During stimulations PS excitatory motor neurons (PSE) were silent and RS excitatory motor neurons (RSE) were continuously active. This is in line with suggested swimmeret muscle activities of intact animals that are not performing any swimmeret movements.

Since some behaviors require only one side of the swimmerets to be active, Wiersma and Ikeda [1964] suggested the existence of ipsilateral inhibition to the swimmeret system. They based this suggestion on occasional terminations of only one side of their preparations but did not state if this side-specificity occurred ipsi- or contralateral to the stimulation. Occasionally I also observed side-specific inhibitory effects, mainly in terms of qualitatively stronger inhibition on one side but rarely also in terms of complete termination on one side. As also stated by Wiersma and Ikeda [1964], these side-specific differences may arose from the preparation itself, e.g. different levels of excitation, or can be ascribed to influences of the dissection. In this thesis, my goal was to investigate complete termination of fictive locomotion which I defined as the absence of PS activity on both sides of the abdominal ganglia. I consequently

neglected incomplete terminations and I generally aimed to terminate the PS activity of the swimmeret system completely. Therefore, I gradually increased the stimulation amplitude until fictive locomotion was completely terminated or discarded the respective axon bundle. During this experimental procedure, I occasionally observed not only side-specific inhibition but also incomplete termination in terms of reduced PS activity. Acevedo [1990] and Mulloney et al. [1987] stated that the effectiveness of inhibitory command neurons depends on the frequency of stimulation, i.e. that at lower frequencies burst strengths and burst durations are reduced but fictive locomotion continued. This reduction of fictive locomotion may be explained by lower amounts of neuromodulators released at lower stimulation frequencies, i.e. OA.

Octopamine in inhibitory command neurons

OA terminates fictive locomotion in the swimmeret system and is considered to be the neuro-modulator released by inhibitory command neurons [Mulloney et al., 1987]. I reproduced the termination by OA and showed that application of epinastine, a highly specific OA receptor antagonist in arthropods [Roeder et al., 1998], completely removed this termination. Mulloney et al. [1987] demonstrated similar effects with another OA receptor antagonist, phentolamine. They additionally blocked the effect of inhibitory command neurons by bath application of phen-tolamine. They stimulated I_C or I_E but did not state which inhibitory command neuron was stimulated in this specific experiment. As another restriction, they used PR to initiate fictive locomotion, raising the possibility of co-modulatory effects of PR and the released OA. There-fore, I tried to reproduce this experiment with epinastine but could not reliably block the effect of inhibitory command neuron I_A or I_C. However, epinastine occasionally blocked termination during the experimental procedures. This may suggest that epinastine diminished the effect of the inhibitory command neurons but the applied concentration was not sufficient to occupy the entirety of OA receptors. If this is true, a proportion of released OA still bound to these recep-tors and affected the respected targets within the microcircuits. Interestingly, recent work from our research group (Laudenberg, master's thesis, 2019, unpublished) revealed that OA applied at different concentrations can have opposing effects on the swimmeret system. At high con-centrations (50 µM), OA completely terminated fictive locomotion but bath applications of lower concentrations (5 / 10 µM) enhanced the swimmeret system. Periods, duty cycles and burst durations decreased while burst strengths increased. Here, I additionally demonstrated that OA can decrease the period of fictive locomotion while PS burst strengths decreased. This is consistent with the results of Davis and Kennedy [1972b]. They stimulated inhibitory command neurons in the swimmeret system of the lobster (*H. americanus*) and increased the period while

burst strengths decreased. This effect might have been due to the stimulation parameters or the preferred stimulation frequency of the stimulated neurons. Perhaps these stimulations lead to lower concentrations of OA compared to complete terminations and can be compared to the varying effectiveness of different OA concentrations.

In my experiments, OA increased the spiking activity of one intracellularly recorded RSE which may indicate an excitatory effect of OA on this group of motor neurons. How OA acts on PSEs or other neurons of the swimmeret system, however, is unknown. In lobsters (*H. americanus*) OA is released as a neurohormone in the neurohemel organs [Evans et al., 1976]. Interestingly, OA concentrations in the hemolymph of the lobster are multiple times smaller than concentrations that significantly affect the swimmeret system in crayfish [Livingstone et al., 1980; Mulloney et al., 1987; Tschuluun et al., 2009]. Consequently, Mulloney et al. [1987] suggested that OA is locally released within abdominal ganglia to terminate fictive locomotion. In order to test this, I focally applied OA within single hemiganglia. In one experiment OA terminated the local PS activity, suggesting an inhibitory effect on the respective PSEs. In another preparation focal OA application terminated fictive locomotion of the entire swimmeret system, further suggesting that CPG neurons or neurons of the coordinating network may be additionally affected by OA.

In a different set of experiments, I intracellularly recorded from CPG neurons and bath applied OA to the entire system. Membrane potential (V_m) oscillations ceased at a depolarized V_m in both neurons, i.e. one Inhibitor of PS (IPS) and one Inhibitor of RS (IRS), while fictive locomotion was terminated. As the neuronal circuitry of the swimmeret system determines, IPS continuously inhibits PSEs at a depolarized V_m [Heitler and Pearson, 1980; Smarandache-Wellmann et al., 2013]. This is in line with the absence of PS activity when the system is silent. I revealed comparable shifts in V_m during inhibitory stimulations. V_m oscillations in one IPS ceased at a depolarized V_m and two PSEs were locked at a hyperpolarized V_m.

Vice versa, a depolarized V_m of IRS indicates continuous inhibition of RSEs. This is unexpected since I showed that RSEs are continuously active during both spontaneous terminations and inhibitory stimulations. During stimulation, the V_m of one IRS was hyperpolarized. During spontaneous transition, however, the V_m of another IRS was hyperpolarized and cannot explain the continuous depolarization of RSEs. One explanation may be that the two types of IRS, i.e. IRSh and IRSnh, are differently affected at a silent state. Since I only recorded from IRSnh, future investigations of IRSh are necessary to test this explanation.

In general, my results indicate that OA affects the neuronal microcircuits similar to inhibitory stimulations - with the exception of IRS. Therefore, OA is potentially released by inhibitory command neurons in order to terminate fictive locomotion which was already suggested [Mulloney

et al., 1987]. Furthermore, during spontaneous transitions of fictive locomotion, IPSs, PSEs, and RSEs were equally affected as during inhibitory stimulations. Again, activity transitions of IRS proved to be highly variable. This emphasizes the possibility that spontaneously occurring termination is due to spontaneous OA release within the abdominal ganglia.

4.2.3 Initiation through excitatory command neurons

Five pairs of excitatory command neurons of the swimmeret system were repeatedly described in the abdominal nerve cord of crayfishes [Wiersma and Ikeda, 1964; Atwood and Wiersma, 1967; Acevedo et al., 1994]. My results indicate the stimulation of three of these neurons, i.e. E_A, E_B or E_C, but my methodical approach restricted further differentiation. However, initiations of fictive locomotion at different stimulation sites were similar among each other, suggesting that E_A, E_B or E_C represent parallel pathways to activate the swimmeret system in an equal manner. This observation was already stated by Wiersma and Ikeda [1964] and Acevedo et al. [1994]. As mentioned before, it is rather unlikely that three pathways exist which generate the same motor output. The activation of the swimmeret system is probably of a more complex nature and depends on the behavioral context and the required swimmeret movements.

I routinely stimulated at a frequency of 30 Hz since Wiersma and Ikeda [1964] described that "the resulting rhythm is then that preferred during natural beating in the intact animal". Acevedo et al. [1994] tested this observation for stimulations of E_C and confirmed that the initiated fictive locomotion was not significantly different to spontaneous conditions. In a preliminary set of experiments I tested different stimulation frequencies (10 - 50 Hz) and showed that both the period and the burst strength depended on the frequency. In general, the excitation level of the swimmeret system increased with increasing frequency. Periods for example, determined by the CPG neurons, decreased with increasing frequency, as already demonstrated by Acevedo [1990]. Interestingly, burst strengths, a measure for motor neuron recruitment, also increased with the frequency. These observations indicate the possibility of two important mechanisms for initiation of locomotion in the swimmeret system. First, both CPG neurons and motor neurons are likely targeted by excitatory command neurons. Second, faster and stronger PS activity at higher stimulation frequencies may be due to an increased transmitter release under these conditions. Following this, graduated excitation of a single excitatory command neuron might be able to control for a wide range of different motor outputs, e.g. faster or slower swimming, or weaker or stronger swimmeret movements.

Initiation is comparable to fictive locomotion spontaneously expressed

I already mentioned that fictive locomotion initiated by excitatory command neurons is similar to spontaneously expressed fictive locomotion in isolated preparations [Wiersma and Ikeda, 1964; Acevedo et al., 1994]. In my experiments, I found significant differences only regarding the burst strengths and the duty cycles. I additionally showed that burst strengths increase with the stimulation frequency, i.e. more motor neurons are recruited at higher frequencies. Therefore, I assume that the significant differences in burst strengths and duty cycles are due to the stimulation frequency of 30 Hz. Lower frequencies may have recruited smaller numbers of motor neurons during the stimulation of excitatory command neurons. The burst strength is a measure for the amount of motor neurons that are recruited during a single burst of PS activity. Consequently, my results show that within the same preparation more motor neurons were recruited during the stimulation of excitatory command neurons than motor neurons were active during spontaneous PS bursts. The phase at which these motor neurons are recruited, e.g. earlier or later within the PS bursts, in turn influenced the corresponding duty cycles.

Initiation is different to fictive locomotion elicited by carbachol

The neuromodulator commonly used to excite the swimmeret system is carbachol (CCh). CCh initiates and enhances fictive locomotion in the swimmeret system while periods, phase lags and duty cycles are similar to spontaneous conditions [Braun and Mulloney, 1993]. Therefore, Braun and Mulloney [1993] suggested the existence of a cholinergic pathway that excites the system. CCh acts on both muscarinic and nicotinic acetylcholine receptors and was shown to act directly on motor neurons [Tschuluun et al., 2009]. In my experiments, burst strengths of CCh-elicited fictive locomotion were significantly weaker than during excitatory stimulations in the same preparations. As mentioned before, however, these differences may be explained by the used stimulation frequency.

Most interestingly, periods in the presence of CCh were significantly longer than during the stimulation of excitatory command neurons. CCh has an dose-dependent effect on the period but I did not compare different CCh concentrations [Braun and Mulloney, 1993]. Instead I gradually increased the CCh concentration (1 - 5 µM) for each preparation until fictive locomotion was continuously expressed which was 1 - 2 µM CCh in the majority of experiments. By this, I assumed comparable levels of excitation across different preparations. In addition to the effect on motor neurons, CCh acts on unidentified presynaptic neurons within the neuronal microcircuits, most likely CPG neurons since they form inhibitory synapses on motor neurons [Tschuluun

et al., 2009]. CPG neurons determine the period of the system and periods were longer during fictive locomotion elicited by CCh compared to excitatory stimulation. This indicates that the CPGs were differently affected by CCh and through excitatory stimulations. Therefore, my results suggest that the stimulated axons are not part of an cholinergic pathway which is in line with findings that showed that three of the excitatory command neurons (E_A, E_C, E_E) are most likely proctolinergic [Acevedo et al., 1994]. The neurons E_B and E_D remain potential candidates of a cholinergic pathway but my methodical approach excluded stimulation of E_D. From this I conclude that a cholinergic pathway was not always activated during my stimulations. However, E_B was most likely stimulated in a subset of my experiments and might have contributed to the excitatory effects on the swimmeret system.

Proctolin in excitatory command neurons

The assumption that excitatory command neurons represent a proctolinergic pathway to activate the swimmeret system was initially based on morphological and pharmaceutical evidences [Siwicki and Bishop, 1986; Mulloney et al., 1987; Acevedo et al., 1994]. Later on, Acevedo [1990] measured the release of PR during excitatory stimulations and located proctolinergic fibers within the stimulated axon bundles. These are strong indications that excitatory command neurons E_A, E_C and E_E represent three proctolinergic pathways. Moreover, Acevedo et al. [1994] showed that fictive locomotion induced via PR is not different to the stimulation of E_C and suggested that this also applies for E_A and E_E. I successfully revised the stimulation of proctolinergic axons and the initiation of fictive locomotion through bath application of PR. However, how PR acts on individual neurons of the swimmeret system remains unknown.

Analog to OA, Mulloney et al. [1987] suggested that PR is locally released within the abdominal ganglia. I performed focal applications of PR within individual hemiganglia which did not elicit rhythmic PS activity or fictive locomotion. It is possible that this was due to the applied concentration of PR. Acevedo et al. [1994] applied 5 µM PR to the system by perfusion through the ventral artery while I was using 1 µM PR during focal applications. Similar to perfusion through the ventral artery, focal application is used to apply pharmaceuticals as close as possible to the respective target area. However, the final concentrations that both methods produce within these areas are difficult to state. Either the loci of my applications or the caused concentrations of PR within the tissue were not sufficient to elicit rhythmic PS activity in my experiments.

Information about the neuronal targets of PR within the swimmeret system are not available. Due to the circuitry, the most simple explanation would be direct targeting of CPG neurons and

consequential indirect effects on the motor neuron pools. However, previous studies showed that the burst durations in the presence of PR are significantly longer at higher concentrations while the period is not affected [Braun and Mulloney, 1993; Acevedo et al., 1994]. Assuming that duty cycles remained constant, this raises the possibility that only motor neurons are targets of PR. In contrast to that, PR can elicit fictive locomotion in previously silent preparations which strongly suggests that CPG neurons are additional targets. Acevedo et al. [1994] applied PR only to individual ganglia and activated the swimmeret system. Even though rhythmic PS activity was elicited in the entire system, the extracellular recordings may indicate stronger recruitment of motor neurons in the ganglia exposed to PR (Figure 6 in Acevedo et al. [1994]). Even if speculative, these findings could further suggest a direct effect of PR on motor neurons, in addition to direct targeting of the CPG neurons.

4.2.4 Enhancement through excitatory command neurons

One of the most interesting findings in this thesis was the enhancement of fictive locomotion through electrical stimulations of separated axon bundles. This enhancement was predominantly reflected by decreased periods which was independent of the initial excitation level of the preparations. I observed a wide range of periods (0.41 - 0.71 s) that decreased to variable values during the enhancement (0.23 - 0.63 s). This clearly shows that the stimulations did not elicited a specific period of the swimmeret system but rather accelerated fictive locomotion with respect to the initial period. Since the period of the swimmeret system's activity is determined by the CPG neurons, these neurons were likely affected by activated descending pathways. Interestingly, the period in two preparations did not decrease and these preparations expressed relatively long periods compared to the other preparations. On the one hand, this may suggest that the decrease in period is not limited to accelerating exclusively slower swimming speeds. On the other hand, however, these experiments were also characterized as enhancement since PS burst strengths strongly increased which I also defined as another characteristic of enhancement. It is possible that the absence of acceleration was due to the activation of a different descending pathway that only affects the motor neurons.

In contrast to the period, burst strengths increased consistently during enhancement across all preparations. This was also reported by Mulloney et al. [1987] who stated that "the amplitude and duration of power-stroke bursts" increased while they stimulated excitatory command neurons in active preparations. The "amplitude" most likely refers to the PS burst intensity which is related, but not equal to the PS burst strength [Mulloney, 2005]. In contrast to these observations, burst durations were not affected during my enhancements of fictive locomotion.

Mulloney et al. [1987] further stated that their stimulations "decreased period slightly" while my results reflect a rather strong effect on the period. The comparison of my findings with the observations of Mulloney et al. [1987] are somehow restricted since they (1) did not state which excitatory command neuron was stimulated and (2) they used PR to activate initially silent preparations. Therefore, their enhancement was maybe influenced by some additional effects of the applied PR on the swimmeret system. However, both the observations of Mulloney et al. [1987] and the results of this thesis suggest that the enhancement of fictive locomotion was due to the activation of excitatory command neurons. In fact, I performed experiments in which I was able to both initiate and enhance fictive locomotion through stimulations of the same axon bundle (N = 7). These preparations were spontaneously active while they switched in a silent state at a later time of the experimental procedure. Under both conditions the same stimulation amplitude either evoked enhancement or initiation of fictive locomotion. This excludes the possibility that different axons were recruited by the stimulation and may suggest that one descending pathway is able to activate and enhance the swimmeret system depending on the intrinsic excitation.

Enhancement through excitatory command neurons or via proctolin is different

At least two of the excitatory command neurons stimulated in my experiments (E_A and E_C) are most likely proctolinergic. Therefore, PR-release of these neurons may be the reason for the described effects during enhancement. Mulloney et al. [1987] stated that PR "applied to beating preparations intensified [increased burst strengths?] and increased the frequency [i.e. decreased period] of the swimmeret rhythm". A similar statement was made by Acevedo et al. [1994] who stated that bath application of PR increased PS intensities and decreased periods in spontaneously active preparations. These observations may suggest similar enhancement via PR application compared with the enhancement through excitatory stimulations presented in my thesis. When I compared these two conditions within the same preparation, however, enhancement was only partially similar. As already mentioned, excitatory stimulations increased burst strengths and decreased periods. In contrast, bath application of PR increased burst strengths but additionally increased the period. This effect of PR on the swimmeret system was extensively investigated in a recent work from our research group (Laudenberg, master's thesis, 2019, unpublished). This work showed that the period significantly increased when PR is applied to spontaneously active preparations while the burst strengths tended to increase. The differences between enhancement via PR or via excitatory stimulations suggest that another descending pathway was activated or worked in parallel with excitatory command neurons.

Braun and Mulloney [1993] showed that bath applications of nicotine decrease periods in active preparations. Since nicotine acts as an agonist of acetylcholine (ACh) at nicotinic ACh receptors (nAChR), this may suggest that CPG neurons of the swimmeret system are targets of an nicotinic pathway via nAChRs. The effect of nicotine on PS burst strengths is not known but Tschuluun et al. [2009] demonstrated that carbachol (CCh) directly acts on motor neurons. CCh is another agonist of ACh that acts on both nicotinic and muscarinic ACh receptors (mAChR). If the direct effects of CCh on motor neurons is due interactions with nAChRs or mAChRs is not known. However, Tschuluun et al. [2009] measured the appearance of two inward currents that were elicited by CCh in motor neurons. They showed that one current was a direct effect on the motor neurons but the other current was elicited by an unknown presynaptic neuron. The CPG neurons synaptically target motor neurons, suggesting that they are the source of the indirect effect on motor neurons via CCh. The different effects of PR, nicotine, and CCh strongly suggest that multiple descending pathways work in parallel to modulate the activity of the swimmeret system. These pathways also may release other substances that were shown to affect the swimmeret system, e.g. the red pigment concentrating hormone (RPCH, Sherff and Mulloney [1991]) or the crustacean cardioactive peptide (CCAP, Mulloney et al. [1997]), or so far unknown neuromodulators.

Multiple pathways may work in parallel to enhance fictive locomotion

In the experiments of Braun and Mulloney [1993] both nicotine and PR were applied to the swimmeret system. They initially activated the preparations applying PR and modulated the period of fictive locomotion via nicotine applications. In my experiments, the stimulated excitatory command neurons E_A or E_C most likely released PR within the neuronal microcircuits and activated the swimmeret system. During enhancement, however, the periods decreased which is different to the effect of PR. One possible explanation is that I stimulated a descending pathway that targets the CPG neurons via nAChRs. The composition of such a pathway is not known but the excitatory command neuron E_B provides a potential descending neuron of this pathway. Acevedo [1990] gave strong evidence that E_B does not contain PR and suggested its use of a so far unknown neuromodulatory substance. Actually, at each time my stimulations enhanced fictive locomotion, I stimulated axon bundles that were in close distance to previously decried locations of E_B [Wiersma and Ikeda, 1964; Acevedo et al., 1994] (Figure 3.1 C). In combination with decreased periods during enhancement, this may suggest that stimulation of E_B activates a descending pathway that targets CPG neurons. As already mentioned, this pathway is most likely not proctolinergic but may activate nAChRs expressed by CPG neurons. Since

the CPG neurons form the basis of the motor output expressed by the swimmeret system, the same pathway could explain why identical stimulations were able to initiate and enhance fictive locomotion within the same preparations.

The same nicotinic pathway may also affect the activity of the motor neurons since CCh directly acts on motor neurons [Tschuluun et al., 2009] and tends to increase burst strengths [Mulloney and Hall, 2007; Blumenthal, 2018]. However, it remains possible that proctolinergic pathways were additionally activated by the stimulations, e.g. E_A or E_C. This would provide another satisfying explanation for the excitatory effect on motor neurons since PR applications also increase burst strengths (Laudenberg, master's thesis, 2019, unpublished). Consequently, the activation of multiple pathways that contributed to the enhancement of fictive locomotion is a possible explanation and limits the characterization of one specific input on the swimmeret system.

4.3 Microcircuits between a silent and an active state

The finding that individual neurons initiate or terminate the generation of a complex behavior directly raises an important question: Which units of the neuronal circuitry are targeted to elicit the complex activity of the complete network? As mentioned before, I clearly showed that excitatory stimulations affect the activity of both CPG neurons (period) and PS motor neurons (burst strength) of the swimmeret system during enhancement. Interestingly, I could additionally show that both chains of abdominal hemiganglia are differently affected during enhancement. PS burst strengths ipsilateral to the stimulation electrode increased significantly more than PS burst strengths on the contralateral side while periods decreased bilaterally. Since potential mechanisms of intraganglionic coupling are not known, this would suggest that I stimulated descending pathways that targeted (1) the CPGs on both sides of the system equally and (2) the motor neurons in a side-specific fashion. Surprisingly, I revealed synaptic input only on one class of CPG neurons, IRS, that was restricted to IRS neurons ipsilateral to the stimulation electrode. In the following I discuss the silent state of the swimmeret system and possible ways of how descending pathways elicit activity transitions. I hypothesized a silent state of the swimmeret system's microcircuits while the swimmerets are continuously hold in a protracted position (Figure 4.1 A). I confirmed the expected states of neuronal activity for most of the intracellularly recorded neurons (Figure 4.1 B) and showed that these states were predominantly consistent between different types of transitions.

The silent state

The membrane potential (V_m) of all recorded neurons did not oscillate when rhythmic PS activity was absent. Besides small fluctuations, the V_ms were locked at a stable value. This was independent of the type of transition, i.e. spontaneous transitions, initiation through excitatory stimulations, or termination through inhibitory stimulations. Each neuronal class tended to be locked at a specific phase of their V_m oscillations in an active state. These non-oscillating potentials (NOP) tended to be highly specific for individual neuronal classes and are well in line with the known circuitry of swimmeret system.

As expected from extracellular recordings and behavioral observations (Chapter 1.2.2), PS excitatory motor neurons (PSE) were locked around their trough potential (TP) while RS excitatory motor neurons (RSE) were locked around their peak potential (PP). I did not perform intracellular recordings from inhibitory motor neurons, i.e. PS Inhibitors (PSI) or RS Inhibitors (RSI), but in some experiments I extracellularly recorded these motor neurons from the posterior (PSIs) or anterior (RSIs) branches of the first nerve root. PSIs were tonically spiking at a silent state while RSIs were silent, indicating that these neurons were locked at their PP and TP, respectively. In intact crayfishes, the NOPs of the motor neurons would elicit continuous excitation to the RS muscles while the PS muscles are continuously inhibited. Consequently, the respective swimmeret would be hold in a protracted position (Figure 4.1 A).

The NOPs of the motor neuron groups provided an estimate of the NOPs of CPG neurons. Since PSEs were locked at their TP, continuous inhibition from IPS would be a possible explanation. Consequently, I expected depolarized V_ms of IPSs around the TP and confirmed this assumption for IPS *tangent* and IPS *orthogonal*. I did not record from IPS *wedge* but I assume a similar NOP, i.e. around the respective PP, since the three types of IPS were described to have similar effects on the motor neurons [Smarandache-Wellmann et al., 2013].

Due to tonic RS activity at a silent state, I expected hyperpolarized V_ms of IRSs. Interestingly, this was not the case. The NOPs were highly diverse across different IRSs and different types of transitions. One possible explanation is that I only recorded from IRS *nohook* (IRSnh). The other type, IRS *hook*, might be differently affected by descending pathways and both types work in parallel to lock the RSEs at depolarized V_ms. Another explanation is that individual IRSnh neurons are differently affected during transitions. Smarandache-Wellmann et al. [2013] stated that both physiology and morphology of IRSnh were more variable compared to other CPG neurons. They occasionally observed a dye-coupling of two IRSnh neurons and discussed the possibility that these represent a distinct type of IRS neurons that appears as an electri-

cally coupled pair. If this is true, the different types of IRSnh may be affected differently by descending pathways which may explain the variability in my experiment.

I did not analyze the activity of the coordinating neurons in this thesis. Analog to motor neurons, their specific NOPs are most likely determined by graduated synaptic inhibition from the CPG neurons [Skinner and Mulloney, 1998; Mulloney, 2003; Smarandache-Wellmann and Grätsch, 2014; Smarandache-Wellmann et al., 2014]. It was previously shown that the NOPs of Descending Coordinating Neurons (DSC) are around the PP while Ascending Coordinating Neurons E (ASC$_E$) are locked around their TP [Namba and Mulloney, 1999; Mulloney et al., 2006; Schneider, 2017]. Blumenthal [2018] showed one Commissural Interneuron 1 (CI1) whose V_m was around its TP when the swimmeret system was silent. In addition, NOPs of CI1s were also observed to be even more hyperpolarized compared to the TP (personal communication CW). These NOPs of coordinating neurons were expected regarding their synaptic inputs from the CPG neurons but need to be proved for inhibitory and excitatory stimulations.

Figure 4.1 B illustrates the NOPs of the different neuronal classes. It includes both the NOPs revealed in this thesis (dark colors) and the NOPs shown in previous studies or suggested by the circuitry and the motor activity (light colors). Taken together, these NOPs are in line with the known circuitry of the swimmeret system but a possible restriction applies. Since I did not perform my experiments in synaptically isolated neurons, my interpretation of a silent state is predominantly based on synaptic connections within the microcircuit. In contrast to that, differences in the passive membrane properties between neuronal classes (e.g. PSE and RSE) or even between individual neurons of the same class may contribute to the NOPs. Sherff and Mulloney [1997] showed that passive properties of motor neurons are not different between each of the four classes, i.e. PSE, RSE, PSI, RSI, and suggested that these properties do not play a crucial role in the generation of alternating PS and RS activity. Between motor neurons of the same class, however, they described minor differences that they mostly attributed to the sizes of the neurons. Larger motor neurons were more hyperpolarized and had a lower probability to reach spiking thresholds [Sherff and Mulloney, 1997]. I did not investigate the amplitude of extracellularly recorded action potentials for individual neurons but size-related differences may explain some of the variability of motor neurons from the same class. During inhibitory and excitatory stimulations, different pathways may recruited specific subpopulations of PSEs or RSEs since they might be involved in different behaviors.
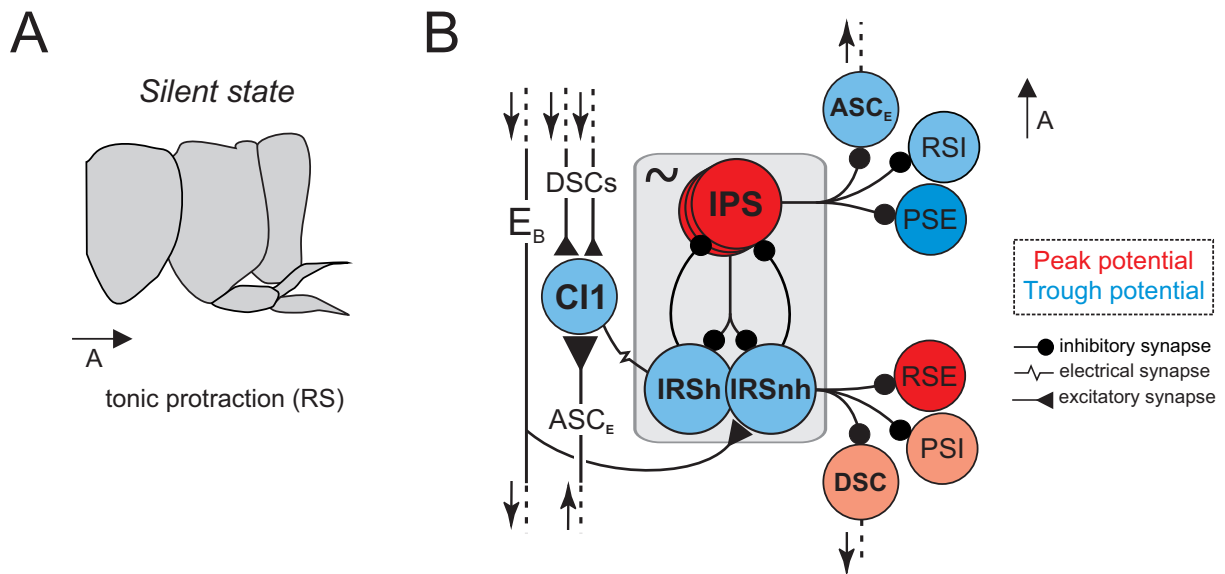
Figure 4.1: Initiation of fictive locomotion in the swimmeret system. **A:** In freely behaving crayfishes, swimmerets are tonically protracted in the return stroke (RS) position, indicating tonic excitation of RS muscles and tonic inhibition of PS muscles. **B:** Illustration of a representative microcircuit at a silent state and the hypothetical targeting via descending neuron E_B. Neurons are either locked at a depolarized (peak potential, red) or hyperpolarized (trough potential, blue) membrane potential (V_m), with respect to V_m oscillations while the system is active. Dark colors refer to the results from this thesis while light colors represent V_ms indicated by the literature or suggested by the circuitry and the behavior. The neuron E_B forms an excitatory synapse on IRSnh and can initiate and enhance fictive locomotion. **RS** *return stroke*, **CI1** *Commissural Interneuron 1*, **DSC** *Descending Coordinating Neuron*, **ASC_E** *Ascending Coordinating Neuron*, **IPS** *Inhibitor of Power Stroke*, **IRS** *Inhibitor of Return Stroke*, **IRSh** *IRS hook*, **IRSnh** *IRS nohook*, **RSI** *Return Stroke Inhibitor*, **RSE** *Return Stroke Exciter*, **PSI** *Power Stroke Inhibitor*, **PSE** *Power Stroke Exciter*.

A possible mechanism for initiation and enhancement

As discussed before, it is likely that my stimulations induced an interplay of parallel pathways that affected the swimmeret system simultaneously. Consequently, the interpretation of inputs from individual pathways is limited. However, initiation and enhancement may be explained in some more detail: Modulating the activity of CPG neurons is necessary to initiate or enhance fictive locomotion and I discovered that one class of CPG neurons, IRSnh, receives synaptic inputs from stimulated axons. These inputs were reflected by small postsynaptic potentials (PSPs) that depolarized the V_m. This is the first time, excitatory input on either class of CPG neurons is described and reflects a possible explanation of how descending pathways excite the swimmeret system.

In the following, I will speculate on one specific excitatory command neuron (E_B) that possibly provided the excitatory input on IRS. Please note that this is highly speculative and only reflects one possible explanation. However, there a some reasons why I assume that E_B is of particular interest: (1) Although stimulation sites were highly variable within my experiments, E_B is located in the middle of the generally targeted portion of the hemiconnectives. (2) Excitatory PSPs

(EPSPs) in IRSnh were elicited through a stimulation that could both initiate and enhance fictive locomotion and E_B was most likely stimulated during enhancement of fictive locomotion. (3) During enhancement, the period decreased which strongly indicates direct input on the CPG neurons, e.g. IRSnh. (4) Since PR does not affect the period similar to excitatory stimulations, I assume that the direct input on IRS was not elicited through a proctolinergic pathway. (5) E_B most likely does not release PR to modulate the swimmeret system.

Figure 4.1 B shows the silent state of a microcircuit and illustrates a possible excitatory synapse from E_B on IRSnh. I showed this synaptic input in two neurons recorded ipsilateral to the stimulation. Interestingly, I additionally recorded from one contralateral IRSnh which was not directly targeted during stimulations. This may suggest that E_B only targets the CPGs of the ipsilateral hemiganglia. This is emphasized by the observation that the stimulated axons projected predominantly to ipsilateral hemiganglia. In addition, the side-specific effect on burst strengths during enhancement indicates unilateral targeting of the swimmeret system but further recordings of ipsilateral and contralateral IRS neurons are necessary to verify this assumption. Acevedo et al. [1994] showed that most of the commissures that cross the midline of each ganglion are not likely to contain proctolinergic fibers, indicating that also proctolinergic pathways may not affect the swimmeret system bilaterally. The initiation of synchronous, rhythmic PS activity on both sides of the swimmeret system might be due to intraganglionic coupling mechanisms that are currently unknown. Therefore, figure 4.1 B only illustrates the microcircuit of one representative hemiganglion. In my experiments I recorded from IRSnh in abdominal ganglion A3 but I assume that each ganglion is equally targeted. I further did not record from IRSh and neglected the possibility that E_B has excitatory synapses on this type of IRS neurons. The other class of CPG neurons, IPS, was not directly targeted by E_B (N = 5 / 5).

During stimulations, E_B seems to provide tonic excitatory input to IRSnh. The question arises how this tonic excitation leads to V_m oscillations in IRSnh. IRSnh forms inhibitory synapses on IPS neurons and vice versa [Skinner and Mulloney, 1998; Mulloney, 2003; Smarandache-Wellmann et al., 2013]. This reciprocal inhibition determines the alternating activity of IRS and IPS when the system is active while intrinsic properties may help the CPG neurons to escape from mutual inhibition. One mechanism to reinduce excitability in a neuron are post-inhibitory rebounds (PIRs). Early computational models suggested that two reciprocally coupled pairs of inhibitory neurons can drive their alternating activity through PIRs [Perkel and Mulloney, 1974]. Schläger [2018] experimentally showed that IPS neurons possess the ability to generate PIRs but information about IRS neurons are so far not available. In the model of Perkel and Mulloney [1974], one pair of neurons with PIR can be entrained by the other pair, suggesting

that direct targeting of one class of CPG neurons may be sufficient to activate the CPGs. In fact, I was able to initiate rhythmic PS activity in a silent preparation through hyperpolarizing current injections in one IPS. However, the initiation of alternating CPG activity through descending pathways might include additional mechanisms. In other systems, descending neurons that activate a locomotor network are tonically active but switch to phasic activity when the network is activated [Dubuc and Grillner, 1989; Perrins and Weiss, 1996]. This transition in the firing pattern is induced by presynaptic inhibition from the targeted circuits and was also found in the stomatogastric nervous system of crustaceans [Nusbaum et al., 1992; Blitz and Nusbaum, 2008]. Synaptic feedback from the swimmeret system's microcircuits may modulate the firing pattern of E_B to produce a precisely timed excitatory input once the system is activated.

Parallel to initiation, excitatory input on IRSnh provides a promising explanation for the enhancement of fictive locomotion. The amplitudes of V_m oscillations in both IRSnh (N = 2 / 3) and IPS (N = 1 / 2) neurons increased in some of the recorded neurons. Interestingly, two IRSnh neurons strongly depolarized which indicates excitatory input from E_B. At the same time, the TP of one IPS neuron hyperpolarized while the PP remained constant. This suggests that the depolarization of IRSnh via E_B increased its inhibitory effect on IPS. This modulation of the CPG activity subsequently affected the postsynaptic motor neurons. V_m oscillations increased in most of the recorded motor neurons and burst strengths strongly increased, indicating that additional motor neurons were recruited. Some motor neurons reached their spiking thresholds while others increased spiking rate. Sherff and Mulloney [1997] showed that the V_ms of large motor neurons oscillate when the excitation level of the system is low but do not generate action potentials. This indicates that some subpopulations of (large) motor neurons can be recruited at higher excitation levels. During enhancement, PSEs tended to depolarize while the TP of most RSEs hyperpolarized. These changes may suggest reduced inhibitory input from IPSs and increased inhibitory input from IRSs and is in line with the changes in CPG neurons. Since motor neurons are known to generate PIRs [Schläger, 2018], increased inhibitory input may contributed to increase the excitation of these neurons. In addition, direct effects on motor neurons from descending pathways can be another possibility. Motor neurons are targeted by an unknown muscarinic or nicotinic pathway [Tschuluun et al., 2009], raising the possibility that they may be affected by E_B. However, proctolinergic pathways may also target motor neurons since PR increases burst strengths (Laudenberg, master's thesis, 2019, unpublished). These pathways may affect different classes of motor neurons, or even subpopulations within these classes differently. As an example, Braun and Mulloney [1993] observed that low concentrations of nicotine "increased the number of larger motor neuron spikes, whereas higher

concentration decreased the number of smaller spikes" on extracellular PS recordings. Therefore, different subpopulation may be recruited for specific behaviors but the specific role that motor neuron targeting plays in initiation or enhancement of fictive locomotion requires further investigations.

Termination or co-modulation?

In contrast to initiation and enhancement, I cannot explain the termination of fictive locomotion by the activation of one individual pathway. Previous studies gave evidence that period [Davis and Kennedy, 1972b] and burst strengths [Davis and Kennedy, 1972b; Mulloney et al., 1987; Acevedo et al., 1994] are affected by inhibitory stimulations which suggests that both CPG neurons and motor neurons are targeted. I did not observe direct synaptic input on either neuronal group during complete termination of fictive locomotion. At a silent state, the NOPs of both CPG neurons and motor neurons were in line with the proposed silent state of the microcircuits which could also be induced by OA application. OA induced a similar NOP in one IPS while PSEs were silent. IRSnh, however, was differently affected by OA. In one experiment, the V_m oscillations of IRSnh ceased around its PP. Although this contradicted my model of a silent state, the experiment was of some particular interest. Excitatory stimulations initiated fictive locomotion even when the system was previously silenced by bath application of OA. This may either suggest that direct excitatory input activated the CPGs, or that neuromodulators released by some excitatory pathway superimposed the effect of OA. In general, the interaction of different neuromodulators might play a crucial role to modulate the swimmeret system's activity. Co-application of OA and PR for example modulates the period differently compared to separate applications of both substances (Laudenberg, master's thesis, 2019, unpublished). Since OA and PR are presumably released by separated pathways that have antagonistic effects on the system, this suggests that co-modulation must be considered to be a key element within the swimmeret system. Within the concept of co-modulation, most likely not only the presence of two (or more) neuromodulators, but also their concentrations determine their effects. I showed that OA can also increase the period of fictive locomotion and a related project in our research group revealed that this effect is caused by low concentrations of OA (Laudenberg, master's thesis, 2019, unpublished).

The interplay of different neuromodulators and their concentrations was extensively studied in other systems that give insights in the complexity (see Svensson et al. [2019] for a review). In isolated preparations of the leech ventral nerve cord, OA elicits fictive swimming but co-application of OA and serotonin inhibits active preparations [Mesce et al., 2001]. In locusts,

OA [Rillich et al., 2013] or CCh [Buhl et al., 2008] elicit fictive flying while only low concentrations of OA were shown to elicit fictive walking [Rillich et al., 2013]. As an example from crayfishes, some motor neurons that innervate the tonic flexor muscle of the abdomen use PR as a co-transmitter [Bishop et al., 1984] which suggests that this mechanism may also play a role in the swimmeret system. A great number of modulatory interneurons were extensively described and characterized in the crustacean stomatogastric nervous system [Coleman et al., 1992; Nusbaum et al., 1992; Wood et al., 2000; Saideman et al., 2007; Blitz and Nusbaum, 2008]. To give an example of the complex nature of neuromodulation within this system, stimulations of the Modulatory Commissural Neuron 1 (MCN1) elicit comparable fictive activity of the gastric mill as bath application of pyrokinin peptides. This is remarkable because MCN1 does not contain pyrokinin peptides and highlights that different pathways that use different neuromodulatory substances can have similar effects on a neuronal network. Analog, multiple pathways are most likely involved in the modulation of fictive locomotion in the swimmeret system and the interplay between different neuromodulators used by these pathways requires detailed investigation.

4.4 Conclusion

Individual command neurons of the swimmeret system can be stimulated to modulate fictive locomotion. However, the method of choice to excite these neurons limits the characterization of distinct descending pathways. The existence of five excitatory and three inhibitory command neurons suggests that their modes of action are not identical but further investigation of their roles in different behaviors requires improved accessibility. Different pathways most likely work in parallel to generate a specific behavior like forward swimming or turning. Since orientation in a three dimensional habitat sometimes requires bilateral differences in the generated motor output, the side-specific recruitment of motor neurons provides first evidence of how descending command neurons may evoke a specific behavior that is not straight forward swimming.

Initiation of locomotion is the prerequisite for any form of goal-directed movement. One class of CPG neurons (IRSnh) is directly targeted by excitatory pathways. In principle, this input may be sufficient to initiate the alternating motor activity of one single swimmeret. Additional inputs on swimmeret motor neurons may be necessary in order to evoke a specific form of locomotion. Furthermore, different subpopulations of motor neurons may be affected by different pathways and different neuromodulators. Co-modulatory effects of these substances are probably involved in the recruitment of the desired populations of neurons.

5 Outlook and future experiments

The generation of fictive locomotion in the swimmeret system is determined by the activation of a coupled chain of separated CPGs. My results show that a subset of CPG neurons is directly targeted by one excitatory pathway and provide evidence that this synaptic input might be sufficient to elicit a coordinated motor output. As already discussed, however, performing a wide range of similar, but not identical behaviors most likely requires the interplay of several pathways that use different mechanisms to control network activities. In this chapter I will briefly describe remaining questions and future experiments that can be performed to gain better insights in descending control of the swimmeret system and of locomotion in general.

Additional targets of descending pathways

The revealing of direct excitatory input on IRSnh is a major step in our understanding of how the swimmeret system's activity is controlled by descending pathways. Further investigation of this synaptic connection will be crucial to better understand its general role in modulating the motor output. Synaptic transmission was very fast which indicates the activation of ionotropic receptors but may also suggest an electrical synapse on IRSnh. The conduction velocities of the stimulated axons allow an estimation of the speed of synaptic transmission and do not fully exclude this possibility. Although these axons were most likely the presynaptic partners of IRSnh, complete clarification was not possible. Previous IRSnh stainings using markers that cross gap junctions, e.g. Lucifer yellow or Neurobiotin, did not shown co-labeling of descending interneurons which may contradict the idea of an electrical synapse [Smarandache-Wellmann et al., 2013]. However, simultaneous recordings from IRSnh and the presynaptic neuron would provide further evidence. My occasional attempts to intracellularly record from excitatory command neurons failed but Davis and Kennedy [1972a] were able to perform such a recording in the lobster. It is not possible to assign their recording to one of the described command neurons but it demonstrates a highly interesting experimental approach.

Information about the possible targeting of the other type of IRS neurons are still missing.

Intracellular recordings from IRSh are necessary to clarify if both types are simultaneously targeted by the same pathways, affected by different pathways, or if IRSh performs a different role in the initiation of locomotion. Maybe IRSnh acts as a relay to transform descending, excitatory information while IRSh is mostly maintaining the CPG activity once the system is activated. Moreover, IRSh, but not IRSnh, is electrically coupled to CI1 and may have a special role in intersegmental coordination. Therefore, different roles of IRSnh and IRSh within the network are possible.

As mentioned before, direct effects of descending pathways on motor neurons are possible and would provide more flexible mechanisms to modulate to motor output. PR is most likely not the neurotransmitter involved in synaptic input on IRSnh but motor neurons, however, remain possible targets of proctolinergic pathways. In the stomatogastric nervous system, PR is released by modulatory interneurons and activates an voltage-dependent inward current that depolarizes spiking neurons in the system [Nusbaum and Marder, 1989; Golowasch and Marder, 1992]. In order to identify a similar effect in the swimmeret system, intracellular recordings from motor neurons that are isolated from presynaptic inputs would allow to measure currents induced by PR. It would be particularly interesting if distinct subpopulations are differently affected by PR which may be important for specific motor neuron recruitment. In addition, intracellular recordings from synaptically isolated neurons would give insights into the contribution of passive membrane properties to the NOPs.

Interactions with the walking system

My results provide evidence that both the swimmeret and the walking system are controlled by the same descending pathways. The command neurons of the swimmeret system are thought to have their somata within the SOG and I most likely stimulated their axons at various portions of the nerve cord. Furthermore, I could initiate rhythmic activity in the walking system through these stimulations. In future experiments, backfills of the stimulated axon bundles would provide first evidence of their projection patterns within the thoracic ganglia and possible interactions with the walking system. Similar to the swimmeret system, the walking system is also activated by cholinergic agonists [Chrachri and Clarac, 1987]. This may suggest that the same pathway that targets IRSnh also modulates CPG activity of the walking legs. In order to verify this assumption, further experiments are necessary in which the thoracic and abdominal nerve cord are intact and the motor activities of both systems are recorded. Moreover, recordings of antagonistic motor activity in the walking system are needed to demonstrate the initiation of fictive locomotion, e.g. depressor and levator activity.

If descending pathways modulate the activity of both locomotor systems, the same pathway may be used to recruit both systems depending on the desired behavior. Salamanders for example show two forms of locomotion, i.e. swimming and walking, and the respective muscle activity differs between both conditions [Delvolvé et al., 1997]. Electrical stimulations in the caudal mesencephalon are able to induce both swimming and walking in semi-intact preparations and evidence is given that the same descending pathway controls both motor outputs [Bem et al., 2003; Cabelguen et al., 2003]. Moreover, salamanders show fluent transitions between walking and swimming [Ashley-Ross and Bechtel, 2004], and Cabelguen et al. [2003] demonstrated that stimulations at low amplitudes induce walking patterns while higher amplitudes induce swimming behavior. Similar serial recruitment of the walking and the swimmeret system in crayfishes is possible and a worthwhile approach in future experiments.

Co-modulation as an important aspect of future experiments

Several different neuromodulatory substances affect the swimmeret system's activity, including neuropeptides, amines or small-molecule neurotransmitters [Mulloney et al., 1987; Sherff and Mulloney, 1991; Barthe et al., 1993; Braun and Mulloney, 1993; Mulloney et al., 1997]. This indicates a huge variety of different ionotropic and metabotropic receptors within the neuronal microcircuits and implies that the neuromodulation of the swimmeret system is highly complex. This is further emphasized by the presence of multiple distinct descending pathways that have similar effects on the swimmeret system's activity. In addition, some substances are most likely brought to the swimmeret neurons as neurohormones via the hemolymph and intensify the complex interplay. The importance to investigate the interactions of different neuromodulators is highlighted in the stomatogastric nervous system (see Marder and Bucher [2007] for a review). Approximately 40 axons project to the stomatogastric ganglion [Coleman et al., 1992] and more than half of them were already shown to provide modulatory input on the CPGs of the system (see Stein [2009] for a review). They contain a vast number of different neuromodulators and can have various effects on the system's activity (e.g. Saideman et al. [2007]).

Another important factor in neuromodulation is co-transmission of more than one neurotransmitter. Neurons can contain multiple neurotransmitters that can be released together or separately, and act together or separately (see Svensson et al. [2019] for a review). It is reasonable to assume that this basic mechanism also applies in the swimmeret system and maybe even for excitatory and inhibitory command neurons. Although Acevedo et al. [1994] stated that the terminals of proctolinergic axons probably contain solely PR, detailed information about the precise neurotransmitter composition are not available. Theoretically, excitatory command

neurons may contain PR and OA. Both substances may be released independently or are simultaneously and their actions may depend on the excitation level of the system. Hence, detailed investigation of the combined effects of multiple neuromodulators is highly necessary to understand the modulation of fictive locomotion in the swimmeret system.

Bibliography

Acevedo, L. D. (1990). *Control of the expression of a simple behavior: activation and inhibition of the crayfish swimmeret rhythm by command neurons and their transmitters*. Ph. D. thesis, University of California, Davis.

Acevedo, L. D., W. M. Hall, and B. Mulloney (1994). Proctolin and excitation of the crayfish swimmeret system. *The Journal of Comparative Neurology 345*(4), 612–627.

Alexandrowicz, J. S. (1926). The innervation of the heart of the cockroach (*Periplaneta orientalis*). *The Journal of Comparative Neurology 41*(1), 291–309.

Alving, B. O. (1968). Spontaneous activity in isolated somata of *Aplysia* pacemaker neurons. *The Journal of General Physiology 51*(1), 29–45.

Ashley-Ross, M. A. and B. F. Bechtel (2004). Kinematics of the transition between aquatic and terrestrial locomotion in the newt *Taricha torosa*. *Journal of Experimental Biology 207*(3), 461–474.

Atwood, H. L. and C. A. G. Wiersma (1967). Command interneurons in the crayfish central nervous system. *Journal of Experimental Biology 46*(2), 249–261.

Bal, T., F. Nagy, and M. Moulins (1988). The pyloric central pattern generator in crustacea: a set of conditional neuronal oscillators. *Journal of Comparative Physiology A 163*(6), 715–727.

Barthe, J.-Y., M. Bévengut, and F. Clarac (1991). The swimmeret rhythm and its relationships with postural and locomotor activity in the isolated nervous system of the crayfish *Procambarus Clarkii*. *Journal of Experimental Biology 157*(1), 205–226.

Barthe, J. Y., M. Bevengut, and F. Clarac (1993). In vitro, protolin and serotonin induced modulations of the abdominal motor system activities in crayfish. *Brain Research 623*(1), 101–109.

Bem, T., J. M. Cabelguen, &. Ekeberg, and S. Grillner (2003). From swimming to walking: a single basic network for two different behaviors. *Biological Cybernetics 88*(2), 79–90.

Bidaye, S. S., C. Machacek, Y. Wu, and B. J. Dickson (2014). Neuronal control of *Drosophila* walking direction. *Science 344*(6179), 97–101.

Bibliography

Bishop, C. A., J. J. Wine, and M. OShea (1984). Neuropeptide proctolin in postural motoneurons of the crayfish. *The Journal of Neuroscience 4*(8), 2001–2009.

Blitz, D. M. and M. P. Nusbaum (2008). State-dependent presynaptic inhibition regulates central pattern generator feedback to descending inputs. *The Journal of Neuroscience 28*(38), 9564–9574.

Blumenthal, F. (2018). *Physiological and morphological analysis of a coordinating circuit.* Ph. D. thesis, University of Cologne, Cologne.

Borgmann, A., S. L. Hooper, and A. Büschges (2009). Sensory feedback induced by front-leg stepping entrains the activity of central pattern generators in caudal segments of the stick insect walking system. *The Journal of Neuroscience 29*(9), 2972–2983.

Bouvier, J., V. Caggiano, R. Leiras, V. Caldeira, C. Bellardita, K. Balueva, A. Fuchs, and O. Kiehn (2015). Descending command neurons in the brainstem that halt locomotion. *Cell 163*(5), 1191–1203.

Bowerman, R. and J. Larimer (1974). Command fibres in the circumoesophageal connectives of crayfish: I. tonic fibres. *Journal of Experimental Biology 60*(1), 95–117.

Braun, G. and B. Mulloney (1993). Cholinergic modulation of the swimmeret motor system in crayfish. *Journal of Neurophysiology 70*(6), 2391–2398.

Brodfuehrer, P. D., E. A. Debski, B. A. O'Gara, and W. O. Friesen (1995). Neuronal control of leech swimming. *Journal of Neurobiology 27*(3), 403–418.

Brodfuehrer, P. D. and W. O. Friesen (1986). Initiation of swimming activity by trigger neurons in the leech subesophageal ganglion. *Journal of Comparative Physiology A 159*(4), 489–502.

Buhl, E., K. Schildberger, and P. A. Stevenson (2008). A muscarinic cholinergic mechanism underlies activation of the central pattern generator for locust flight. *Journal of Experimental Biology 211*(14), 2346–2357.

Büschges, A. (2005). Sensory control and organization of neural networks mediating coordination of multisegmental organs for locomotion. *Journal of Neurophysiology 93*(3), 1127–1135.

Cabelguen, J.-M., C. Bourcier-Lucas, and R. Dubuc (2003). Bimodal locomotion elicited by electrical stimulation of the midbrain in the salamander *Notophthalmus viridescens*. *The Journal of Neuroscience 23*(6), 2434–2439.

Cang, J. and W. O. Friesen (2000). Sensory modification of leech swimming: Rhythmic activity of ventral stretch receptors can change intersegmental phase relationships. *The Journal of Neuroscience 20*(20), 7822–7829.

Bibliography

Carlson, A. J. (1904). Nervous pacemaker in limulus heart. *American Journal of Physiology 12*, 67–74.

Cattaert, D., J.-Y. Barthe, D. M. Neil, and F. Clarac (1992). Remote control of the swimmeret central pattern generator in crayfish (*Procambarus clarkii* and *Pacifastacus leniusculus*): Effect of a walking leg proprioceptor. *Journal of Experimental Biology 169*(1), 181–206.

Cattaert, D. and E. Clarac (1983). Influence of walking on swimmeret beating in the lobster *Homarus gammarus*. *Journal of Neurobiology 14*(6), 421–439.

Chrachri, A. and F. Clarac (1987). Induction of rhythmic activity in motoneurons of crayfish thoracic ganglia by cholinergic agonists. *Neuroscience Letters 77*(1), 49–54.

Cohen, I., H. Kita, and W. Van Der Kloot (1974). Stochastic properties of spontaneous transmitter release at the crayfish neuromuscular junction. *The Journal of Physiology 236*(2), 363–371.

Coleman, M. J., M. P. Nusbaum, I. Cournil, and B. J. Claiborne (1992). Distribution of modulatory inputs to the stomatogastric ganglion of the crab, *Cancer borealis*. *The Journal of Comparative Neurology 325*(4), 581–594.

Cooke, I. M. (2002, apr). Reliable, responsive pacemaking and pattern generation with minimal cell numbers: the crustacean cardiac ganglion. *The Biological Bulletin 202*(2), 108–136.

Copp, N. H. and S. Hodes (2001). Asynchronous swimmeret beating during defense turns in the crayfish, *Procambarus clarkii*. *Journal of Comparative Physiology A 187*(9), 737–745.

Daghfous, G., F. Auclair, F. Clotten, J.-L. Létourneau, E. Atallah, J.-P. Millette, D. Derjean, R. Robitaille, B. S. Zielinski, and R. Dubuc (2018). GABAergic modulation of olfactomotor transmission in lampreys. *PLOS Biology 16*(10).

Davis, W. (1968a). Lobster righting responses and their neural control. *Proceedings of the Royal Society of London B: Biological Sciences 170*(1021), 435–456.

Davis, W. (1968b). Quantitative analysis of swimmeret beating in the lobster. *Journal of Experimental Biology 48*(3), 643–662.

Davis, W. J. (1969). The neural control of swimmeret beating in the lobster. *Journal of Experimental Biology 50*(1), 99–117.

Davis, W. J. and D. Kennedy (1972a). Command interneurons controlling swimmeret movements in the lobster: I. types of effects on motoneurons. *Journal of Neurophysiology 35*(1), 1–12.

Davis, W. J. and D. Kennedy (1972b). Command interneurons controlling swimmeret move-
ments in the lobster: II. Interaction of effects on motoneurons. *Journal of Neurophysiol-
ogy 35*(1), 13–19.

Delvolvé, I., T. Bem, and J. M. Cabelguen (1997). Epaxial and limb muscle activity during
swimming and terrestrial stepping in the adult newt, *Pleurodeles waltl. Journal of Neurophys-
iology 78*(2), 638–650.

Derjean, D., A. Moussaddy, E. Atallah, M. St-Pierre, F. Auclair, S. Chang, X. Ren, B. Zielinski,
and R. Dubuc (2010). A novel neural substrate for the transformation of olfactory inputs into
motor output. *PLOS biology 8*(12).

Di Prisco, G. V., E. Pearlstein, R. Robitaille, and R. Dubuc (1997). Role of sensory-evoked
NMDA plateau potentials in the initiation of locomotion. *Science 278*(5340), 1122–1125.

Dubuc, R., F. Brocard, M. Antri, K. Fénelon, J.-F. Gariépy, R. Smetana, A. Ménard, D. Le Ray,
G. V. Di Prisco, and É. Pearlstein (2008). Initiation of locomotion in lampreys. *Brain research
reviews 57*(1), 172–182.

Dubuc, R. and S. Grillner (1989). The role of spinal cord inputs in modulating the activity of
reticulospinal neurons during fictive locomotion in the lamprey. *Brain Research 483*(1), 196–
200.

Dudel, J. and S. W. Kuffler (1961). The quantal nature of transmission and spontaneous minia-
ture potentials at the crayfish neuromuscular junction. *The Journal of Physiology 155*(3),
514–529.

Dudel, J. and R. K. Orkand (1960). Spontaneous potential changes at crayfish neuromuscular
junctions. *Nature 186*(4723), 476–477.

Eaton, R. C., R. K. K. Lee, and M. B. Foreman (2001). The mauthner cell and other identified
neurons of the brainstem escape network of fish. *Progress in Neurobiology 63*(4), 467–485.

Edwards, D. H., W. J. Heitler, and F. B. Krasne (1999). Fifty years of a command neuron: the
neurobiology of escape behavior in the crayfish. *Trends in Neurosciences 22*(4), 153–161.

Evans, P. D., E. A. Kravitz, and B. R. Talamo (1976). Octopamine release at two points along
lobster nerve trunks. *The Journal of Physiology 262*(1), 71–89.

Fatt, P. and B. Katz (1952). Spontaneous subthreshold activity at motor nerve endings. *The
Journal of Physiology 117*(1), 109–128.

Finger, W. and H. Stettmeier (1981). Analysis of miniature spontaneous inhibitory postsynaptic

currents (sIPSCs) from current noise in crayfish opener muscle. *Pfluegers Archiv European Journal of Physiology 392*(2), 157–162.

Fraser, P. J. (1975). Three classes of input to a semicircular canal interneuron in the crab, *Scylla serrata*, and a possible output. *Journal of Comparative Physiology A 104*(3), 261–271.

Friesen, W., M. Poon, and G. Stent (1976). An oscillatory neuronal circuit generating a locomotory rhythm. *Proceedings of the National Academy of Sciences 73*(10), 3734–3738.

Golowasch, J. and E. Marder (1992). Proctolin activates an inward current whose voltage dependence is modified by extracellular Ca^2. *The Journal of Neuroscience 12*(3), 810–817.

Grätsch, S., F. Auclair, O. Demers, E. Auguste, A. Hanna, A. Büschges, and R. Dubuc (2018). A brainstem neural substrate for stopping locomotion. *The Journal of Neuroscience 39*(6), 1044–1057.

Hama, N. and M. Takahata (2003). Effects of leg movements on the synaptic activity of descending statocyst interneurons in crayfish, *Procambarus clarkii*. *Journal of Comparative Physiology A 189*(12), 877–888.

Hama, N. and M. Takahata (2005). Modification of statocyst input to local interneurons by behavioral condition in the crayfish brain. *Journal of Comparative Physiology A 191*(8), 747–759.

Heitler, W. J. (1978). Coupled motoneurones are part of the crayfish swimmeret central oscillator. *Nature 275*(5677), 231–234.

Heitler, W. J. and K. G. Pearson (1980). Non-spiking interactions and local interneurones in the central pattern generator of the crayfish swimmeret system. *Brain Research 187*(1), 206–211.

Ikeda, K. and C. Wiersma (1964). Autogenic rhythmicity in the abdominal ganglia of the crayfish: the control of swimmeret movements. *Comparative Biochemistry and Physiology 12*(1), 107–115.

Josset, N., M. Roussel, M. Lemieux, D. Lafrance-Zoubga, A. Rastqar, and F. Bretzner (2018). Distinct contributions of mesencephalic locomotor region nuclei to locomotor control in the freely behaving mouse. *Current Biology 28*(6), 884–901.e3.

Karayannidou, A., P. V. Zelenin, G. N. Orlovsky, and T. G. Deliagina (2007). Responses of reticulospinal neurons in the lamprey to lateral turns. *Journal of Neurophysiology 97*(1), 512–521.

Bibliography

Kavalali, E. T. (2014). The mechanisms and functions of spontaneous neurotransmitter release. *Nature Reviews Neuroscience 16*(1), 5–16.

Kristan, W. B. and R. L. Calabrese (1976). Rhythmic swimming activity in neurones of the isolated nerve cord of the leech. *Journal of Experimental Biology 65*(3), 643–668.

Livingstone, M. S., R. M. Harris-Warrick, and E. A. Kravitz (1980). Serotonin and octopamine produce opposite postures in lobsters. *Science 208*(4439), 76–79.

Marder, E. and D. Bucher (2001). Central pattern generators and the control of rhythmic movements. *Current Biology 11*(23), R986–R996.

Marder, E. and D. Bucher (2007). Understanding circuit dynamics using the stomatogastric nervous system of lobsters and crabs. *Annual Review of Physiology 69*(1), 291–316.

Mesce, K. A., K. M. Crisp, and L. S. Gilchrist (2001). Mixtures of octopamine and serotonin have nonadditive effects on the CNS of the medicinal leech. *Journal of Neurophysiology 85*(5), 2039–2046.

Mulloney, B. (1997). A test of the excitability-gradient hypothesis in the swimmeret system of crayfish. *The Journal of Neuroscience 17*(5), 1860–1868.

Mulloney, B. (2003). During fictive locomotion, graded synaptic currents drive bursts of impulses in swimmeret motor neurons. *The Journal of Neuroscience 23*(13), 5953–5962.

Mulloney, B. (2005). A method to measure the strength of multi-unit bursts of action potentials. *Journal of Neuroscience Methods 146*(1), 98 – 105.

Mulloney, B., L. D. Acevedo, and A. G. Bradbury (1987). Modulation of the crayfish swimmeret rhythm by octopamine and the neuropeptide proctolin. *Journal of Neurophysiology 58*(3), 584–597.

Mulloney, B. and W. M. Hall (2000). Functional organization of crayfish abdominal ganglia. III. swimmeret motor neurons. *Journal of Comparative Neurology 419*(2), 233–243.

Mulloney, B. and W. M. Hall (2003). Local commissural interneurons integrate information from intersegmental coordinating interneurons. *Journal of Comparative Neurology 466*(3), 366–376.

Mulloney, B. and W. M. Hall (2007). Not by spikes alone: Responses of coordinating neurons and the swimmeret system to local differences in excitation. *Journal of Neurophysiology 97*(1), 436–450.

Bibliography

Mulloney, B., P. I. Harness, and W. M. Hall (2006). Bursts of information: Coordinating interneurons encode multiple parameters of a periodic motor pattern. *Journal of Neurophysiology 95*(2), 850–861.

Mulloney, B., H. Namba, H.-J. Agricola, and W. M. Hall (1997). Modulation of force during locomotion: Differential action of crustacean cardioactive peptide on power-stroke and return-stroke motor neurons. *The Journal of Neuroscience 17*(18), 6872–6883.

Mulloney, B. and C. Smarandache-Wellmann (2012). Neurobiology of the crustacean swimmeret system. *Progress in Neurobiology 96*(2), 242–267.

Murchison, D., A. Chrachri, and B. Mulloney (1993). A separate local pattern-generating circuit controls the movements of each swimmeret in crayfish. *Journal of Neurophysiology 70*(6), 2620–2631.

Nakagawa, H. and M. Hisada (1989). Morphology of descending statocyst interneurons in the crayfish *Procambarus clarkii* (Girard). *Cell and Tissue Research 255*(3), 539–551.

Namba, H. and B. Mulloney (1999). Coordination of limb movements: three types of intersegmental interneurons in the swimmeret system and their responses to changes in excitation. *Journal of Neurophysiology 81*(5), 2437–2450.

Negro, C. A. D., G. D. Funk, and J. L. Feldman (2018, may). Breathing matters. *Nature Reviews Neuroscience 19*(6), 351–367.

Nusbaum, M. P. and E. Marder (1989). A modulatory proctolin-containing neuron (MPN). I. identification and characterization. *The Journal of Neuroscience 9*(5), 1591–1599.

Nusbaum, M. P., J. M. Weimann, J. Golowasch, and E. Marder (1992). Presynaptic control of modulatory fibers by their neural network targets. *The Journal of Neuroscience 12*(7), 2706–2714.

O'Gara, B. A. and W. O. Friesen (1995). Termination of leech swimming activity by a previously identified swim trigger neuron. *Journal of Comparative Physiology A 177*(5), 627–636.

Paul, D. H. and B. Mulloney (1985a). Local interneurons in the swimmeret system of the crayfish. *Journal of Comparative Physiology A 156*(4), 489–502.

Paul, D. H. and B. Mulloney (1985b). Nonspiking local interneuron in the motor pattern generator for the crayfish swimmeret. *Journal of Neurophysiology 54*(1), 28–39.

Pearson, K. G. and J. F. Iles (1970). Discharge patterns of coxal levator and depressor motoneurones of the cockroach, *Periplaneta americana*. *Journal of Experimental Biology 52*(1), 139–165.

Bibliography

Perkel, D. H. and B. Mulloney (1974). Motor pattern production in reciprocally inhibitory neurons exhibiting postinhibitory rebound. *Science 185*(4146), 181–183.

Perrins, R., A. Walford, and A. Roberts (2002). Sensory activation and role of inhibitory reticulospinal neurons that stop swimming in hatchling frog tadpoles. *The Journal of Neuroscience 22*(10), 4229–4240.

Perrins, R. and K. R. Weiss (1996). A cerebral central pattern generator in *Aplysia* and its connections with buccal feeding circuitry. *The Journal of Neuroscience 16*(21), 7030–7045.

Ramirez, J.-M. (1988). Interneurons in the suboesophageal ganglion of the locust associated with flight initiation. *Journal of Comparative Physiology A 162*(5), 669–685.

Rillich, J., P. A. Stevenson, and H. J. Pflueger (2013). Flight and walking in locusts–cholinergic co-activation, temporal coupling and its modulation by biogenic amines. *PLOS ONE 8*(5).

Roeder, T., J. Degen, and M. Gewecke (1998). Epinastine, a highly specific antagonist of insect neuronal octopamine receptors. *European Journal of Pharmacology 349*(2-3), 171–177.

Saideman, S. R., D. M. Blitz, and M. P. Nusbaum (2007). Convergent motor patterns from divergent circuits. *Journal of Neuroscience 27*(25), 6664–6674.

Schläger, L. (2018). *Ionic currents and intrinsic properties of key interneurons and their influence on network activity in a chain of coupled oscillators*. Ph. D. thesis, University of Cologne, Cologne.

Schneider, A. C. (2017). *Encoding of Coordinating Information in a Network of Coupled Oscillators*. Ph. D. thesis, University of Cologne, Cologne.

Schneider, H., B. A. Trimmer, J. Rapus, M. Eckert, D. E. Valentine, and E. A. Kravitz (1993). Mapping of octopamine-immunoreactive neurons in the central nervous system of the lobster. *The Journal of Comparative Neurology 329*(1), 129–142.

Schoofs, A., S. Hückesfeld, P. Schlegel, A. Miroschnikow, M. Peters, M. Zeymer, R. Spieß, A. S. Chiang, and M. J. Pankratz (2014). Selection of motor programs for suppressing food intake and inducing locomotion in the *Drosophila* brain. *PLOS Biology 12*(6).

Seichter, H. A., F. Blumenthal, and C. R. Smarandache-Wellmann (2014). The swimmeret system of crayfish: A practical guide for the dissection of the nerve cord and extracellular recordings of the motor pattern. *Journal of Visualized Experiments* (93).

Sen, R., M. Wu, K. Branson, A. Robie, G. M. Rubin, and B. J. Dickson (2017). Moonwalker descending neurons mediate visually evoked retreat in *Drosophila*. *Current Biology 27*(5), 766–771.

Bibliography

Sherff, C. M. and B. Mulloney (1991). Red pigment concentrating hormone is a modulator of the crayfish swimmeret system. *Journal of Experimental Biology 155*(1), 21–35.

Sherff, C. M. and B. Mulloney (1996). Tests of the motor neuron model of the local pattern-generating circuits in the swimmeret system. *The Journal of Neuroscience 16*(8), 2839–2859.

Sherff, C. M. and B. Mulloney (1997). Passive properties of swimmeret motor neurons. *Journal of Neurophysiology 78*(1), 92–102.

Siwicki, K. K. and C. A. Bishop (1986). Mapping of proctolinlike immunoreactivity in the nervous systems of lobster and crayfish. *The Journal of Comparative Neurology 243*(4), 435–453.

Skinner, F. K. and B. Mulloney (1998). Intersegmental coordination of limb movements during locomotion: mathematical models predict circuits that drive swimmeret beating. *The Journal of Neuroscience 18*(10), 3831–3842.

Smarandache-Wellmann, C. and S. Grätsch (2014). Mechanisms of coordination in distributed neural circuits: encoding coordinating information. *The Journal of Neuroscience 34*(16), 5627–5639.

Smarandache-Wellmann, C., C. Weller, and B. Mulloney (2014). Mechanisms of coordination in distributed neural circuits: decoding and integration of coordinating information. *The Journal of Neuroscience 34*(3), 793–803.

Smarandache-Wellmann, C., C. Weller, T. M. Wright, and B. Mulloney (2013). Five types of nonspiking interneurons in local pattern-generating circuits of the crayfish swimmeret system. *Journal of Neurophysiology 110*(2), 344–357.

Stein, P. S. (1971). Intersegmental coordination of swimmeret motoneuron activity in crayfish. *Journal of Neurophysiology 34*(2), 310–318.

Stein, W. (2009). Modulation of stomatogastric rhythms. *Journal of Comparative Physiology A 195*(11), 989–1009.

Sutherland, R. M. and R. F. Nunnemacher (1968). Microanatomy of crayfish thoracic cord and roots. *Journal of Comparative Neurology 132*(4), 499–517.

Svensson, E., J. Apergis-Schoute, G. Burnstock, M. P. Nusbaum, D. Parker, and H. B. Schioeth (2019). General principles of neuronal co-transmission: Insights from multiple model systems. *Frontiers in Neural Circuits 12*(117).

Sylva, M., M. J. van den Hoff, and A. F. Moorman (2013). Development of the human heart. *American Journal of Medical Genetics Part A 164*(6), 1347–1371.

Bibliography

Takahata, M. and M. Hisada (1982). Statocyst interneurons in the crayfish *Procambarus clarkii* Girard. *Journal of Comparative Physiology A 149*(3), 287–300.

Takahata, M., H. Komatsu, and M. Hisada (1984). Positional orientation determined by the behavioural context in *Procambarus clarkii* Girard (decapoda: Macrura). *Behaviour 88*(3), 240–264.

Takakusaki, K., J. Kohyama, and K. Matsuyama (2003). Medullary reticulospinal tract mediating a generalized motor inhibition in cats: iii. functional organization of spinal interneurons in the lower lumbar segments. *Neuroscience 121*(3), 731–746.

Tschuluun, N., W. Hall, and B. Mulloney (2009). State-changes in the swimmeret system: a neural circuit that drives locomotion. *Journal of Experimental Biology 212*(22), 3605–3611.

Ullén, F., T. Deliagina, G. Orlovsky, and G. S (1995). Spatial orientation in the lamprey. I. Control of pitch and roll. *Journal of Experimental Biology 198*, 665–673.

Wernicke, R. (1876). *Zur Physiologie des embryonalen Herzens*. Ph. D. thesis, Friedrich-Schiller-Universität, Jena.

Westberg, K.-G. and A. Kolta (2011). The trigeminal circuits responsible for chewing. In *International Review of Neurobiology*, pp. 77–98.

Whelan, P. (1996). Control of locomotion in the decerebrate cat. *Progress in Neurobiology 49*(5), 481–515.

Wiersma, C. (1947). Giant nerve fiber system of the crayfish. A contribution to comparative physiology of synapse. *Journal of Neurophysiology 10*(1), 23–38.

Wiersma, C. and G. Hughes (1961). On the functional anatomy of neuronal units in the abdominal cord of the crayfish, *Procambarus clarkii* (Girard). *Journal of Comparative Neurology 116*(2), 209–228.

Wiersma, C. and K. Ikeda (1964). Interneurons commanding swimmeret movements in the crayfish, *Procambarus clarki* (Girard). *Comparative Biochemistry and Physiology 12*(4), 509–525.

Wilson, D. M. (1961). The central nervous control of flight in a locust. *Journal of Experimental Biology 38*(2), 471–490.

Wood, D. E., W. Stein, and M. P. Nusbaum (2000). Projection neurons with shared cotransmitters elicit different motor patterns from the same neural circuit. *The Journal of Neuroscience 20*(23), 8943–8953.

Bibliography

Yoshino, M., M. Takahata, and M. Hisada (1980). Statocyst control of the uropod movement in response to body rolling in crayfish. *Journal of Comparative Physiology A 139*(3), 243–250.

Zelenin, P. V., T. G. Deliagina, S. Grillner, and G. N. Orlovsky (2000). Postural control in the lamprey: A study with a neuro-mechanical model. *Journal of Neurophysiology 84*(6), 2880–2887.

Zill, S., J. Schmitz, and A. Büschges (2004). Load sensing and control of posture and locomotion. *Arthropod structure & development 33*(3), 273–286.

Zorović, M. and B. Hedwig (2012). Descending brain neurons in the cricket *Gryllus bimaculatus* (de Geer): auditory responses and impact on walking. *Journal of Comparative Physiology A 199*(1), 25–34.

Appendix

Calculation of the distance between stimulation site and hook recording
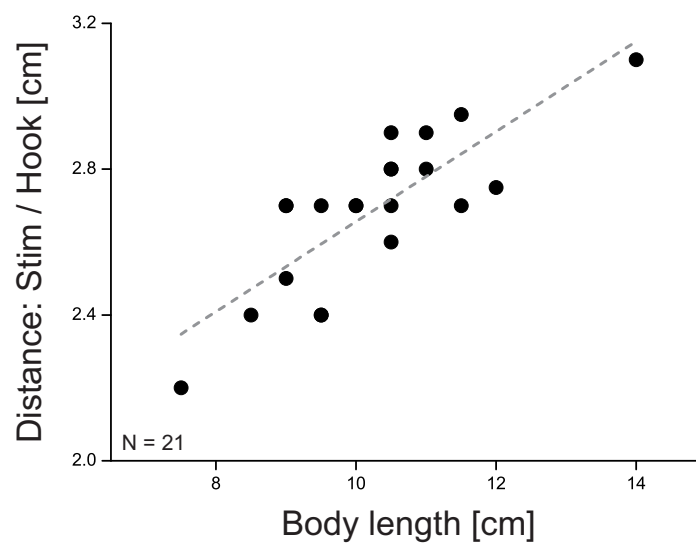
Figure 5.1: Distance between the stimulation and the hook electrodes. In order to calculate the conduction velocities of stimulated neurons, I measured the distance between the stimulation and the hook electrodes for individual experiments. However, if this information was not available I calculated the distance in relation to the animal's body length ($y = 0.123x + 1.420$, Pearson R = 0.811, R^2 = 0.640, N = 21).

Parameters for stimulations at different frequencies

Table 5.1: Parameters for stimulations at different frequencies. Data is presented for three different experiments (mean ± SD, n = 11) and refers to experiments presented in Figure 3.9.

		10 Hz	20 Hz	30 Hz	40 Hz	50 Hz
Period [s]	1	(no rhythm)	0.74 ± 0.04	0.60 ± 0.01	0.50 ± 0.02	0.43 ± 0.02
	2	0.73 ± 0.10	0.60 ± 0.08	0.59 ± 0.04	0.57 ± 0.15	0.58 ± 0.10
	3	0.87 ± 0.04	0.57 ± 0.02	0.42 ± 0.01	0.37 ± 0.05	0.36 ± 0.07
Phase PS3 [%]	1	(no rhythm)	24.3 ± 3.9	21.8 ± 3.4	15.3 ± 2.9	10.5 ± 3.9
	2	34.7 ± 8.0	33.1 ± 9.5	38.6 ± 5.9	21.6 ± 14.3	21.6 ± 10.8
	3	n/a	n/a	n/a	n/a	n/a
Phase PS4 [%]	1	(no rhythm)	12.1 ± 4.0	10.7 ± 3.1	5.3 ± 2.5	3.0 ± 2.2
	2	23.9 ± 5.8	17.0 ± 4.1	12.4 ± 3.1	9.2 ± 4.2	13.1 ± 4.4
	3	n/a	n/a	n/a	n/a	n/a
Duty cycle [%]	1	(no rhythm)	53.2 ± 0.04.9	55.6 ± 6.1	60.1 ± 3.1	66.4 ± 5.0
	2	62.7 ± 13.6	62.7 ± 0.11.3	57.6 ± 6.0	67.9 ± 18.3	72.8 ± 14.4
	3	62.0 ± 5.0	55.9 ± 0.04.8	46.7 ± 3.1	65.4 ± 13.2	72.6 ± 10.5
Burst duration [s]	1	(no rhythm)	0.39 ± 0.03	0.33 ± 0.02	0.30 ± 0.01	0.29 ± 0.02
	2	0.45 ± 0.09	0.37 ± 0.07	0.34 ± 0.03	0.37 ± 0.11	0.43 ± 0.08
	3	0.54 ± 0.06	0.31 ± 0.02	0.19 ± 0.01	0.24 ± 0.04	0.26 ± 0.05
Burst strength	1	(no rhythm)	0.56 ± 0.13	1 ± 0.13	0.93 ± 0.13	1.01 ± 0.09
	2	0.42 ± 0.11	0.92 ± 0.15	1 ± 0.16	1.14 ± 0.16	1.37 ± 0.17
	3	0.37 ± 0.05	0.73 ± 0.11	1 ± 0.15	1.01 ± 0.12	0.94 ± 0.16

Motor neurons during enhancement

Table 5.2: **Parameters of motor neurons during enhancement**. Data (mean ± SD, n = 10) refers to neurons recorded ipsilateral (i) or contralateral (c) to the stimulation that are presented in figures 3.23 and 3.24. **PSE** *Power Stroke Exciter*, **RSE** *Return Stroke Exciter*.

(n = 10)		Period [s]	Amplitude [mV]	PP [mV]	TP [mV]
PSEi 1	Pre-Stim	0.72 ± 0.03	3.1 ± 0.2	- 63.4 ± 0.1	- 66.6 ± 0.2
	Stim	0.57 ± 0.03	6.1 ± 0.5	- 57.1 ± 0.5	- 63.2 ± 0.3
PSEi 2	Pre-Stim	0.70 ± 0.04	6.3 ± 0.6	- 43.7 ± 0.5	- 50.1 ± 0.6
	Stim	0.48 ± 0.01	10.7 ± 0.3	- 39.3 ± 0.2	- 50.1 ± 0.2
PSEc	Pre-Stim	0.46 ± 0.02	9.1 ± 0.6	- 50.4 ± 0.4	- 59.5 ± 0.4
	Stim	0.37 ± 0.02	7.3 ± 0.3	- 51.2 ± 0.2	- 58.5 ± 0.2
RSEi 1	Pre-Stim	0.58 ± 0.02	5.2 ± 0.5	- 53.1 ± 0.5	- 58.3 ± 0.3
	Stim	0.39 ± 0.01	16.2 ± 0.9	- 45.8 ± 0.4	- 62.0 ± 0.8
RSEi 2	Pre-Stim	0.70 ± 0.03	5.6 ± 0.6	- 53.7 ± 0.4	- 59.3 ± 0.3
	Stim	0.64 ± 0.03	10.4 ± 0.4	- 50.0 ± 0.4	- 60.4 ± 0.4
RSEi 3	Pre-Stim	0.89 ± 0.02	7.5 ± 0.7	- 57.0 ± 0.2	- 64.6 ± 0.7
	Stim	0.61 ± 0.02	8.6 ± 0.7	- 55.3 ± 0.3	- 63.8 ± 0.7
RSEi 4	Pre-Stim	0.86 ± 0.02	9.0 ± 0.6	- 44.0 ± 0.4	- 53.0 ± 0.5
	Stim	0.55 ± 0.10	8.5 ± 1.0	- 47.3 ± 0.7	- 55.8 ± 0.7
RSEc	Pre-Stim	0.56 ± 0.03	4.6 ± 0.3	- 52.7 ± 0.3	- 57.3 ± 0.2
	Stim	0.35 ± 0.02	4.1 ± 0.4	- 52.4 ± 0.3	- 56.5 ± 0.3

Table 5.3: **Parameters of CPG neurons during enhancement**. Data (mean ± SD, n = 10) refers to neurons recorded ipsilateral (i) or contralateral (c) to the stimulation that are presented in figures 3.25 and 3.26. **IPS** *Inhibitor of Power Stroke*, **IRS** *Inhibitor of Return Stroke*.

(n = 10)		Period [s]	Amplitude [mV]	PP [mV]	TP [mV]
IPSi 1	Pre	0.75 ± 0.09	6.44 ± 0.78	- 45.7 ± 0.8	- 52.2 ± 1.2
	Stim	0.44 ± 0.04	13.69 ± 0.45	- 43.8 ± 0.5	- 57.5 ± 0.4
IPSi 2	Pre	0.52 ± 0.04	7.15 ± 0.64	- 49.1 ± 0.5	- 56.2 ± 0.3
	Stim	0.46 ± 0.04	5.71 ± 0.75	- 52.9 ± 0.6	- 58.6 ± 0.3
IRSi	Pre	0.60 ± 0.02	4.66 ± 0.17	- 60.4 ± 0.1	- 65.0 ± 0.1
	Stim	0.37 ± 0.01	8.50 ± 0.32	- 52.9 ± 0.1	- 61.4 ± 0.3
IRSc 1	Pre	0.75 ± 0.04	8.09 ± 0.98	- 38.3 ± 0.2	- 46.4 ± 1.0
	Stim	0.46 ± 0.03	6.48 ± 0.48	- 38.8 ± 0.4	- 45.3 ± 0.4
IRSc 2	Pre	0.82 ± 0.04	6.25 ± 0.24	- 55.4 ± 0.2	- 61.7 ± 0.2
	Stim	0.51 ± 0.03	10.96 ± 0.32	- 52.2 ± 0.2	- 63.2 ± 0.3

PSPs in IRS during enhancement of fictive locomotion
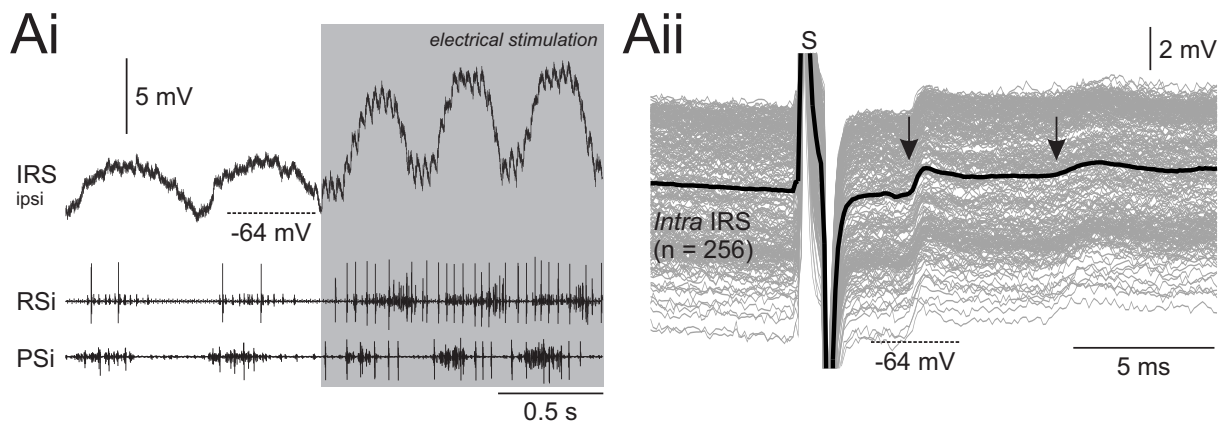
Figure 5.2: Individual stimulation pulses evoked postsynaptic potentials (PSP) in IRS during enhancement of fictive locomotion. Stimulations are depicted in gray. **Ai:** Intracellular recording of one ipsilateral IRS during enhancement of fictive locomotion. During stimulation, the membrane potential depolarized and oscillation amplitudes increased. The same neuron is presented in figure 3.28. **Aii:** An stimulus-triggered overdraw (n = 256, black line illustrates the average), illustrating the generation of two stimulus-triggered PSPs (left arrow, latency: 4.1 ms, amplitude: 1.3 mV; right arrow, latency: 9.2 ms, amplitude: 0.7 mV) in IRS. **IRS** *inhibitor of return stroke*, **RSi** *ipsilateral return stroke*, **PSi** *ipsilateral power stroke*, **S** *stimulus artifact*, **PSP** *postsynaptic potential*.

Danksagung

Mein größter Dank gebührt meiner Betreuerin PD Dr. Carmen Wellmann. Carmen, Du warst eine herausragende Doktormutter und ich bin Dir wirklich überaus dankbar für Deinen immensen Beitrag bei der Planung und Durchführung meiner Experimente, bei der kritischen Reflexion meiner Ergebnisse, und natürlich auch bei der Zusammenstellung dieser Arbeit. Ohne Dich hätte das nicht funktioniert - Danke!

Danken möchte ich auch den weiteren Mitgliedern meiner Prüfungskommission, Prof. Dr. Ansgar Büschges und Prof. Dr. Sigrun Korsching. Ein besonderer Dank geht hierbei an Prof. Dr. Ansgar Büschges, auf dessen Unterstützung ich mich immer verlassen konnte und mich als ein vollwertiger Teil der AG Büschges gefühlt habe.

Der gesamten AG Büschges, der AG Gruhn und auch der AG Kloppenburg möchte ich für die unvergleichliche Arbeitsatmosphäre über die vergangenen Jahre danken. Es hat sich wirklich nicht wie Arbeit angefühlt und ich habe sehr gute Freunde gefunden die mich hoffentlich noch mein weiteres Leben begleiten werden. Den Elektroboys, HP und allen weiteren Mitarbeitern möchte ich insbesondere auch für die technische Unterstützung danken!

An die gesamte Swimmeret-Crew um Carmen, Heike, Anna, Laura, Berenike, Felix und Nils: Ich hätte mir keine besseren Arbeitskollegen wünschen können! Ihr habt mich immer unterstützt und mir bei allen Problemen geholfen. Angefangen von der ersten Präparation und den frühen experimentellen Schritten, über unzählige Ohrwürmer, bis hin zur Auswertung und Korrektur dieser Arbeit. Ihr seid tolle Menschen und noch dazu sehr, sehr k-l-u-k.

Hier fehlen dürfen auch nicht mein phänomenaaler Freundeskreis - Danke Euch aalen! *Greifvogelgruß* - und meine gesamte Familie, der ich jedes Mal gerne erneut erkläre was ich eigentlich genau mache. Zum Schluss noch der vielleicht größte Dank an die Person, die mich während den letzten Monaten ertragen hat, immer die richtigen Worte fand und mir so unendlich viel abgenommen hat - Danke Iva und ab jetzt koche ich!

Eigenständigkeitserklärung

Ich versichere, dass ich die von mir vorgelegte Dissertation selbständig angefertigt, die benutzten Quellen und Hilfsmittel vollständig angegeben und die Stellen der Arbeit – einschließlich Tabellen, Karten und Abbildungen –, die anderen Werken im Wortlaut oder dem Sinn nach entnommen sind, in jedem Einzelfall als Entlehnung kenntlich gemacht habe; dass diese Dissertation noch keiner anderen Fakultät oder Universität zur Prüfung vorgelegen hat; dass sie noch nicht veröffentlicht worden ist, sowie, dass ich eine solche Veröffentlichung vor Abschluss des Promotionsverfahrens nicht vornehmen werde. Die Bestimmungen der Promotionsordnung sind mir bekannt. Die von mir vorgelegte Dissertation ist von PD Dr. Carmen Wellmann betreut worden.

Köln, den 05.05.2020